3D data processing 1

Geometric modeling

- Modeling real objects in 3D manner using cameras and laser range sensors

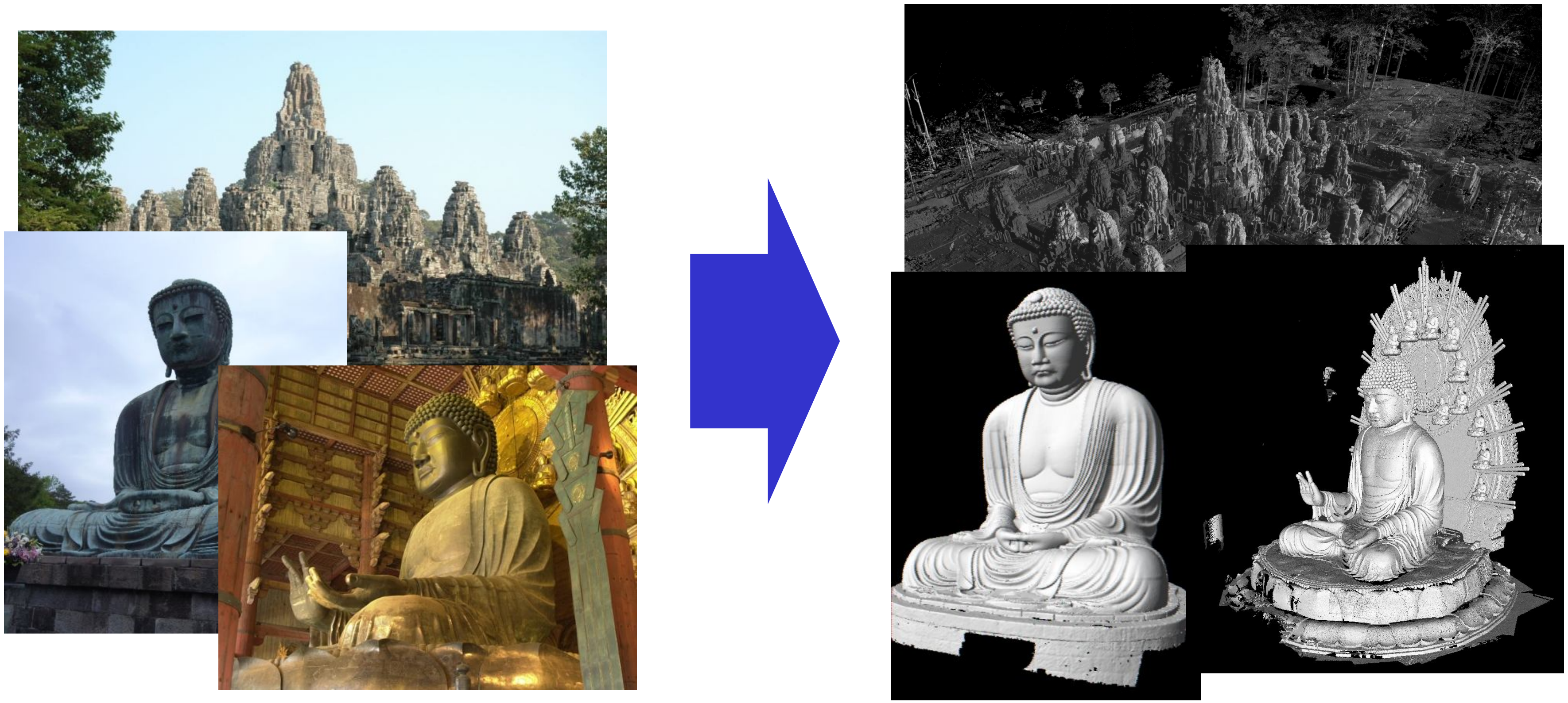

Modeling procedures

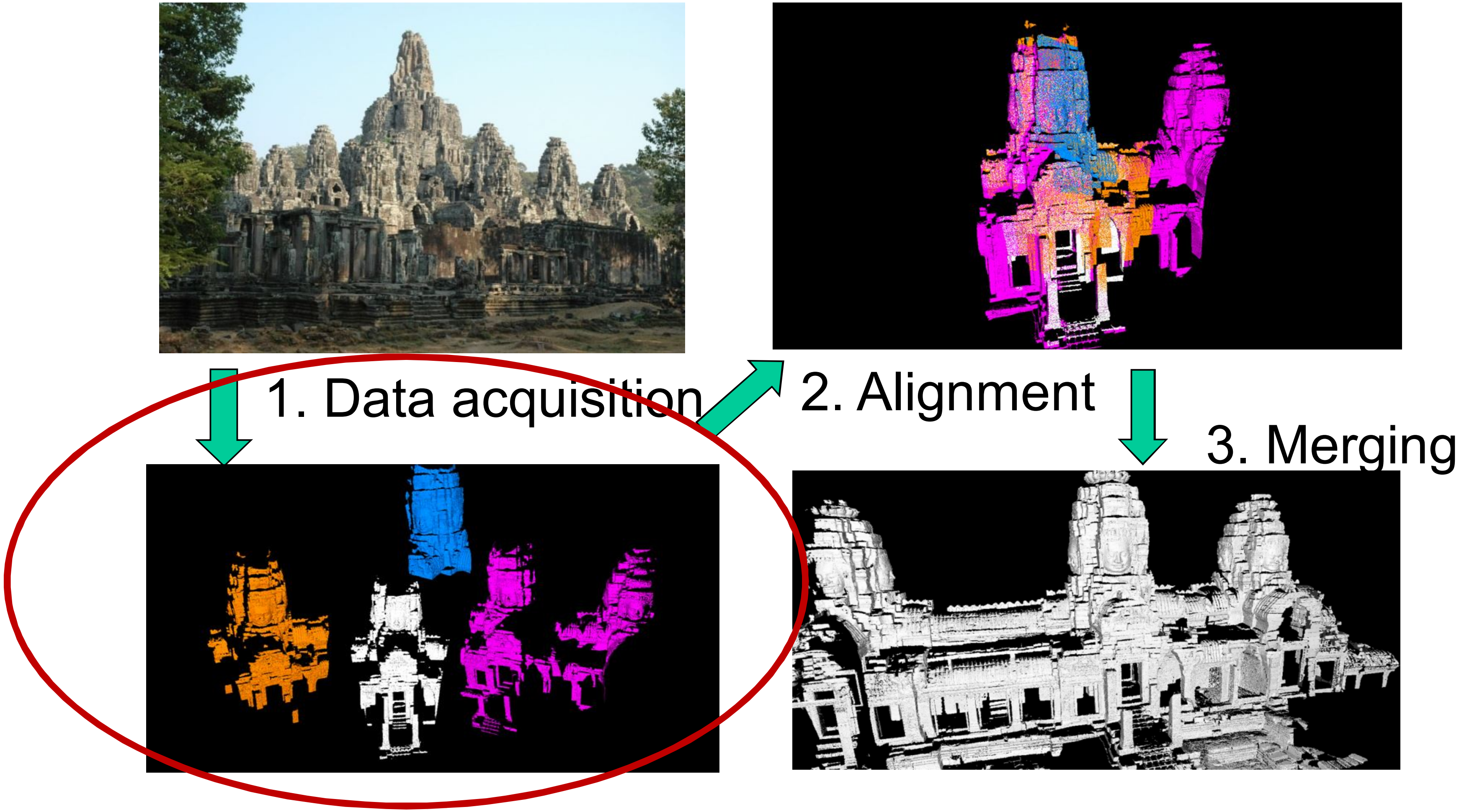

1. DATA ACQUISITION

Color image vs. Range image

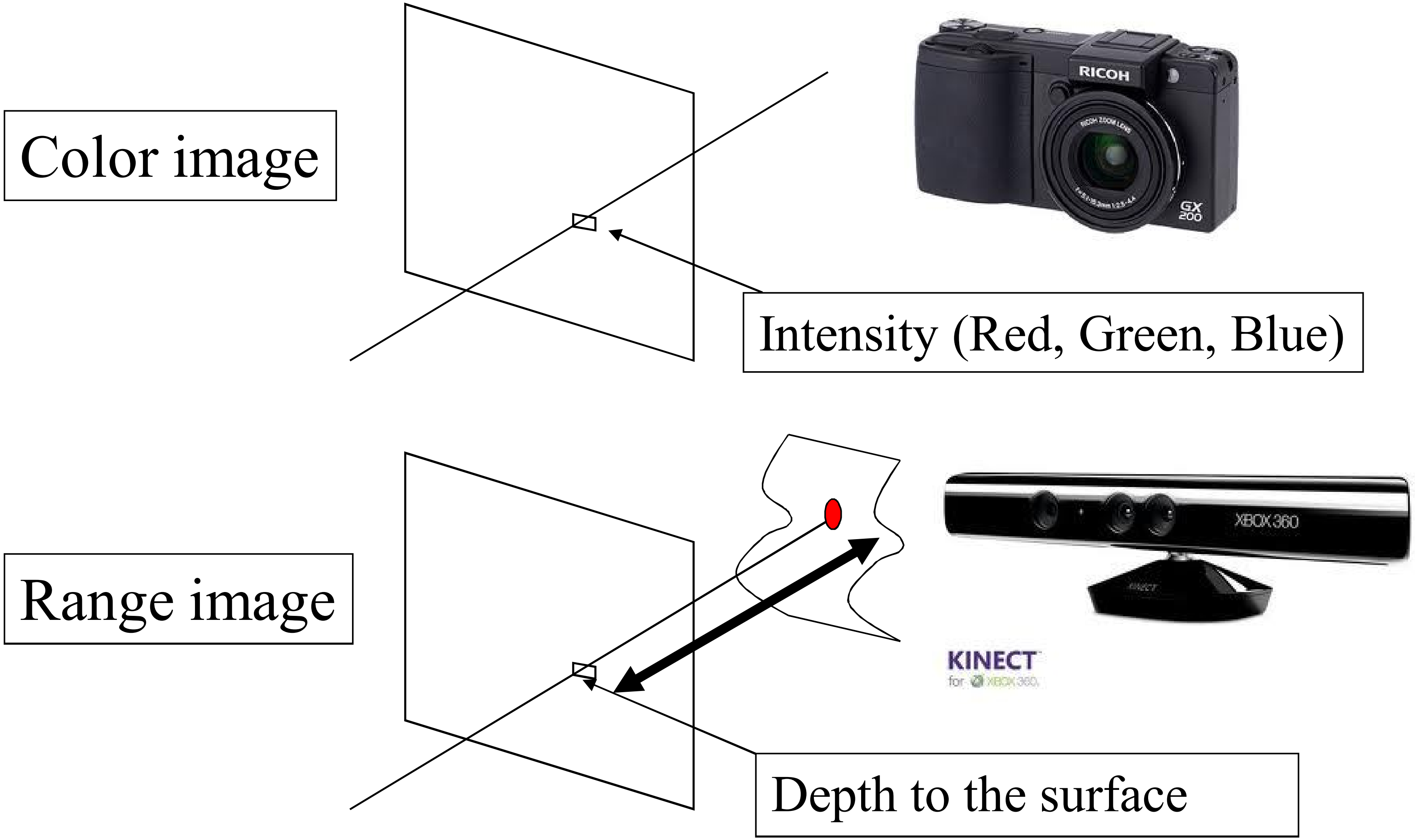

Range image example

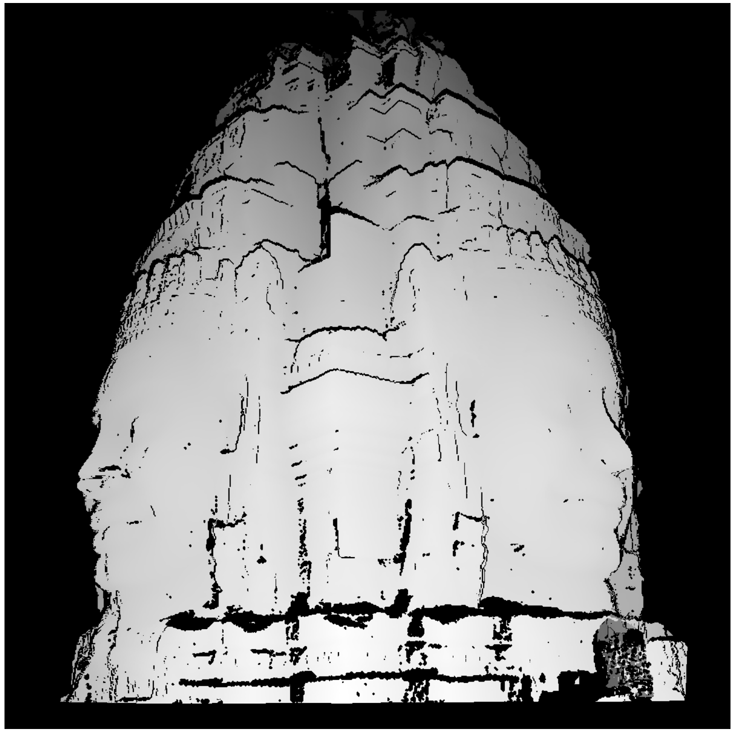

Range image (2.5D)

Reconstructed partial 3D model

Measurement method (non-contact)

[redacted]

- Active
  - Structured light
  - Laser range sensor

Grey code structured lighting

[Inokuchi ICPR'84]

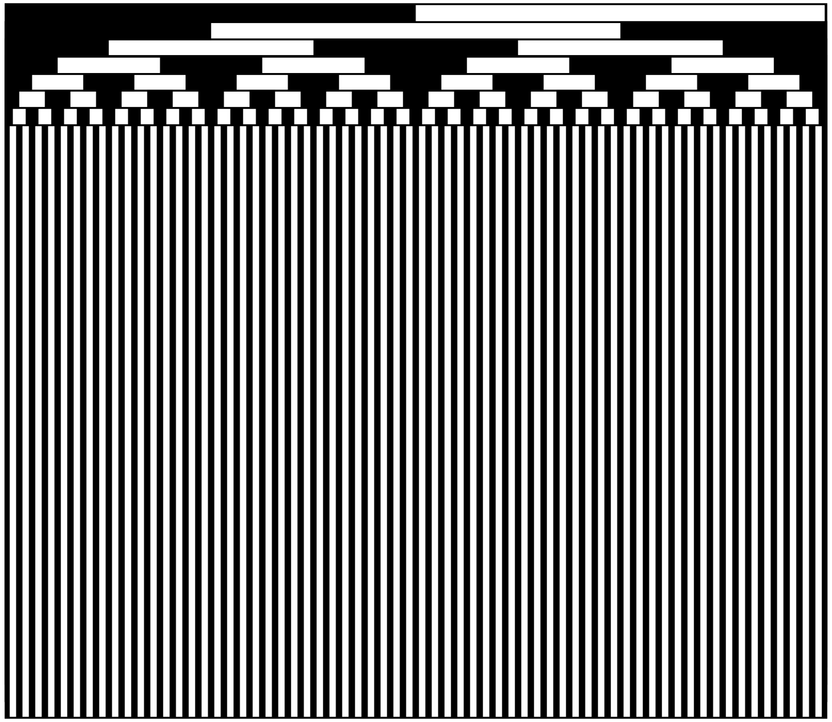

integer row/column index -> binary code -> Gray code

Structured light

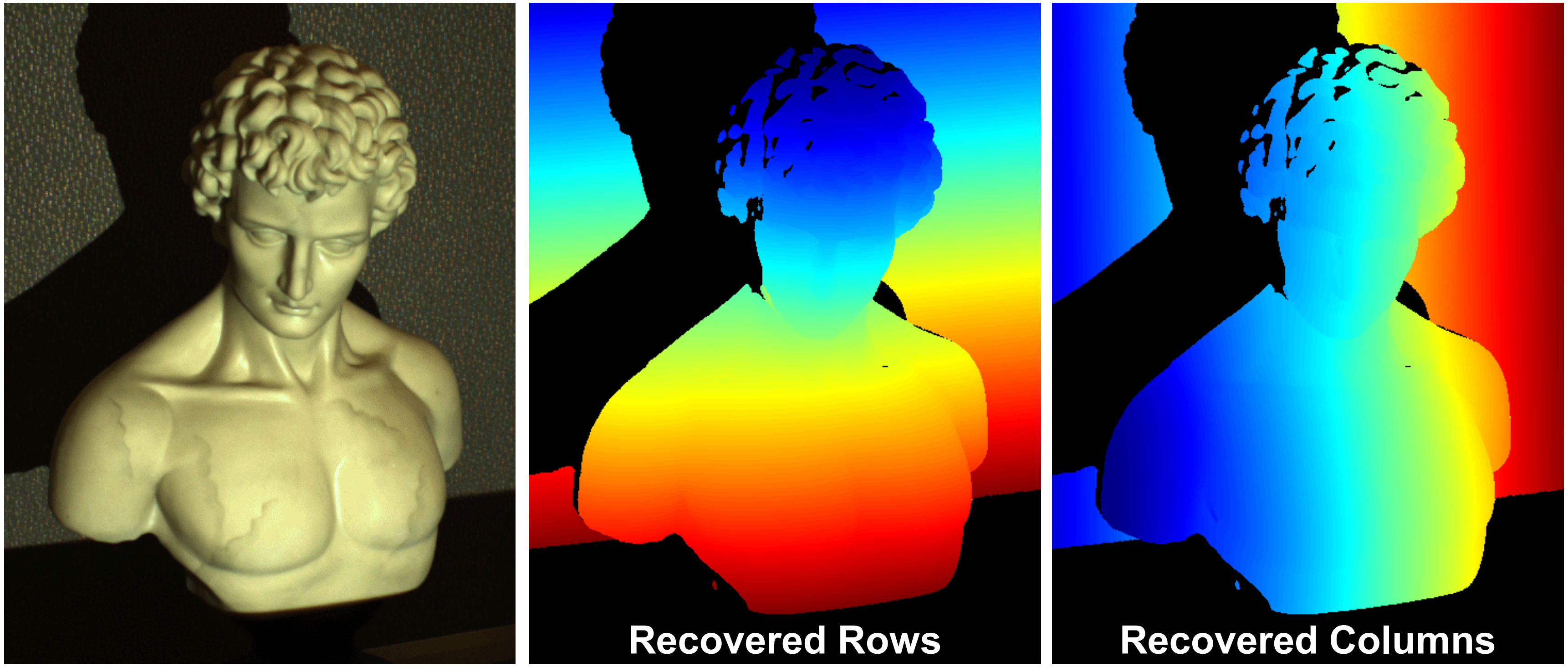

Gray code -> binary code -> integer row/column index

[Lanman et al.]

Triangulation

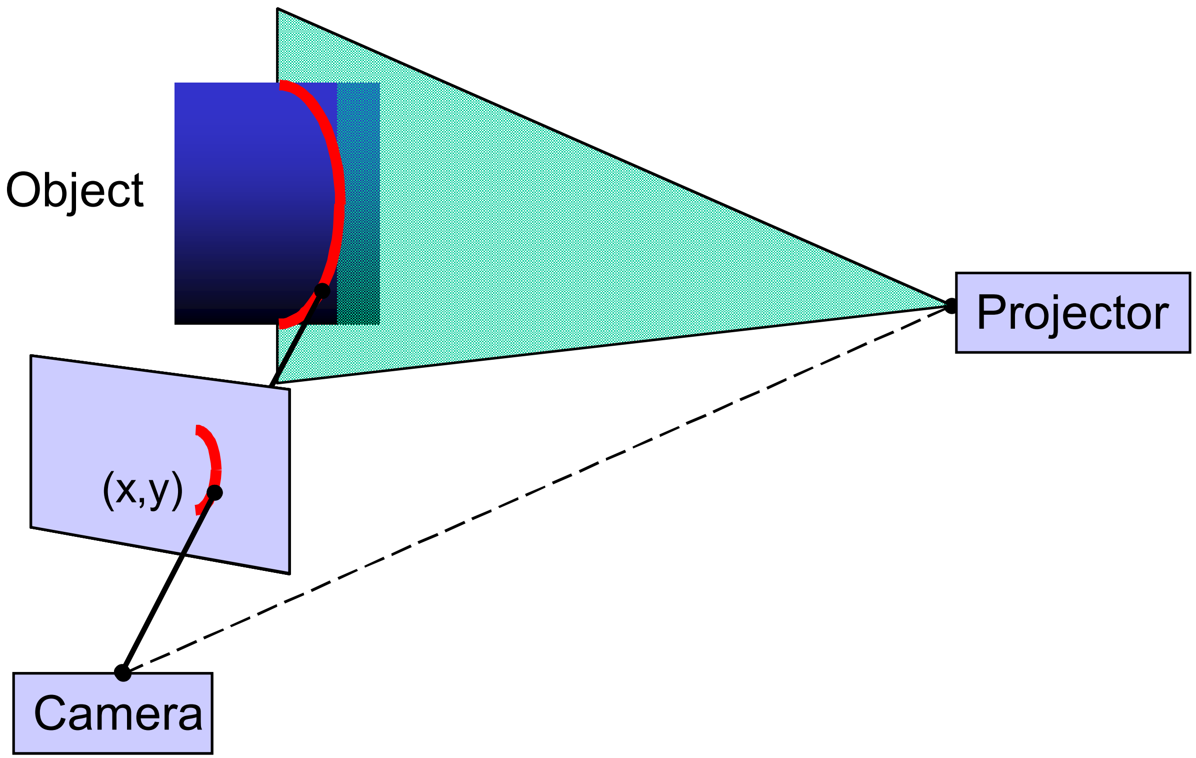

- Depth from ray-plane triangulation

Measurement result

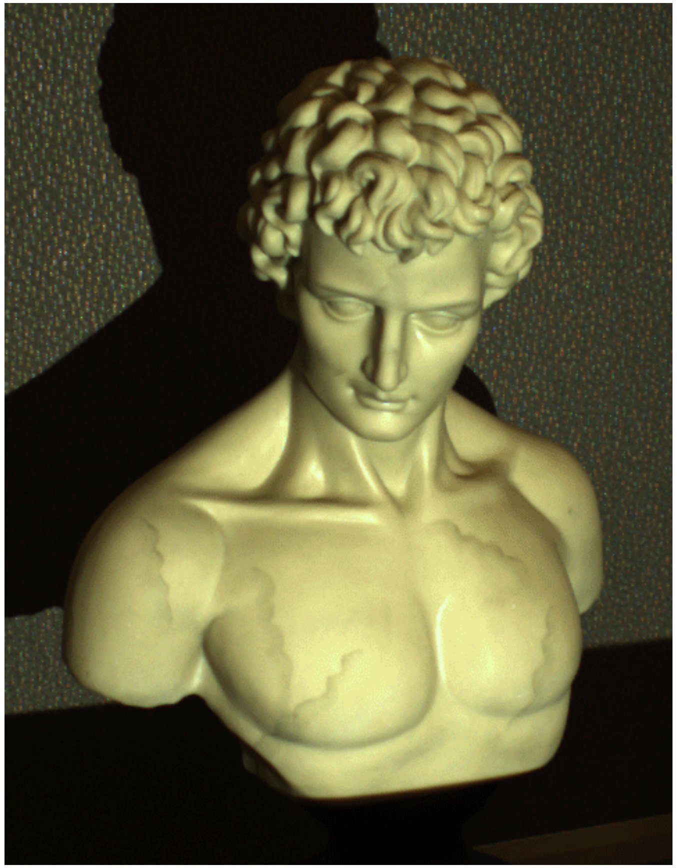

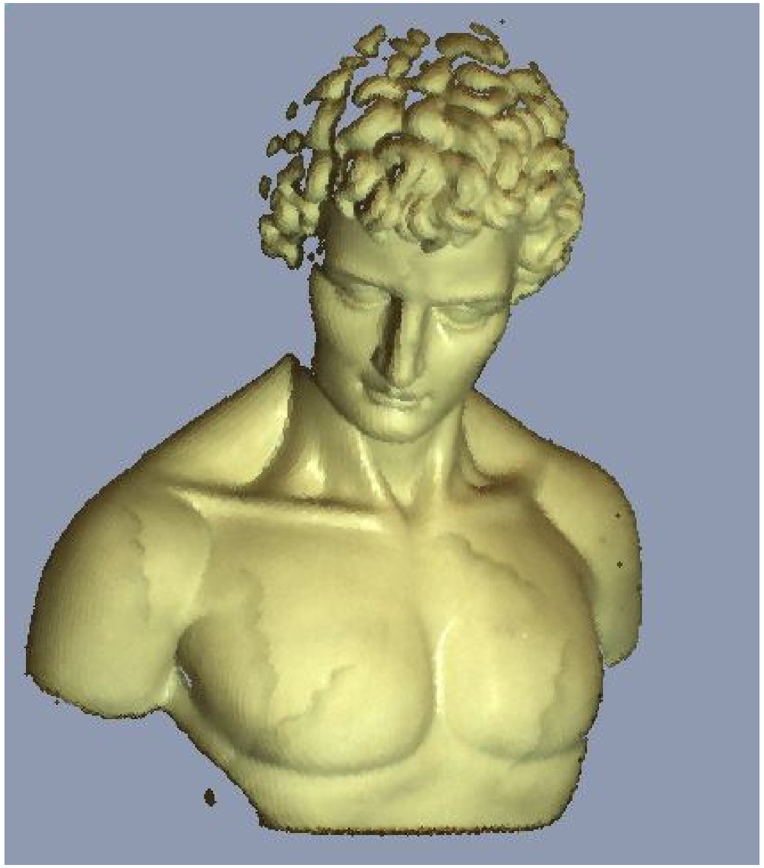

[Lanman et al.]

Real-time full-field 3-D surface-shape measurement using off-the-shelf components and a single processor

P. Jia*, J. Kofman†, C. English†
*University of Ottawa, Laval University
†University of Waterloo

Time-Coded Light Patterns

- Assign each stripe a unique illumination code over time [Posdamer 82]

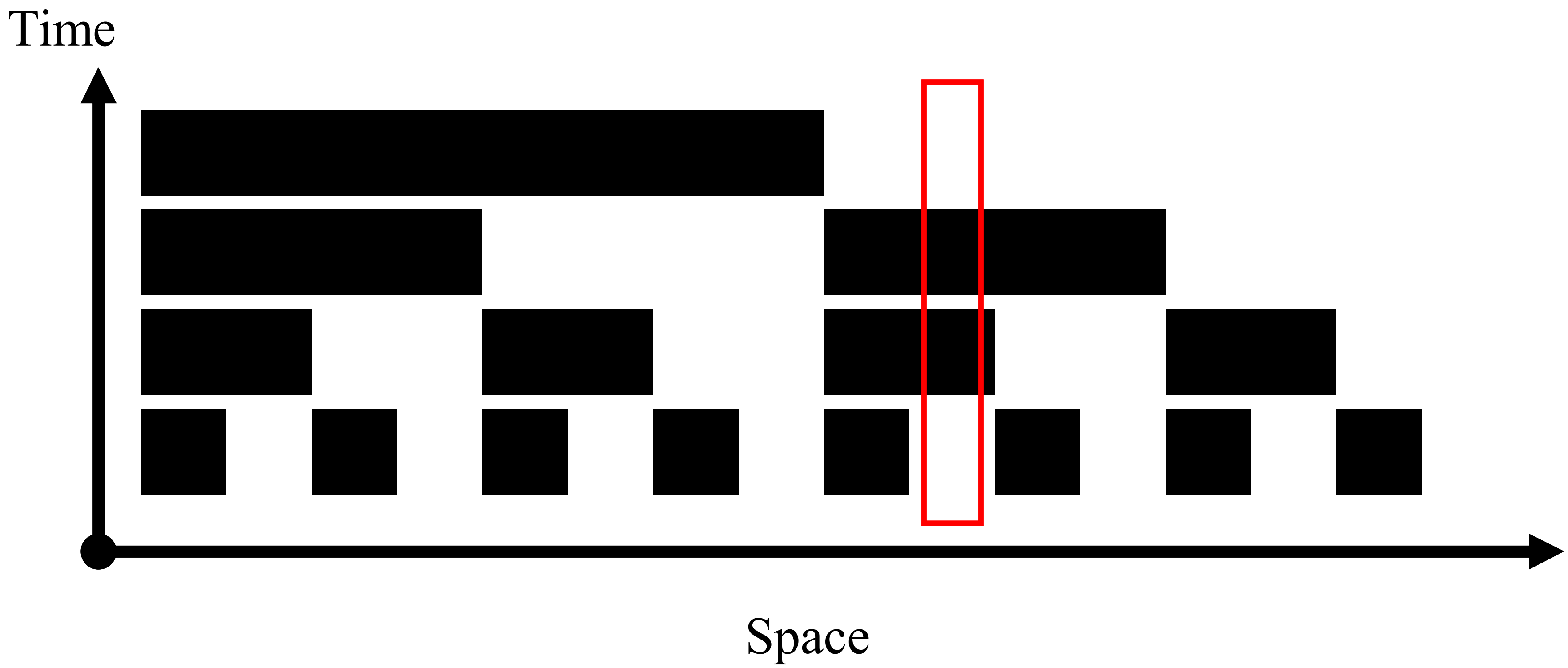

Proposed method

- Real-time Structured Light
  - Triangular-pattern & phase-shifting
  - Software synchronization (projector & camera)

Triangular pattern

(a)

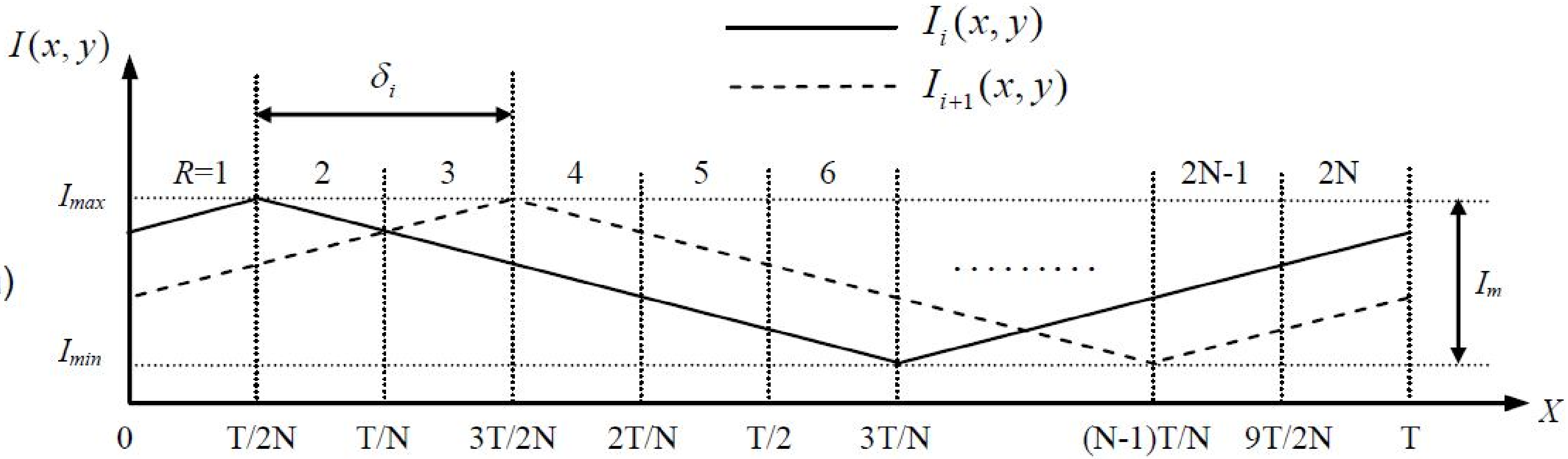

$$I_i(x,y)=\begin{cases}\dfrac{2I_m(x,y)}{T}(x+\delta_i)+I_{\min}(x,y)+\dfrac{I_m(x,y)}{2} & x+\delta_i\in[0,\dfrac{T}{4})\\ -\dfrac{2I_m(x,y)}{T}(x+\delta_i)+I_{\min}(x,y)+\dfrac{3I_m(x,y)}{2} & x+\delta_i\in[\dfrac{T}{4},\dfrac{3T}{4})\\ \dfrac{2I_m(x,y)}{T}(x+\delta_i)+I_{\min}(x,y)-\dfrac{3I_m(x,y)}{2} & x+\delta_i\in[\dfrac{3T}{4},T)\end{cases}$$

Intensity ratio

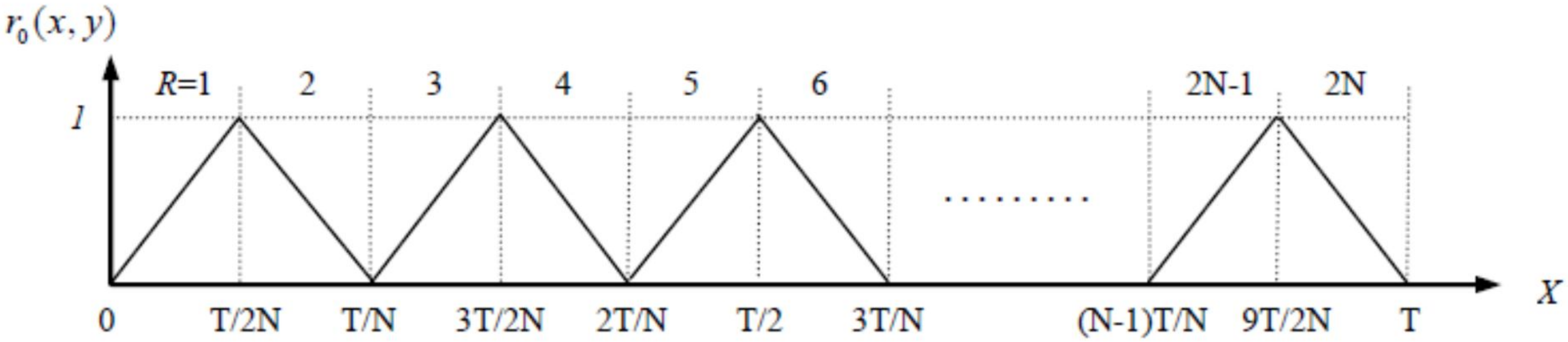

Phase Step	Equation for $r_0(x,y)$
2	$r_0(x,y)=\lvert I_1(x,y)-I_2(x,y)\rvert / I_m(x,y)$ where $I_1(x,y)$ and $I_2(x,y)$ are the intensities for the two shifted triangular patterns, respectively.
3	$r_0(x,y)=\left[I_{high}(x,y)-I_{med}(x,y)+I_{low}(x,y)-I_{min}(x,y)\right]/I_m(x,y)$ where $I_{high}(x,y)$, $I_{med}(x,y)$ and $I_{low}(x,y)$ are the highest, median and lowest intensities of the three shifted triangular patterns at the same position in the range of the pitch, respectively.
4	$r_0(x,y)=\big\lVert I_1(x,y)-I_3(x,y)\rvert-\lvert I_2(x,y)-I_4(x,y)\big\rVert / I_m(x,y)$ where $I_1(x,y)$, $I_2(x,y)$, $I_3(x,y)$ and $I_4(x,y)$ are the intensities for the four shifted triangular patterns, respectively.
	$r(x,y)=[I\ (x,y)-I\ (x,y)+I\ (x,y)-I\ (x,y)+I\ (x,y)-I\ (x,y)]/I\ (x,y)$

Intensity ratio unwrapping

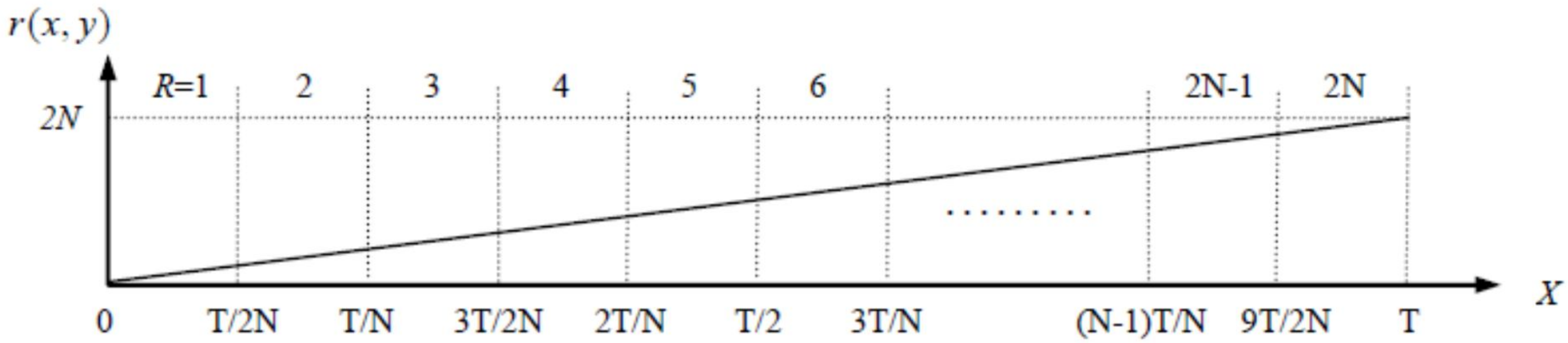

$$r(x,y) = 2 \times round\left(\frac{R-1}{2}\right) + (-1)^{R+1} r_0(x,y)$$

$$R = 1, 2, 3, \cdots\cdots$$

R is the region number

Intensity ratio unwrapping

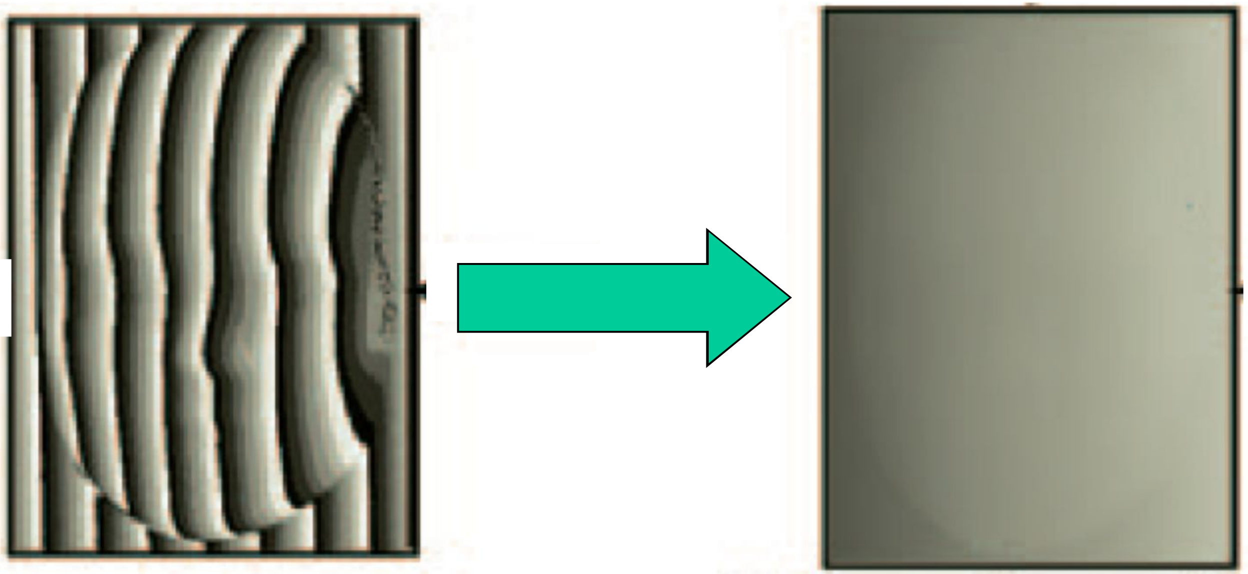

Intensity-ratio wrapped image

Intensity-ratio unwrapped image

Measurement Pipeline

- Image acquisition
- Intensity-ratio wrapping
- Intensity-ratio unwrapping
- 3D data reconstruction

Multi-thread Programming

System setup

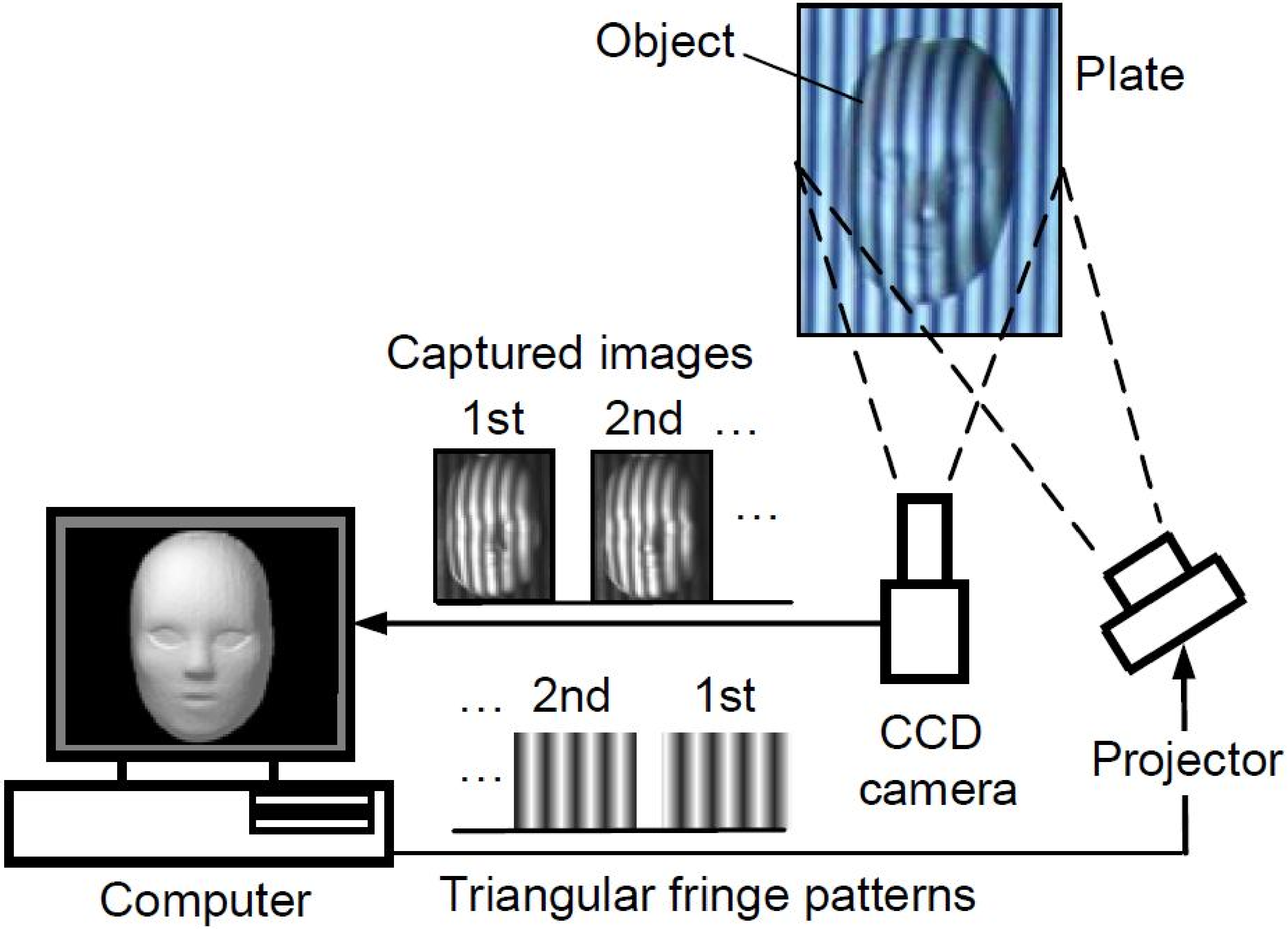

Measurement of a human face

Photo

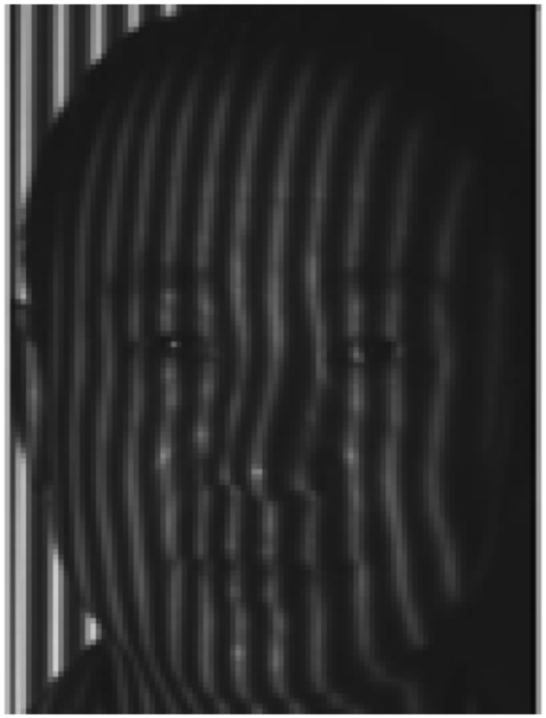

Fringe image

3D model

Results 1: 2-step pattern

Measurement speed : 5.6 fps

Results 2: 6-step pattern

Measurement speed : 4.2 fps

Summary

- Triangular-pattern & phase-shifting
- Software synchronization (projector & camera)

- Measurement speed: 5.6 fps (2-step)
  4.2 fps (6-step)

A Sensor for Simultaneously Capturing Texture and Shape by Projecting Structured Infrared Light

K. Akasaka, R. Sagawa, Y. Yagi
Osaka University

Color coded pattern

[Zhang 3DPVT2002]

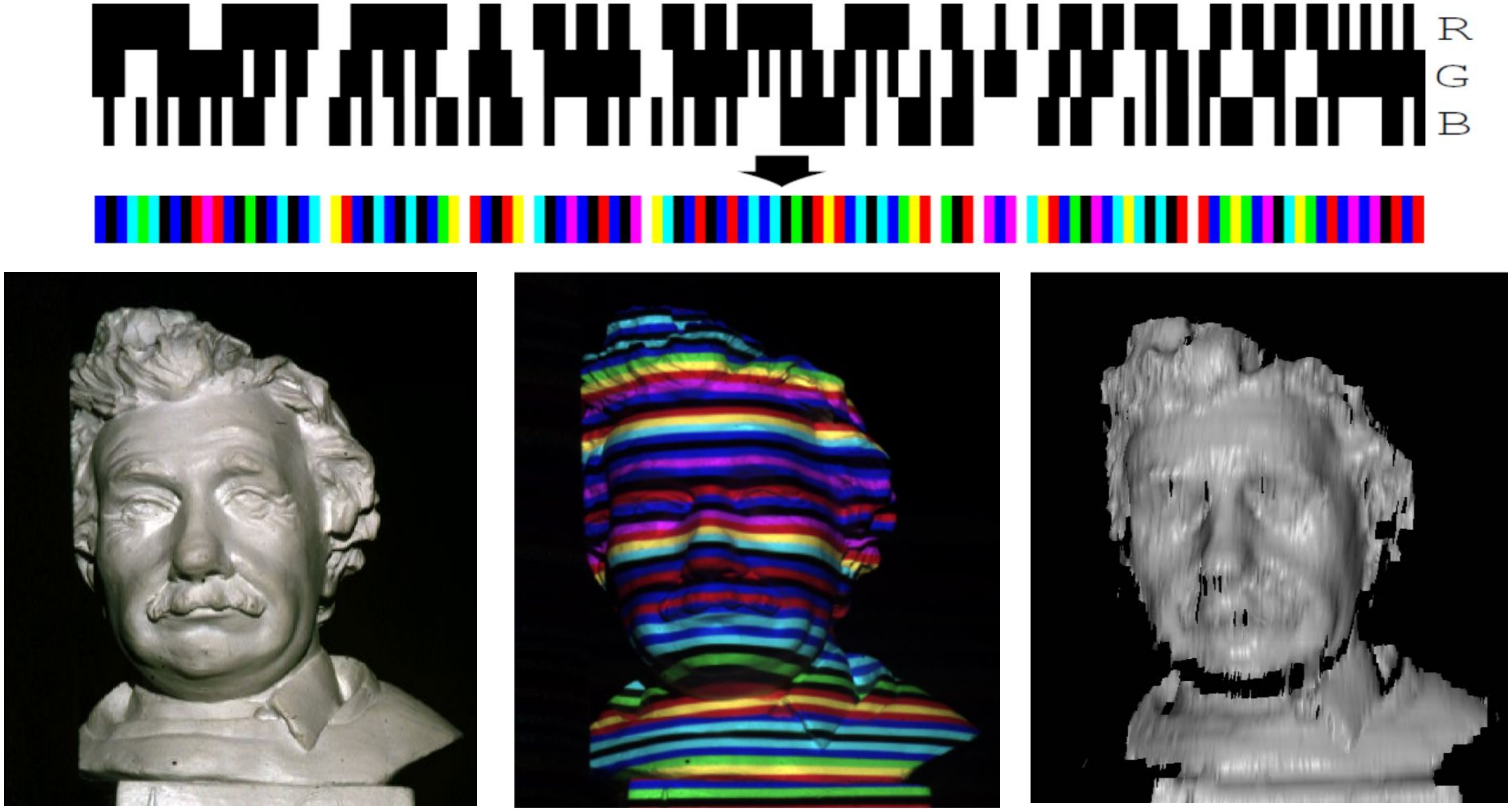

Capturing texture and shape

- Color patterns method requires two shots for capturing both texture and shape

- Texture: Visible light
- Shape: Infrared structured light

Distribution of wavelengths

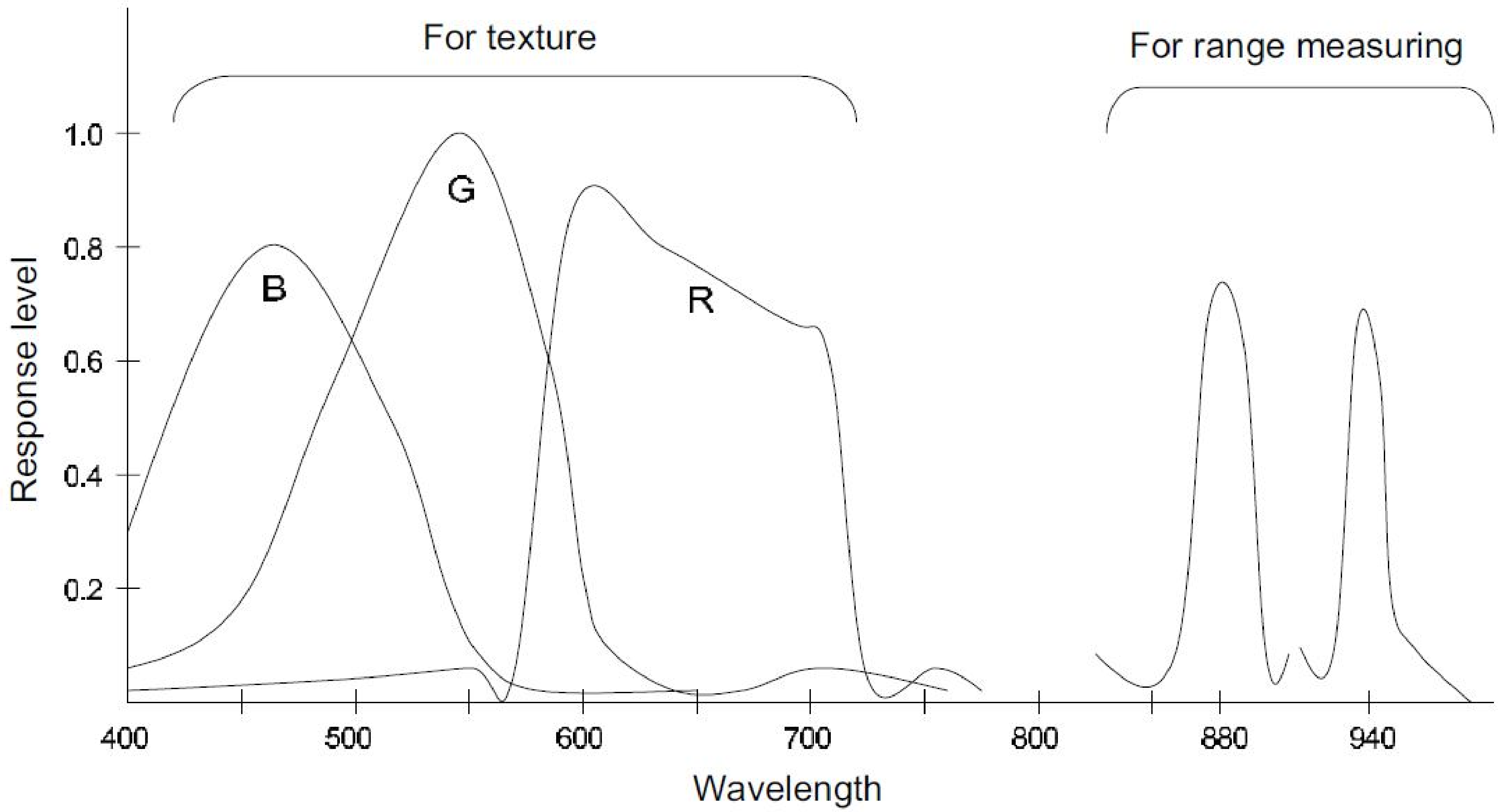

System overview

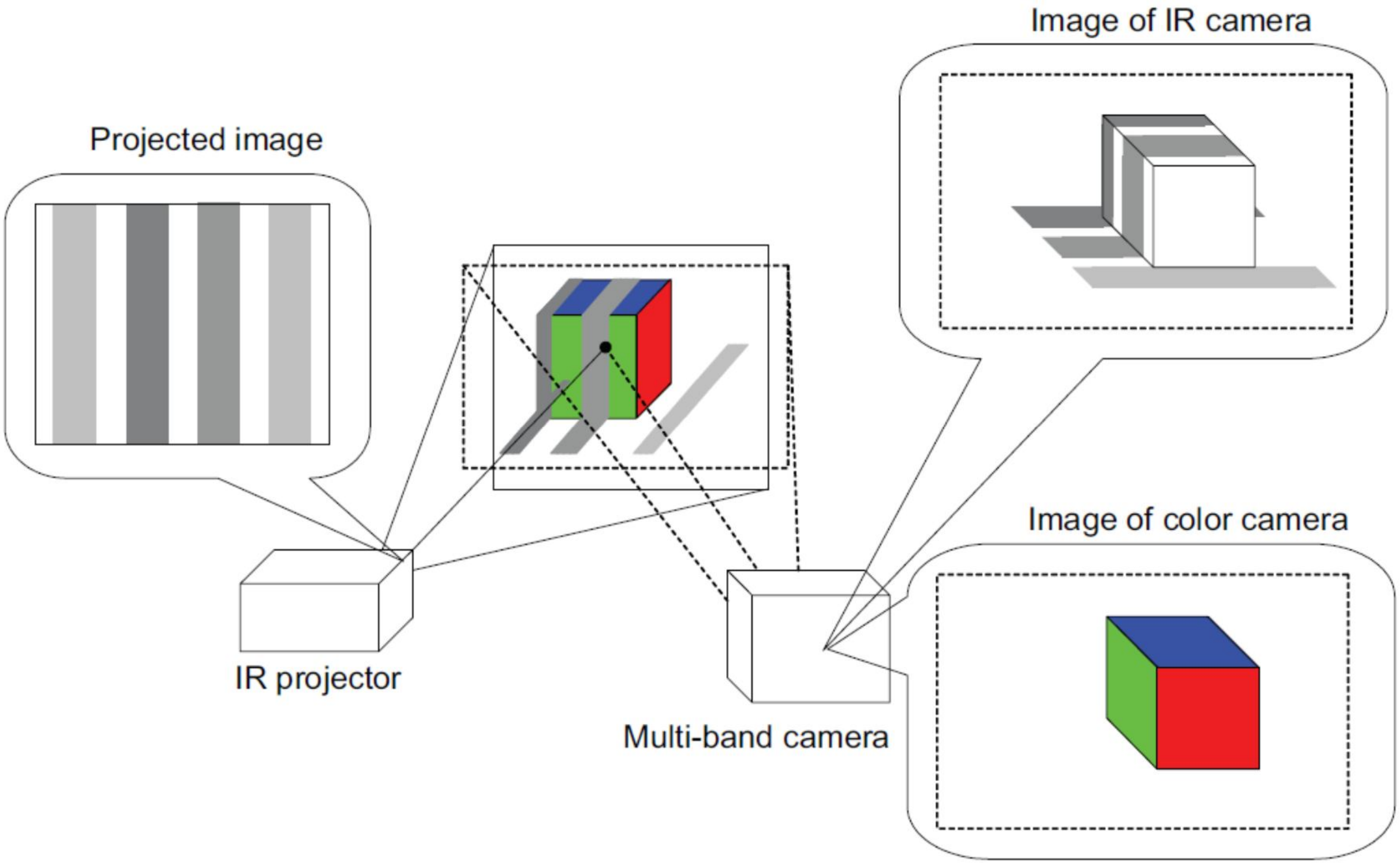

Structured light patterns

- De Bruijn sequence
  - n=8, q=2 (2colors: 880nm, 940nm)
  - The number of symbols=150

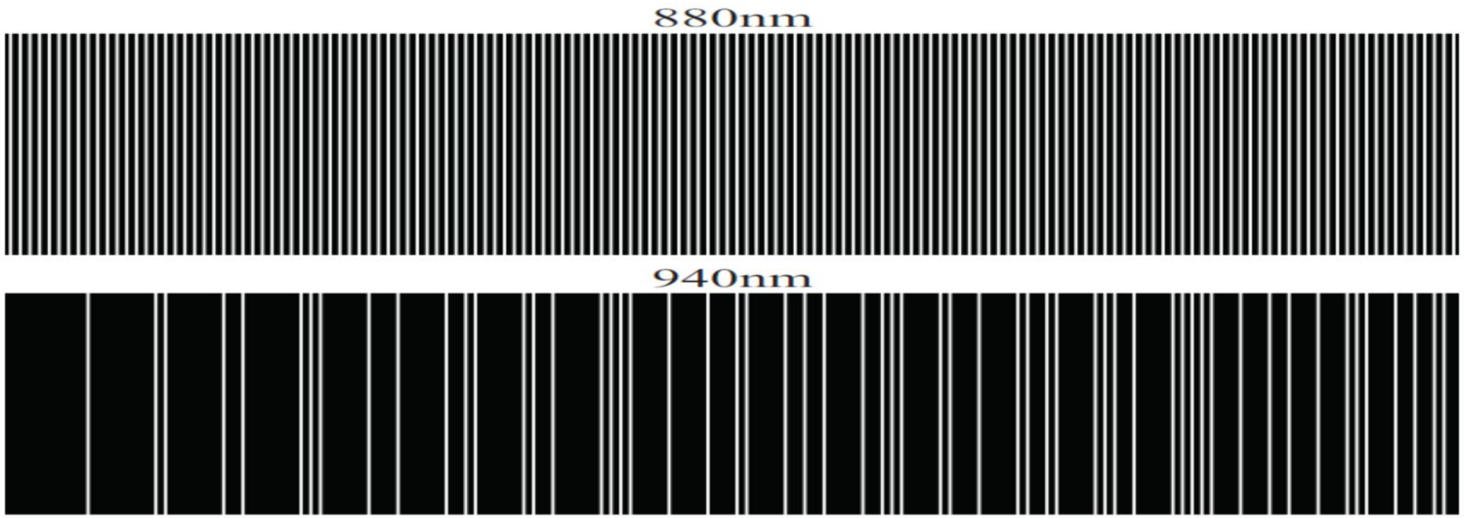

- Matching: DP matching

IR Projector

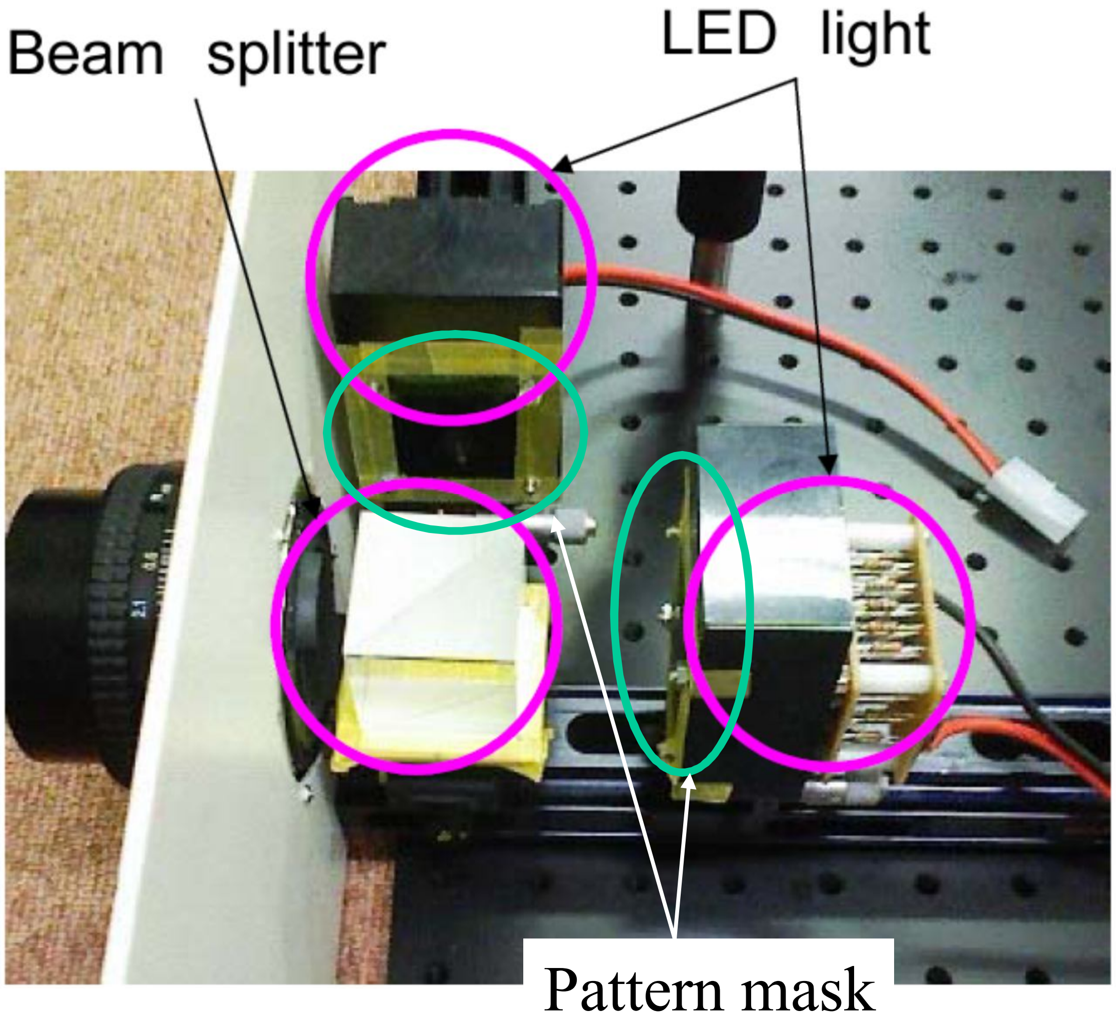

Multi-band camera

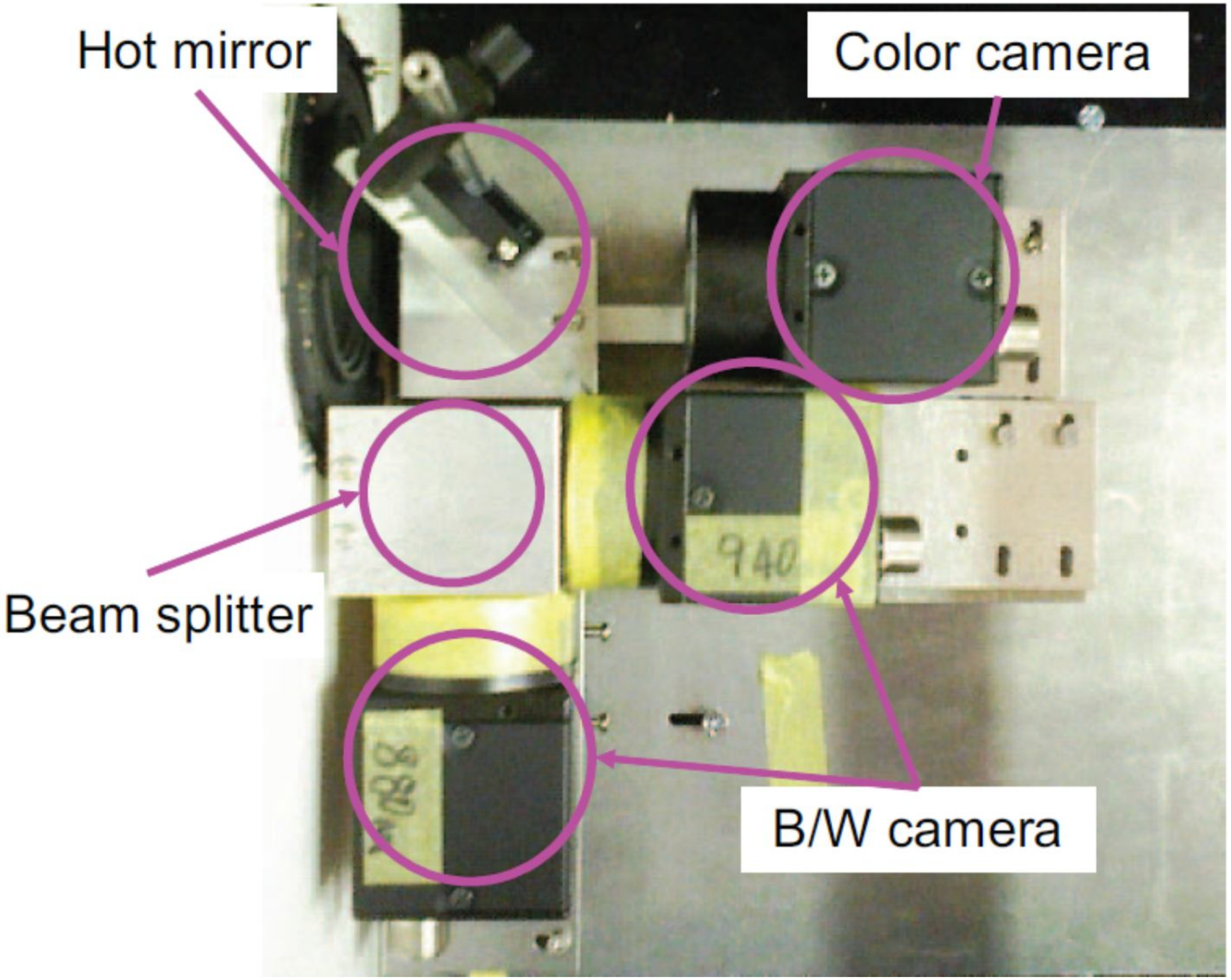

Experimental overview

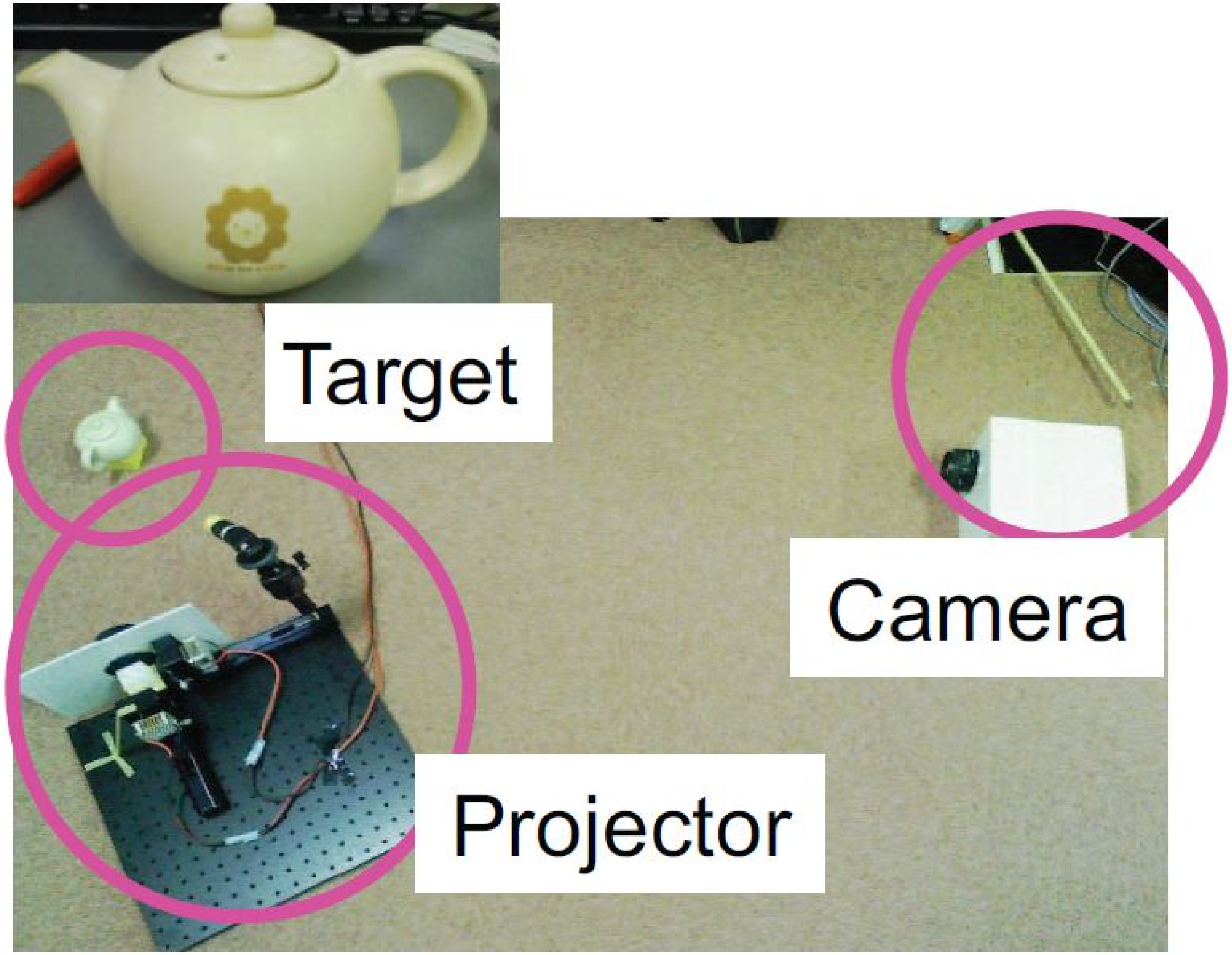

Captured images

Texture image

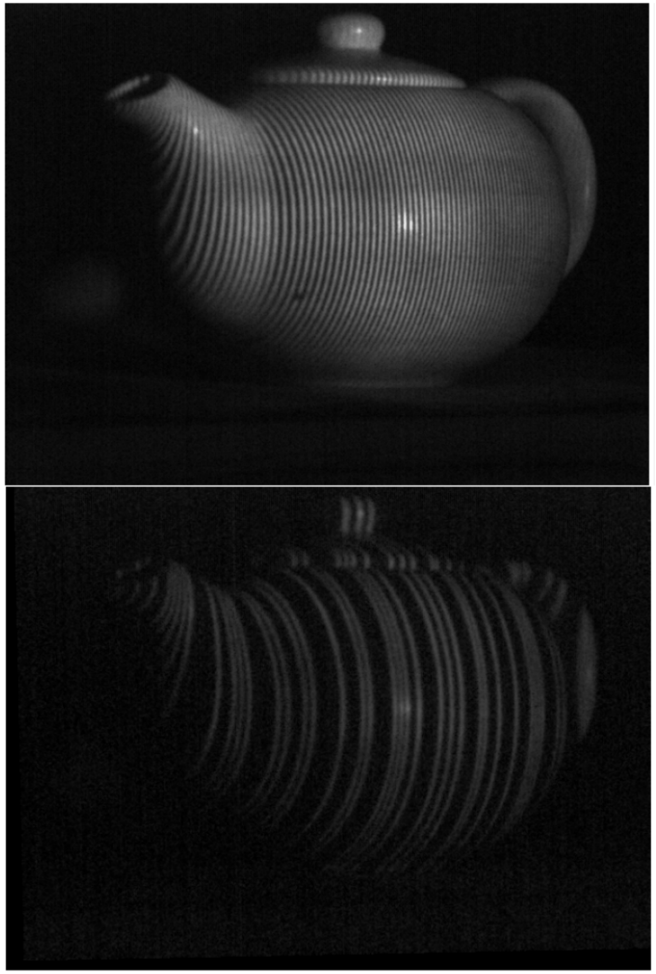

IR filtered image

Detected lines

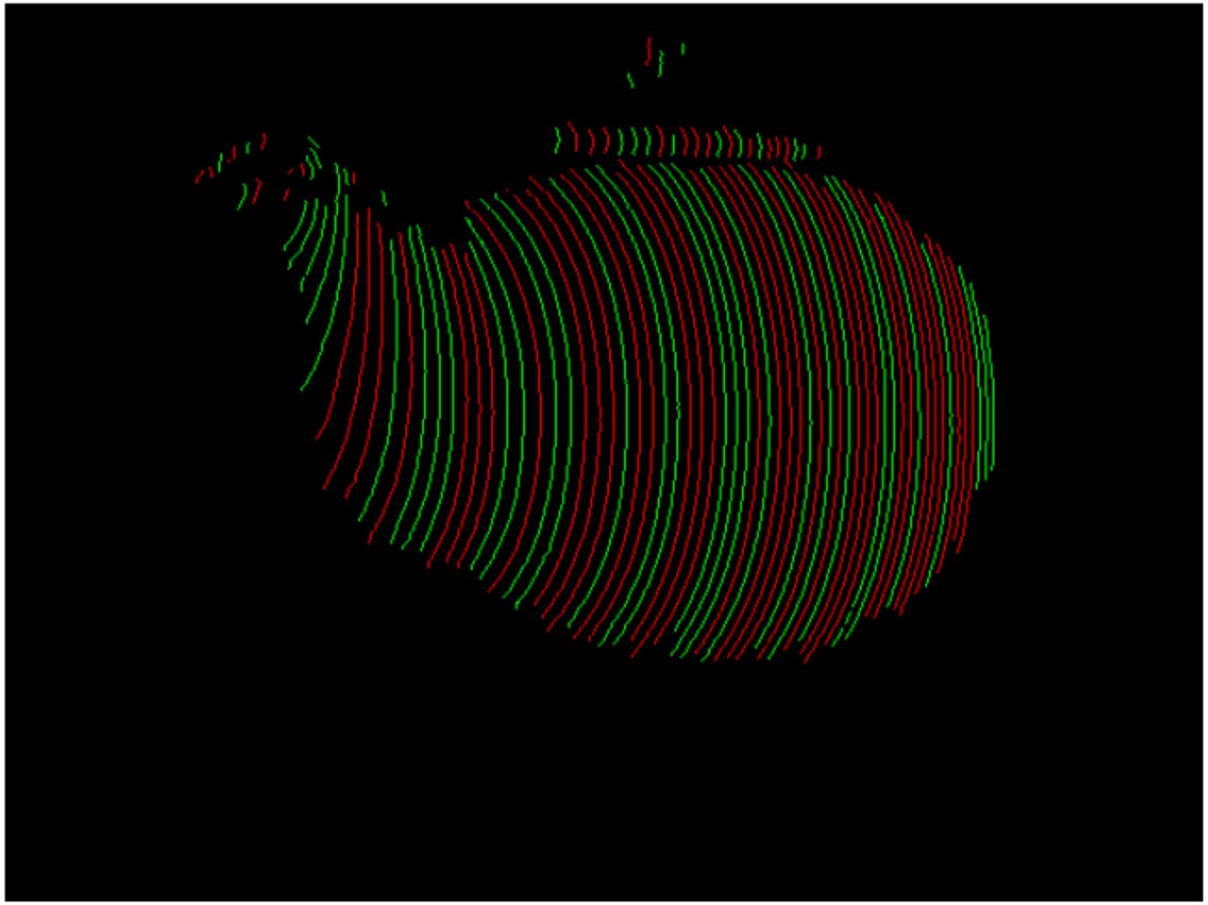

Generated 3D mesh model

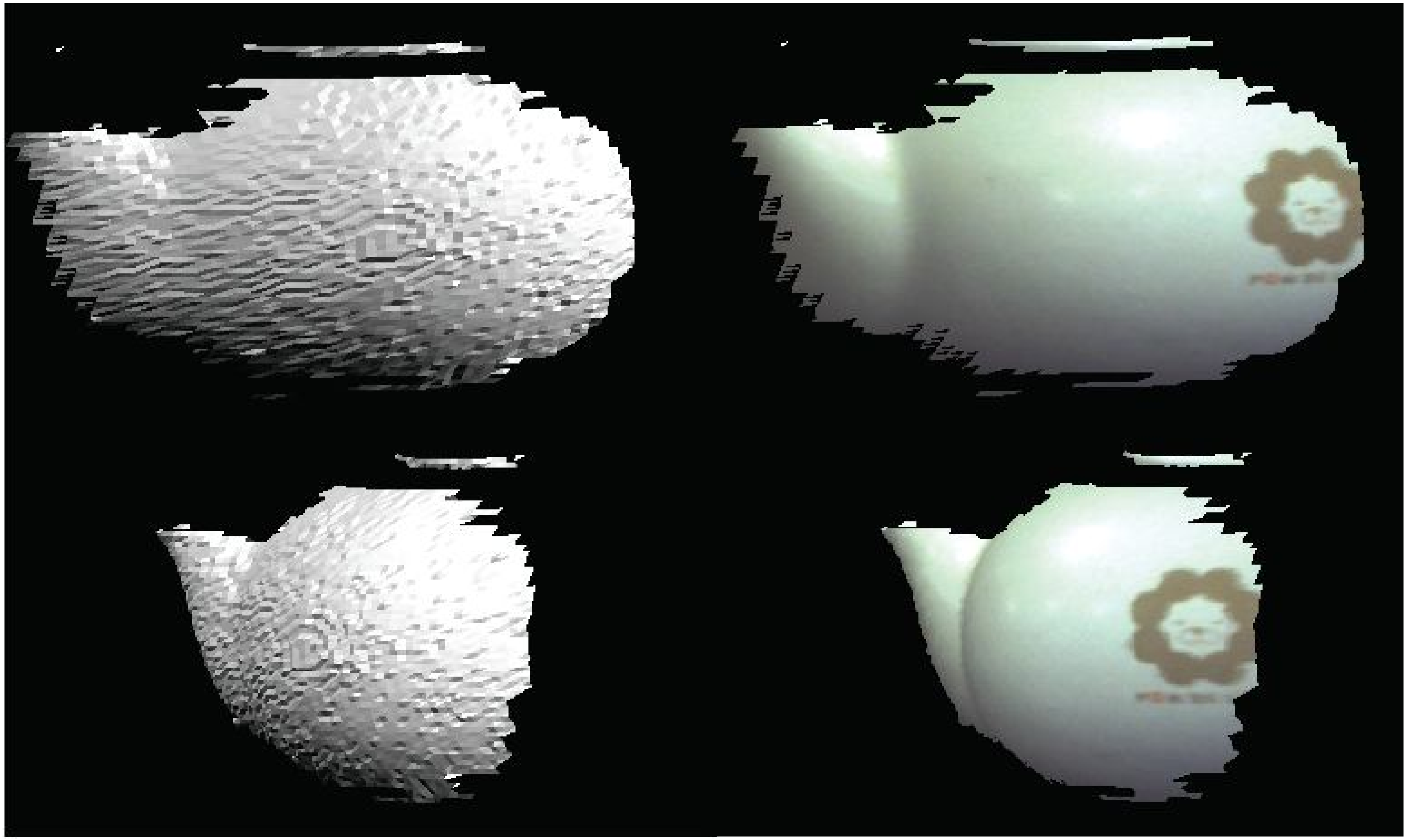

Measurement time: 60 ms (16.7fps)
with Intel Pentium 4 3.0GHz

Summary

- Simultaneously capturing texture and shape
  - Texture: Visible light
  - Shape: Infrared structured light (880nm, 940nm)

  - De Bruijn sequence (n=8, q=2)
  - DP matching

Dense 3D reconstruction

[Sagawa et al. ICCV'09]

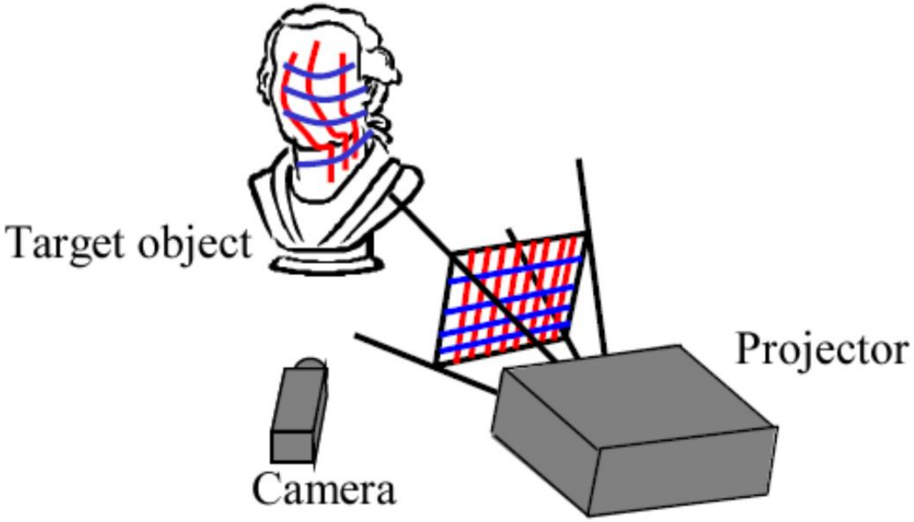

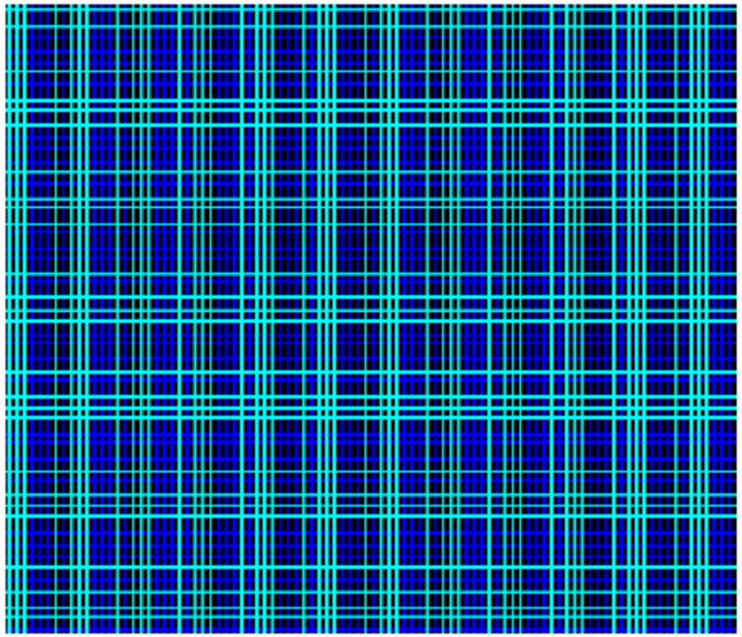

Demo video

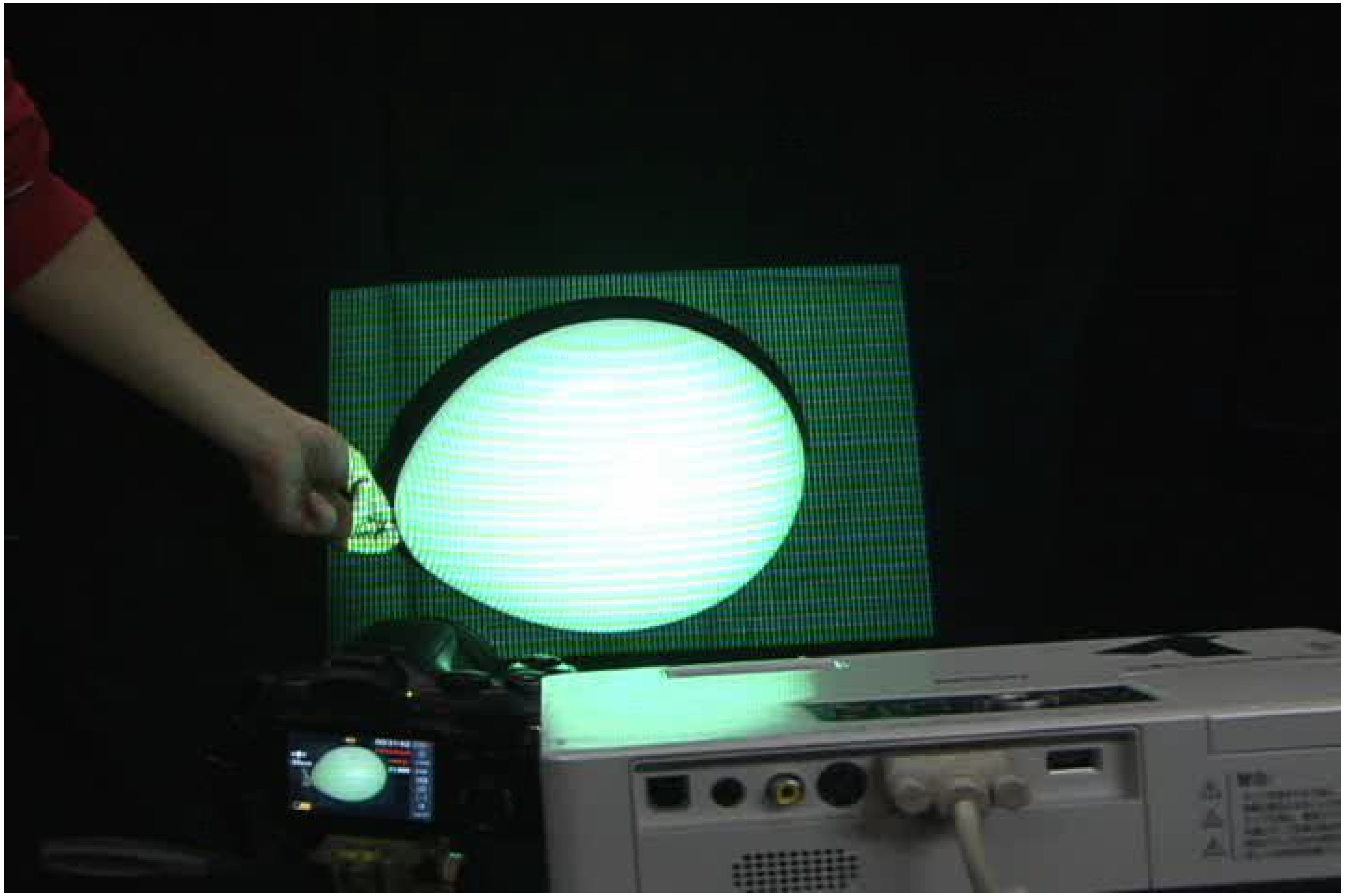

Codes for moving scenes

- Assign time codes to stripe boundaries
- Perform frame-to-frame tracking of corresponding boundaries
  - Propagate illumination history

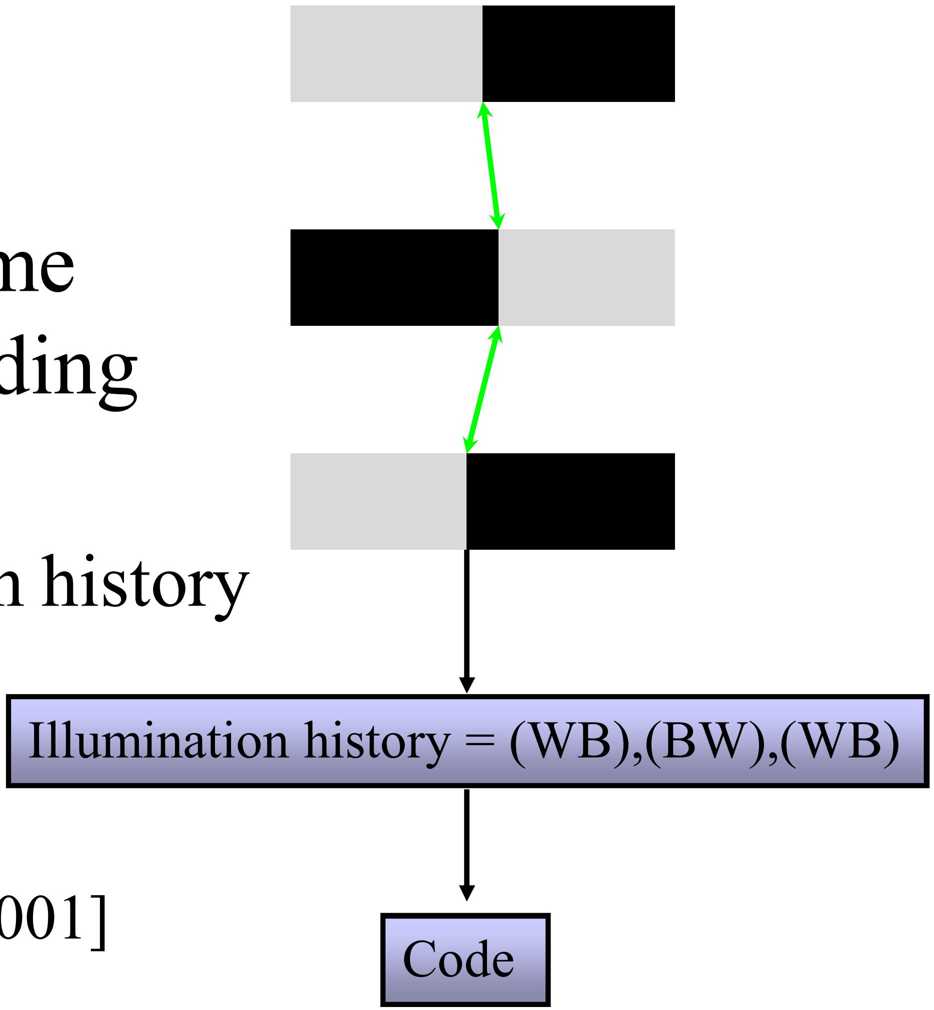

[Hall-Holt & Rusinkiewicz, ICCV 2001]

Kinect (Microsoft)

- Near-infrared laser
- Dot patterns

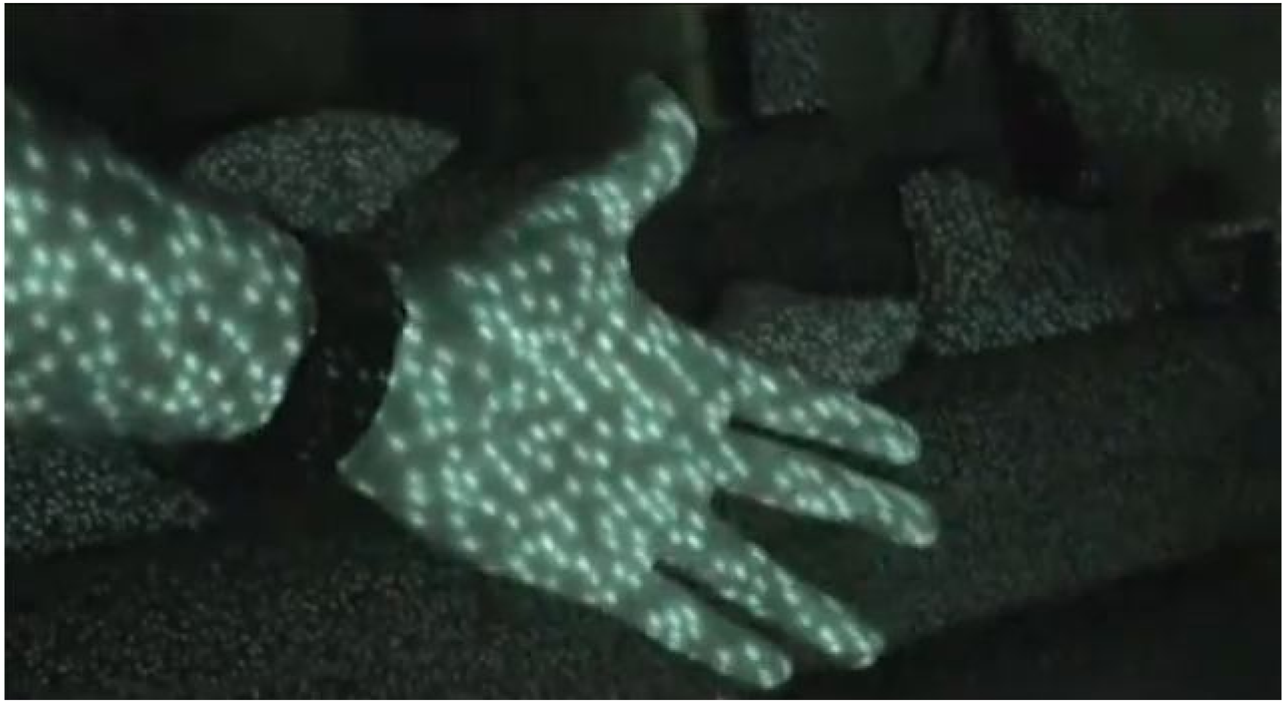

LASER RANGE SENSOR

Light sectioning method

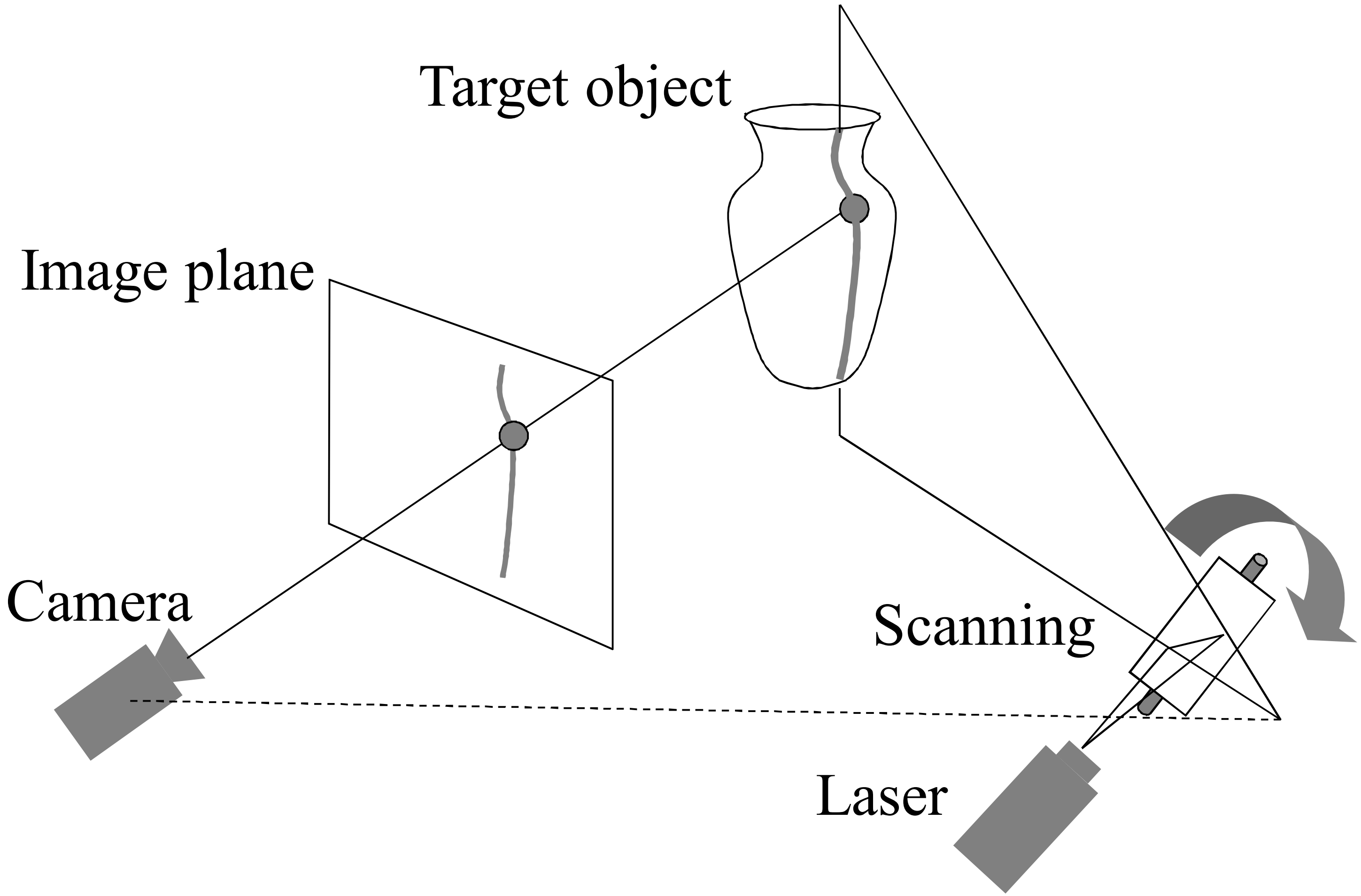

VIVID910 (Konica Minolta)

- Range : 0.6-1.0m
- Accuracy : 0.05-0.4mm
- Time : 2.5 sec
- Resolution : 640×480
- Laser class : 2

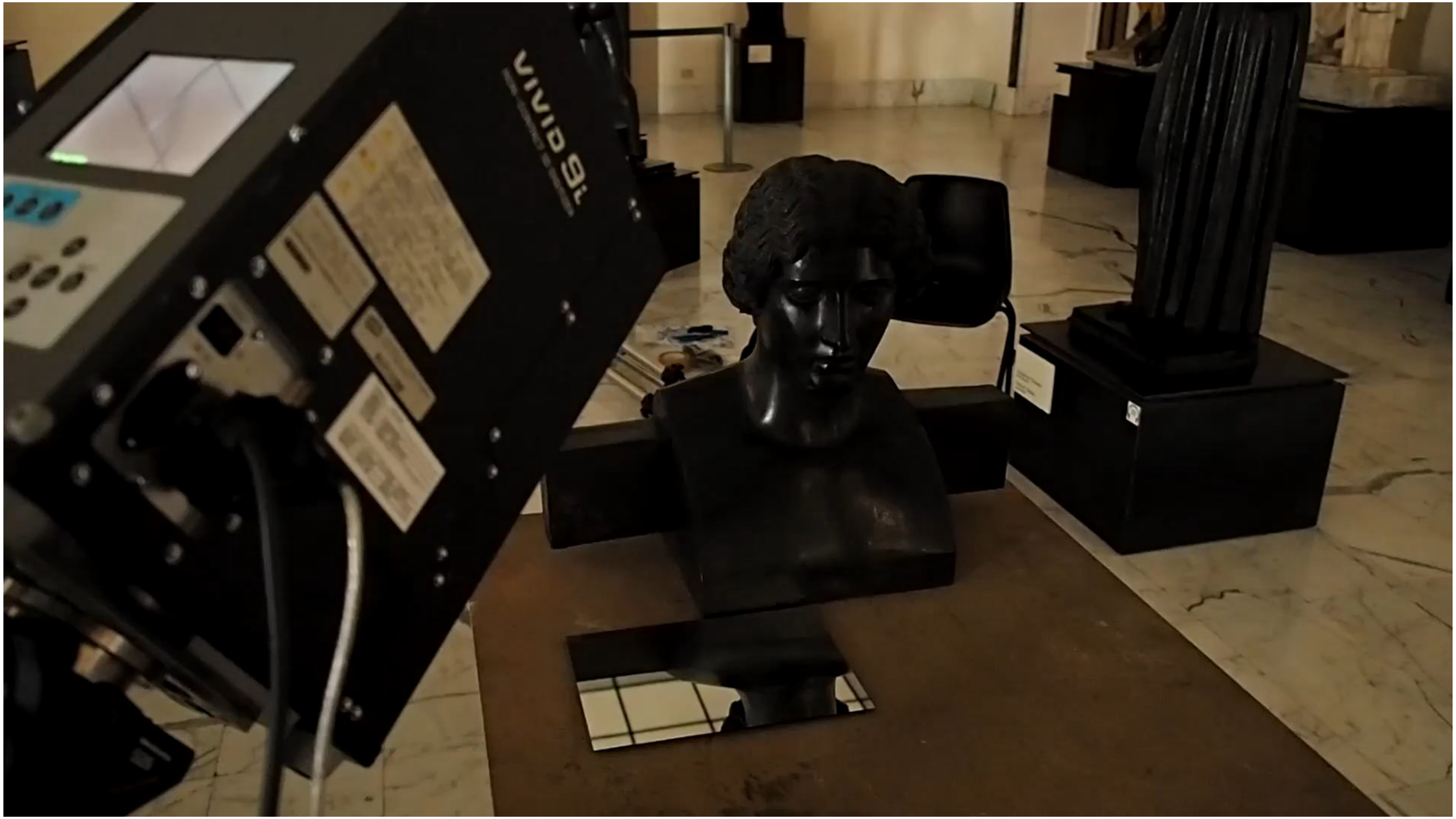
VIVID 9i

Measured Data

Issue of triangulation methods

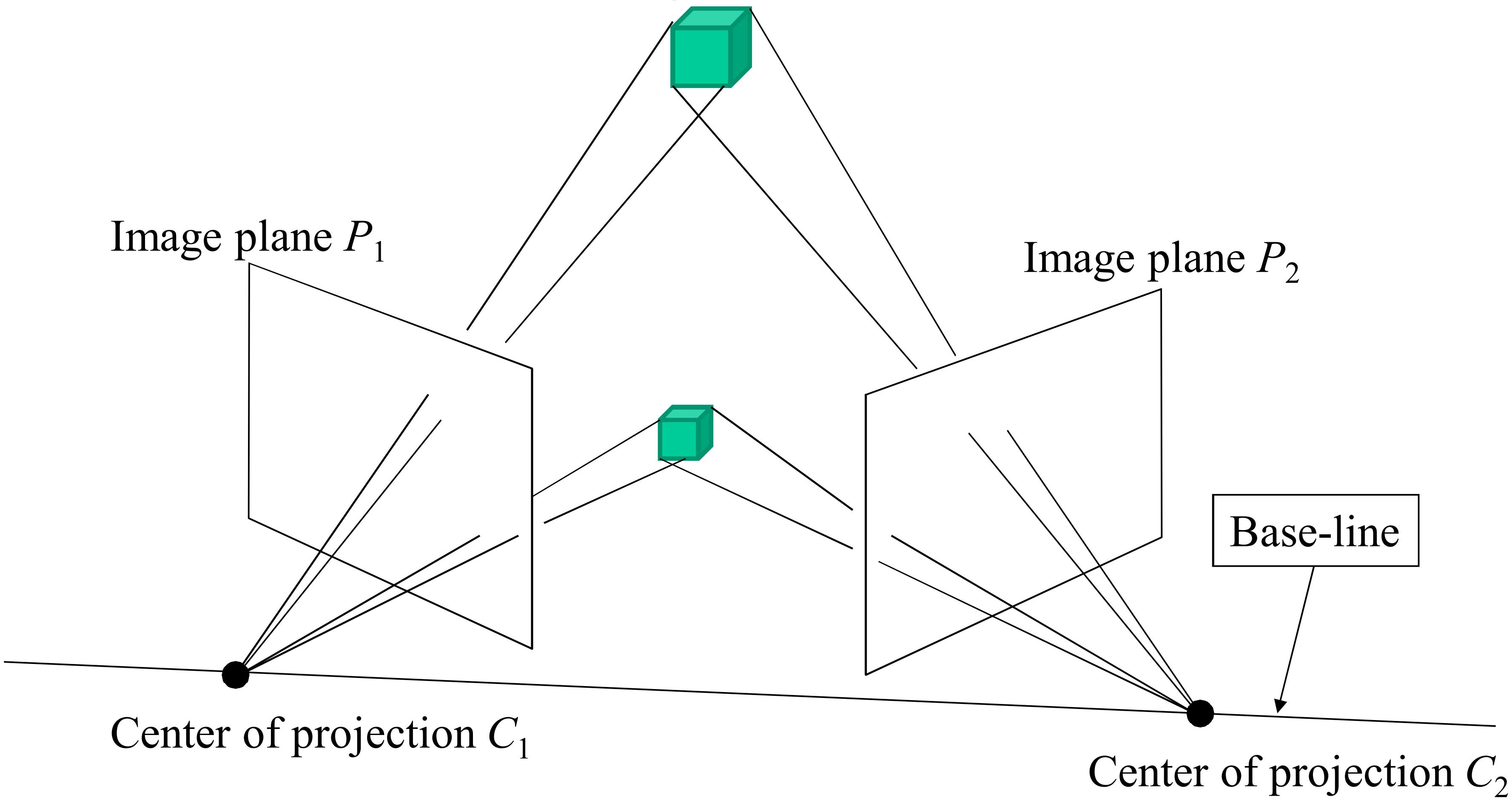

Distance <-->Accuracy

Time-of-flight (TOF)

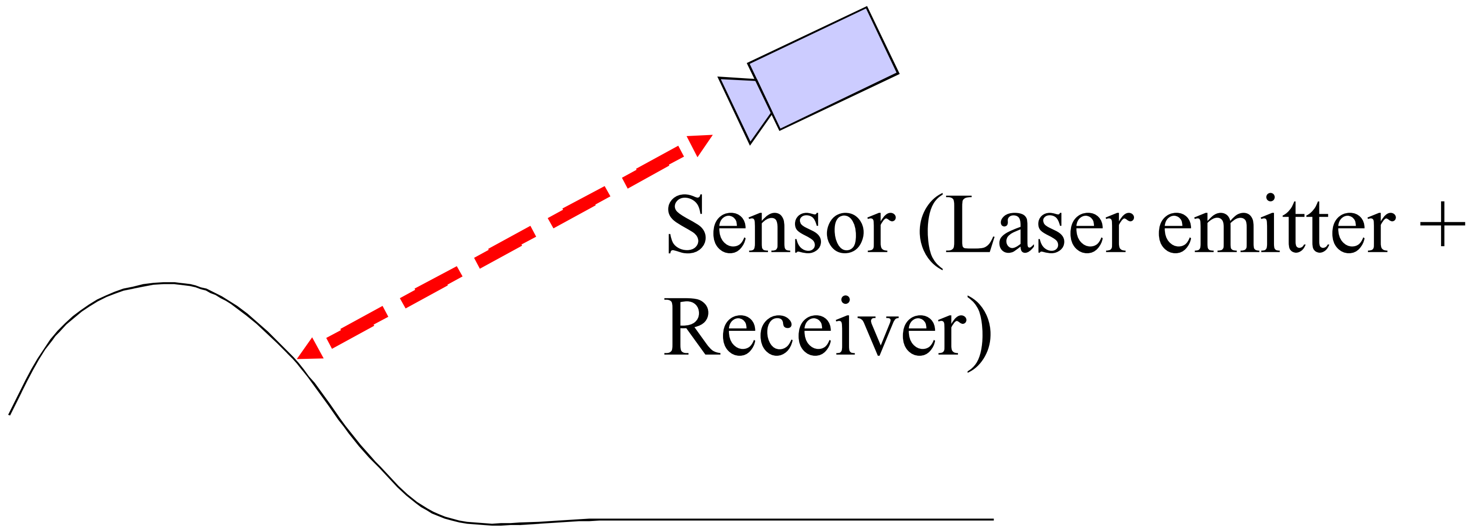

Time to travel ➡ Distance

Scanning mechanism

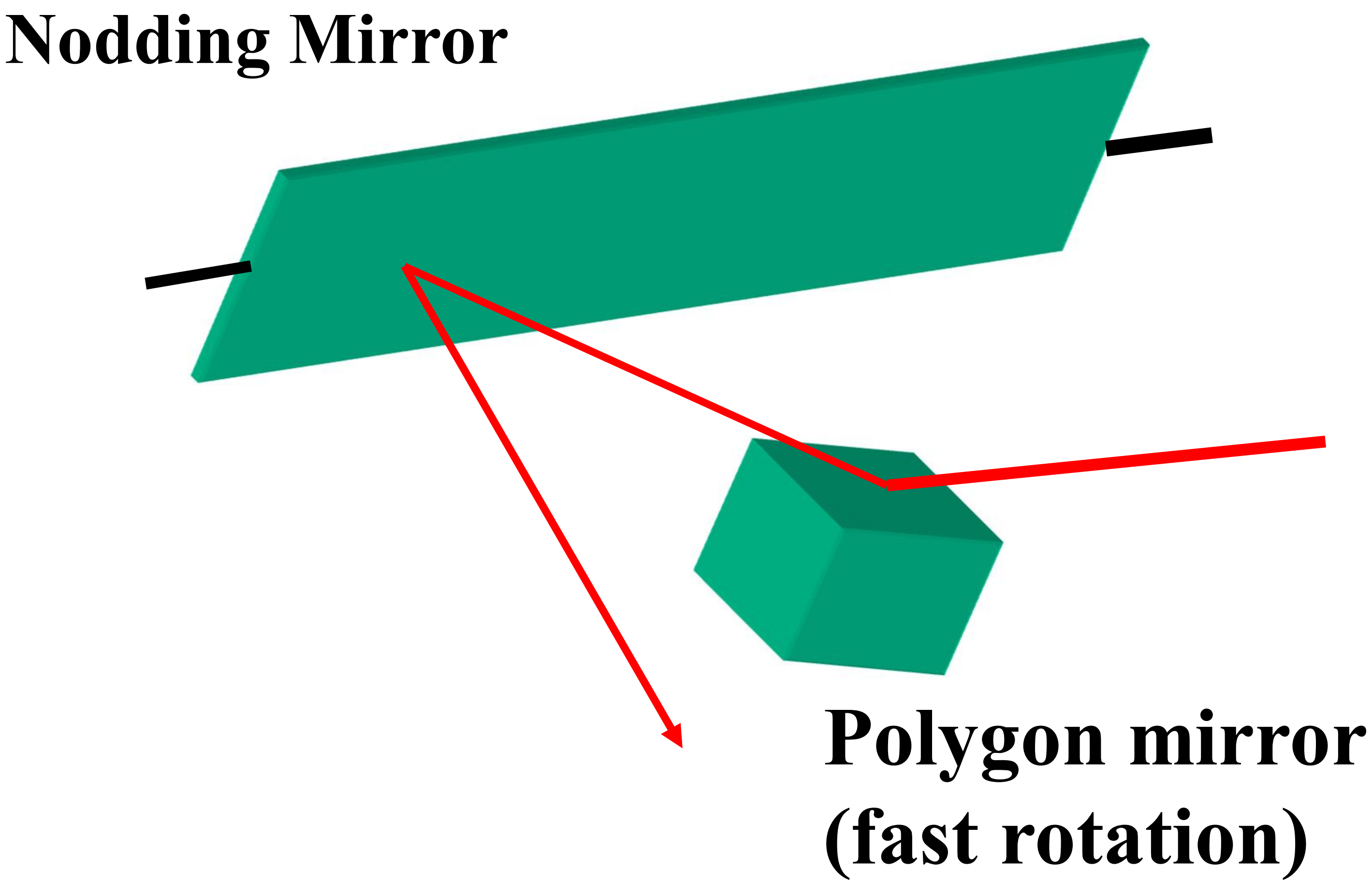

Scan Station C10 (Leica geosystems)

- Range: 0.1-300m
  - – 360 x 270 degrees
- Accuracy: 6mm (Depth: 4mm)
- Speed: 5,0000 pt / sec
- Laser class: 3R

Measured data (Cyrax)

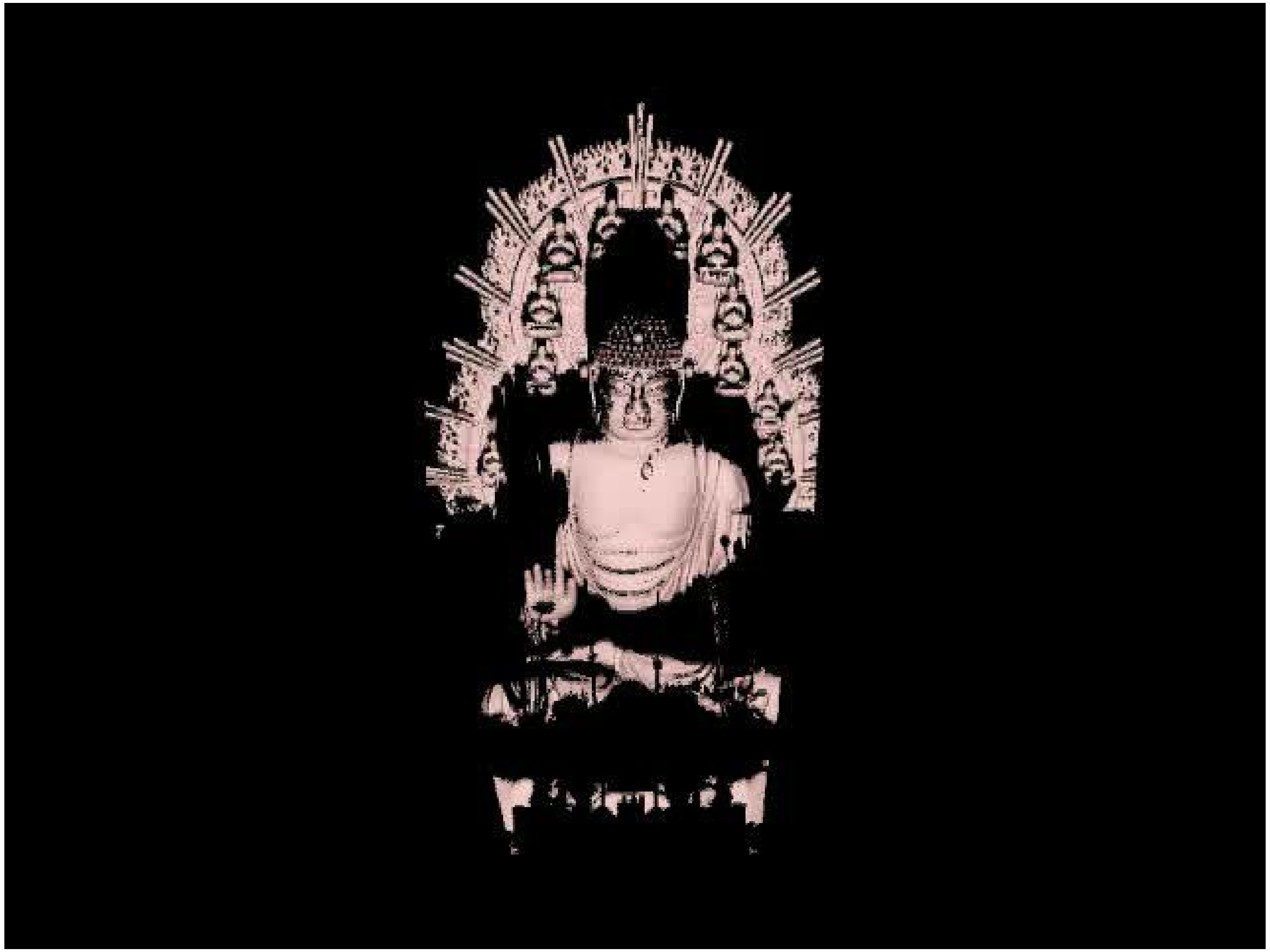

Phase shift method

Amplitude Modulation

$$D = (\lambda/4\pi)\,\Delta\Phi$$

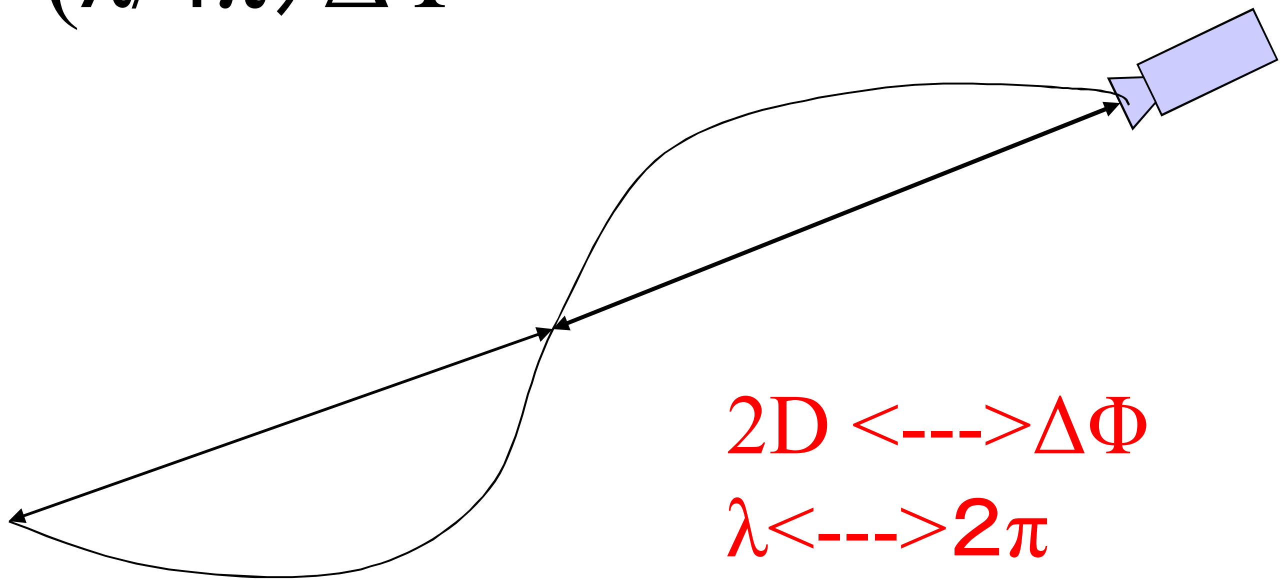

$2D <---> \Delta\Phi$

$\lambda <---> 2\pi$

Imager5003（Z+F）

- Range :   - 187.3m
  :   310° (v) × 360° (h)
- Accuracy: 0.4 - 1.6mm
- Speed :   1,000,000 pt/sec

- Phase shift method
  (Amplitude modulation)

Measured data (Imager)

Velodyne LiDAR

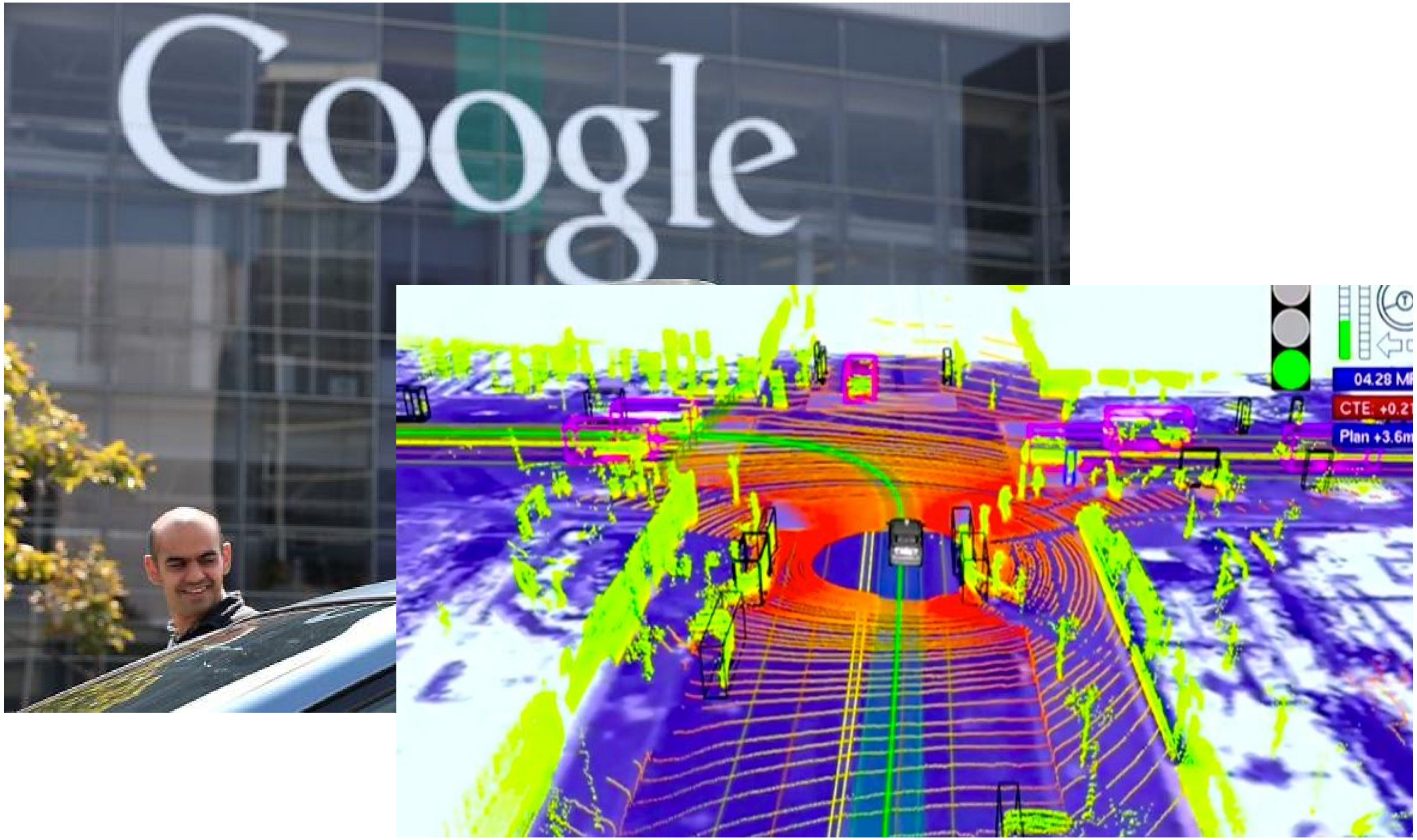

Climbing Sensor

-- Narrow Corridors – [Ono et al.]

Balloon sensor

[Banno et al.]

2. ALIGNMENT (REGISTRATION)

Modeling procedures

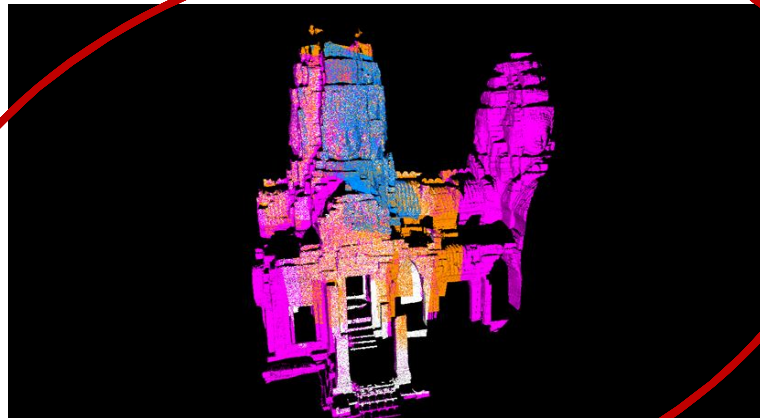

1. Data acquisition

2. Alignment

3. Merging

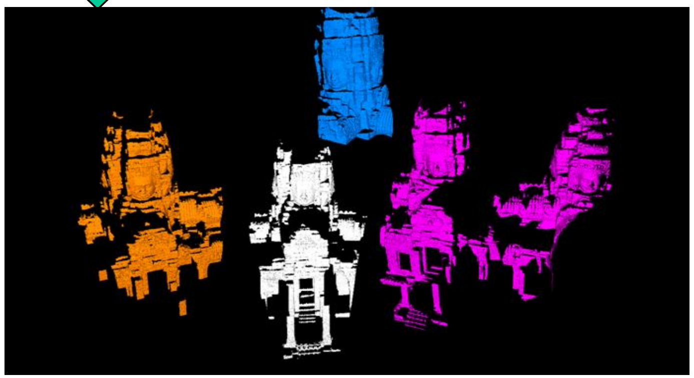

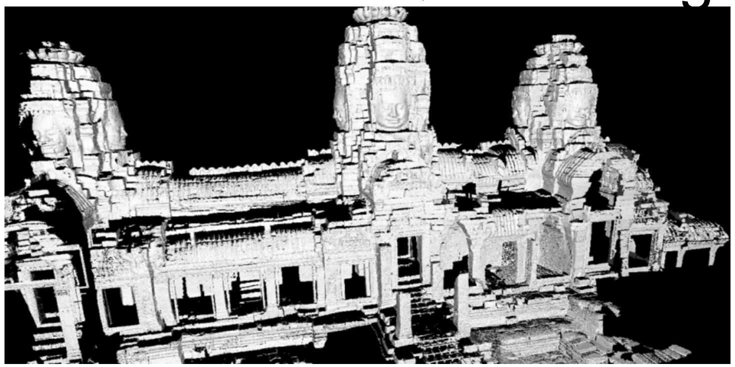

Alignment of range images

- Estimation of relative positions

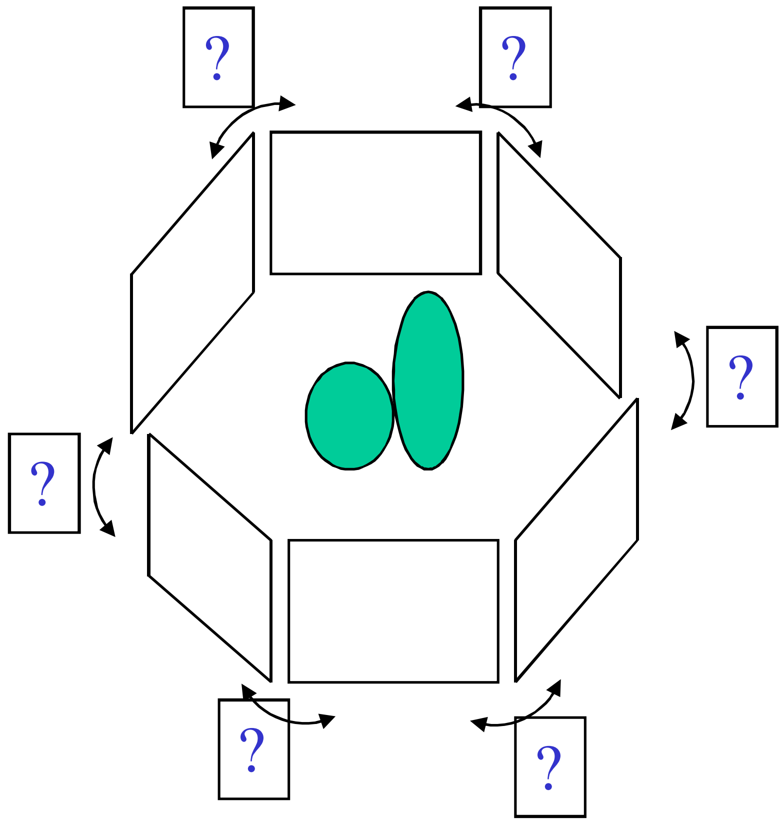

Self positioning

GPS measurement

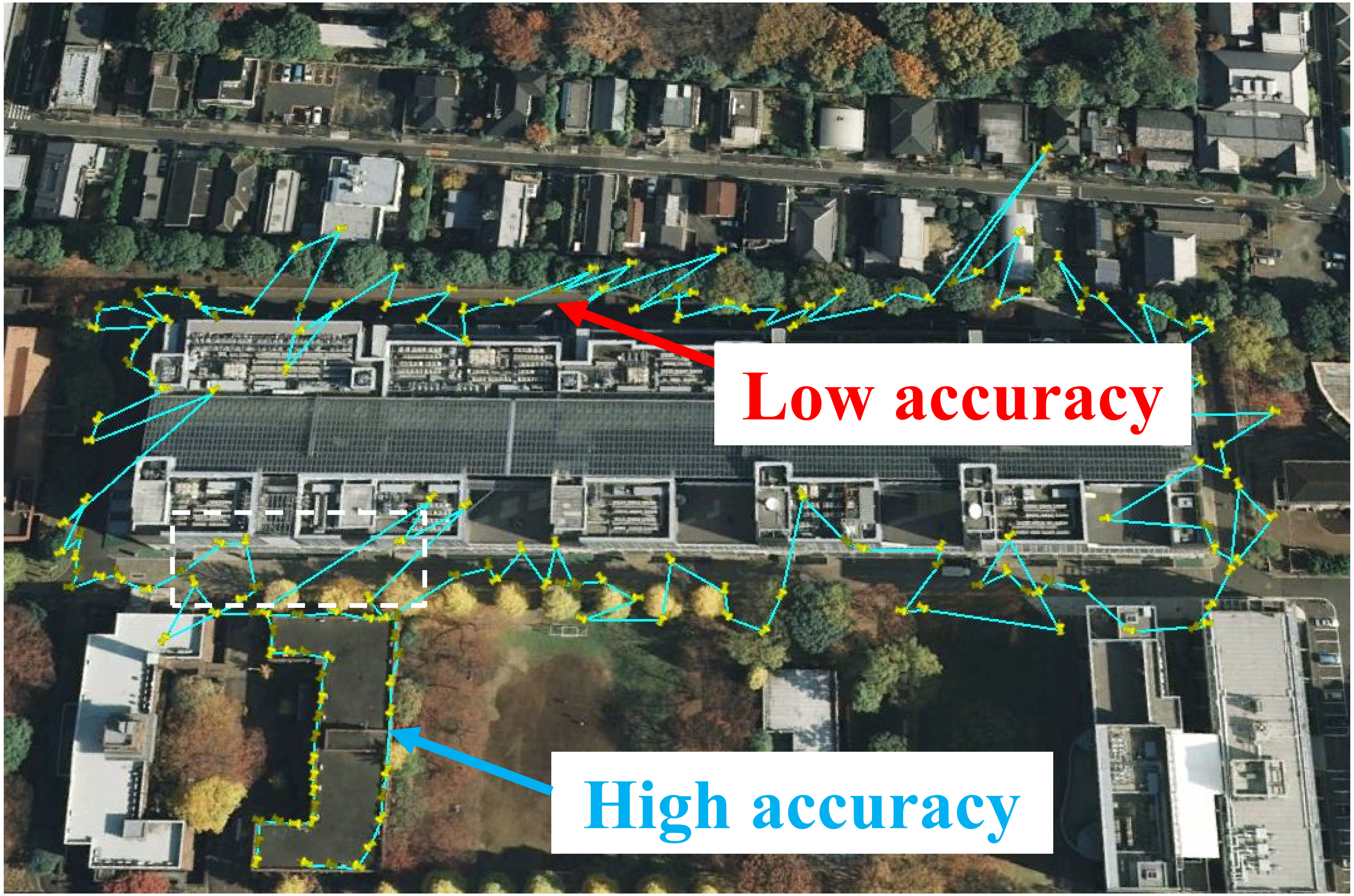

3D laser measurement system for large scale architectures using multiple mobile robots

R. Kurazume, Y. Tobata, Y. Iwashita,
and T. Hasegawa

Kyushu University

3D measurement of large scale architectures

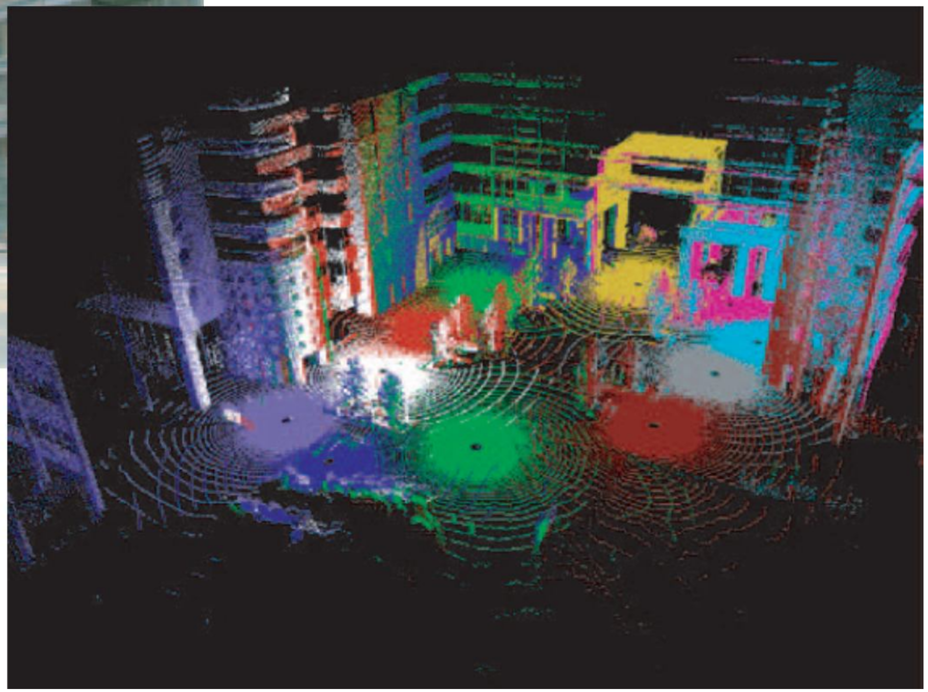

Alignment of multiple range images

- Post-processing
  - ICP algorithm etc.
    - Requires initial positions: Laborious & time consuming
- Directly measuring positions
  - GPS (RTK, VRS)
    - Limited to outdoor environment & low accuracy

Proposed method

- Cooperative Positioning System (CPS)
  - Multiple mobile robots
  - Measurement devices of mutual positions

Positioning method

- Odometry (Wheel encoder, Acceleration sensor)
  - low accuracy
- Landmarks (Camera, Range sensor)
  - require prior knowledge
- GPS
  - outdoor only

Cooperative Positioning System

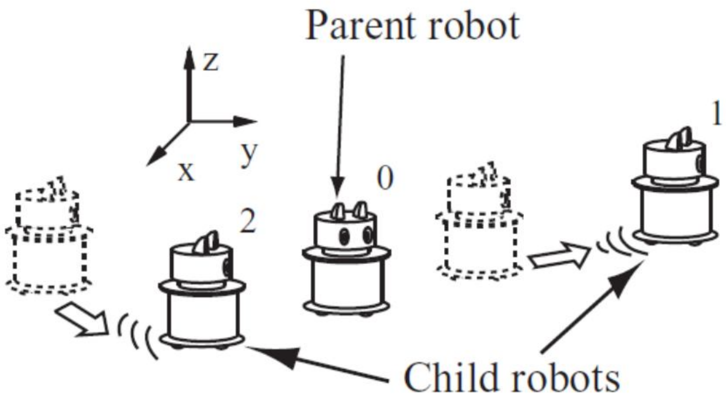

(1) Robot 1 and 2 move.

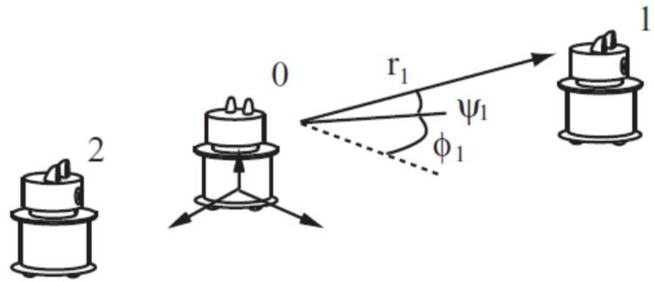

(2) Robot 0 measures the position of robot 1.

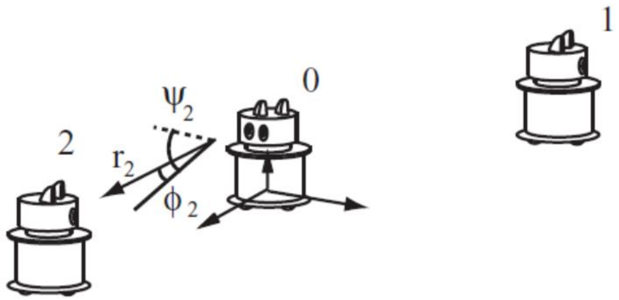

(3) Robot 0 measures the position of robot 2.

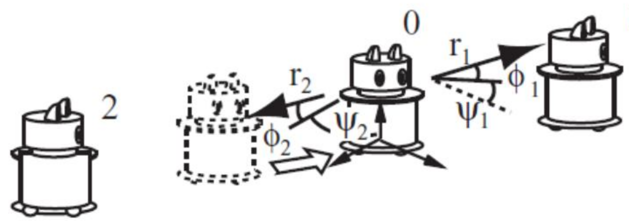

(4) Robot 0 moves and measures the position of robots 1 and 2.

Measurement system with CPS V

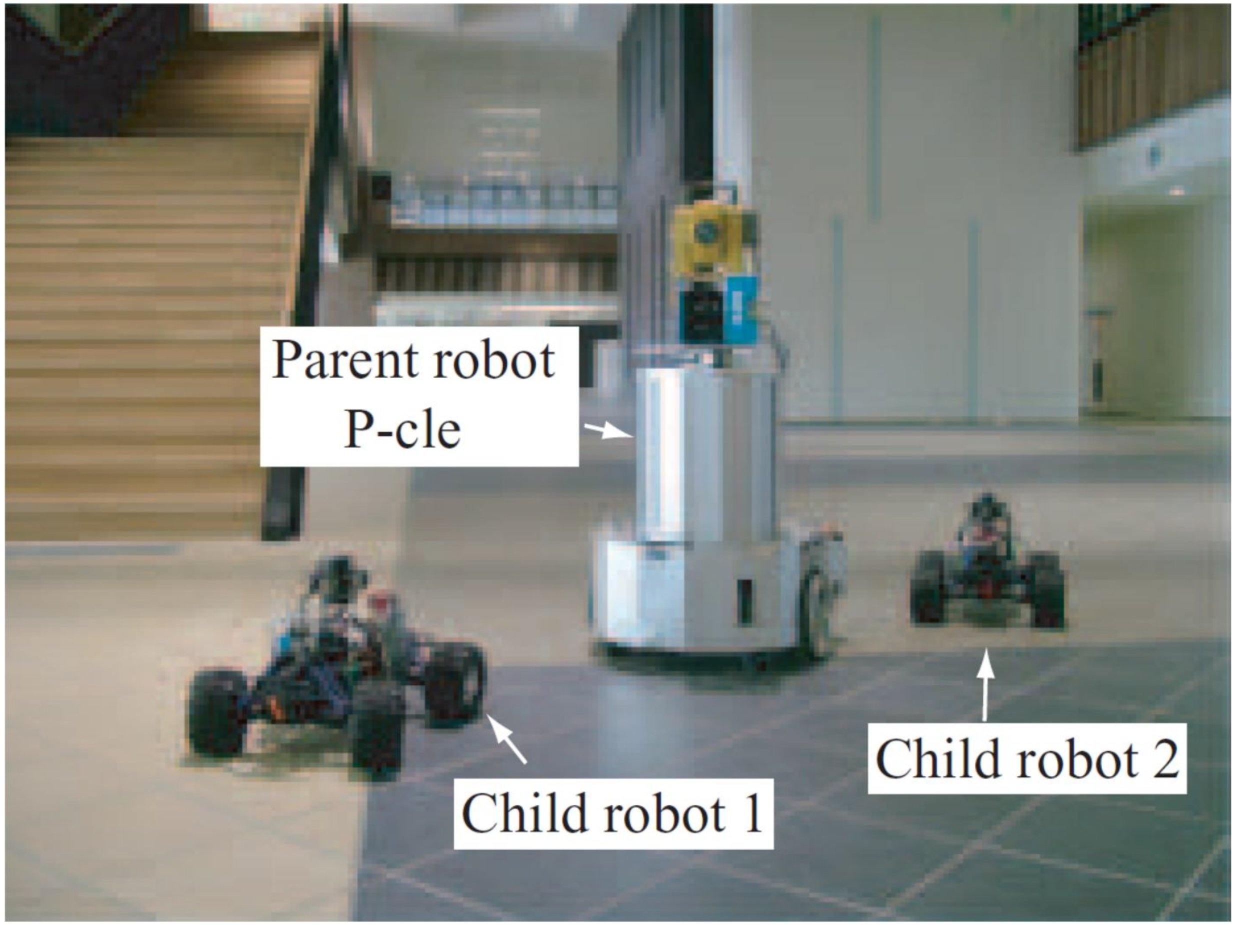

Parent robot (P-cle)

- 3D measurement: Rotating table + 2D laser range sensor
- Position:
  Total station
- Measurement time:
  37.8 sec

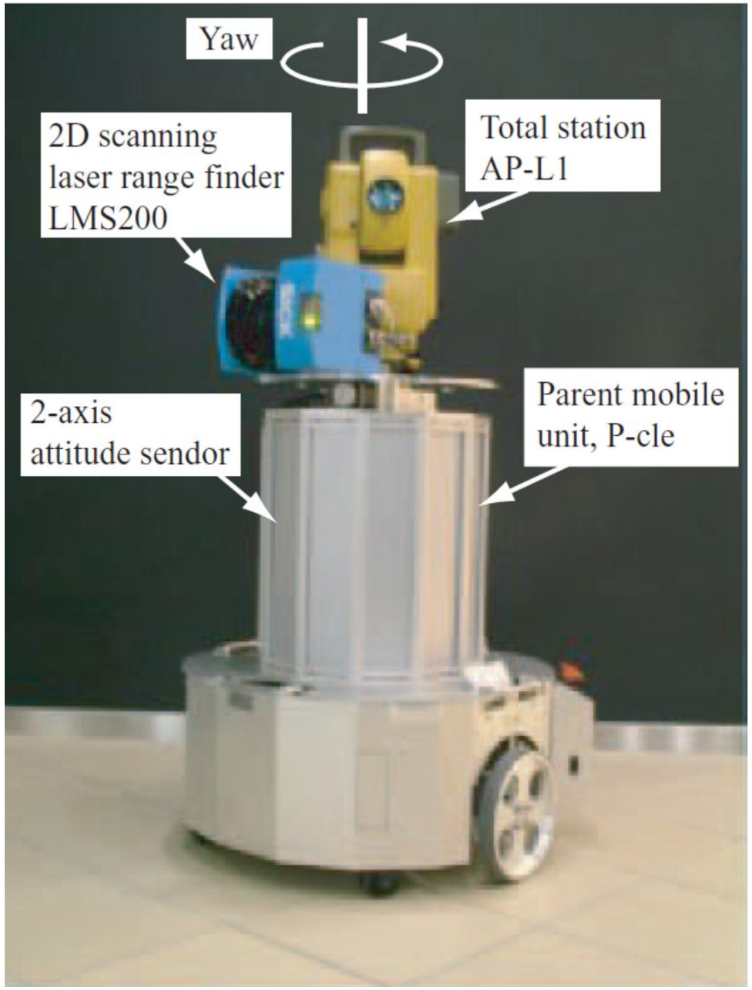

Child robot

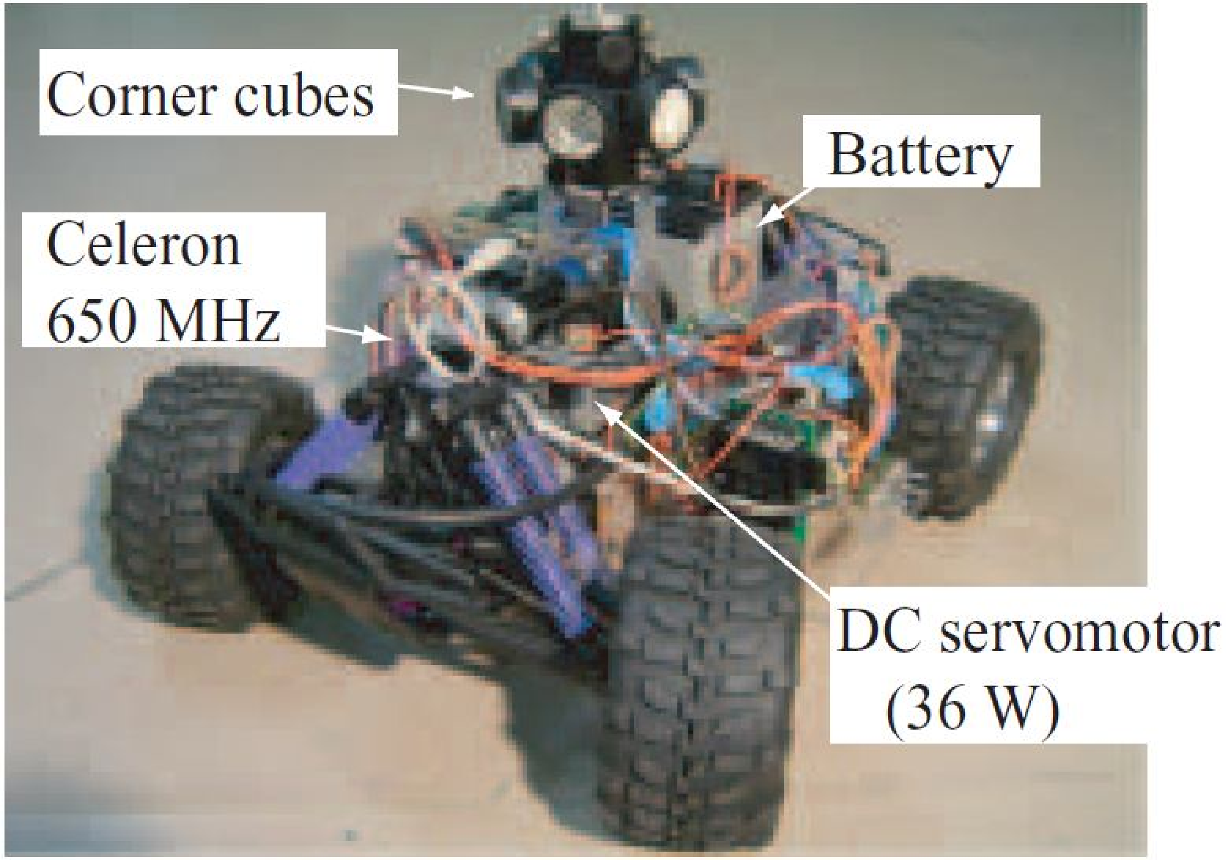

Experimental result

Experimental result

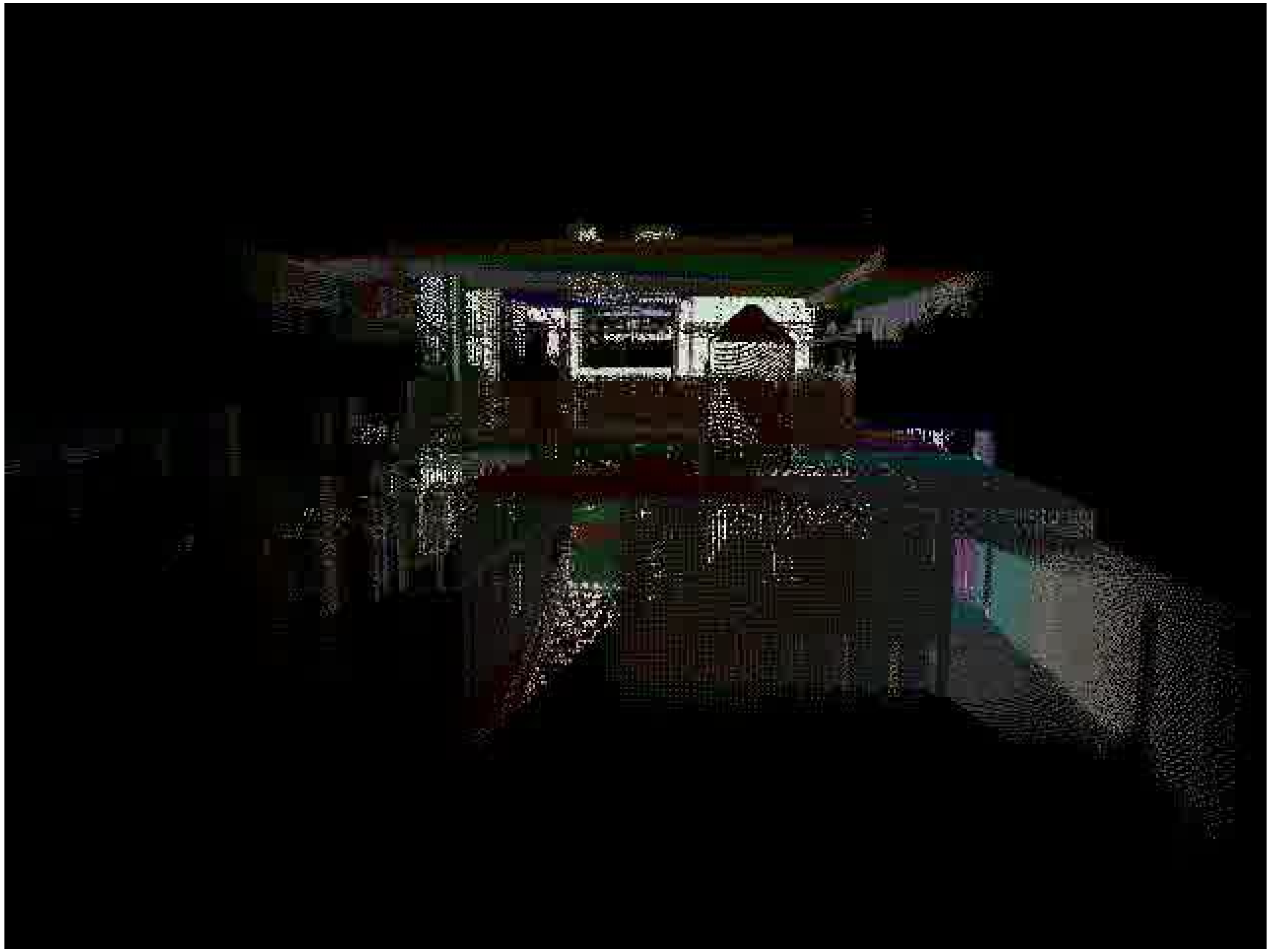

Experimental result

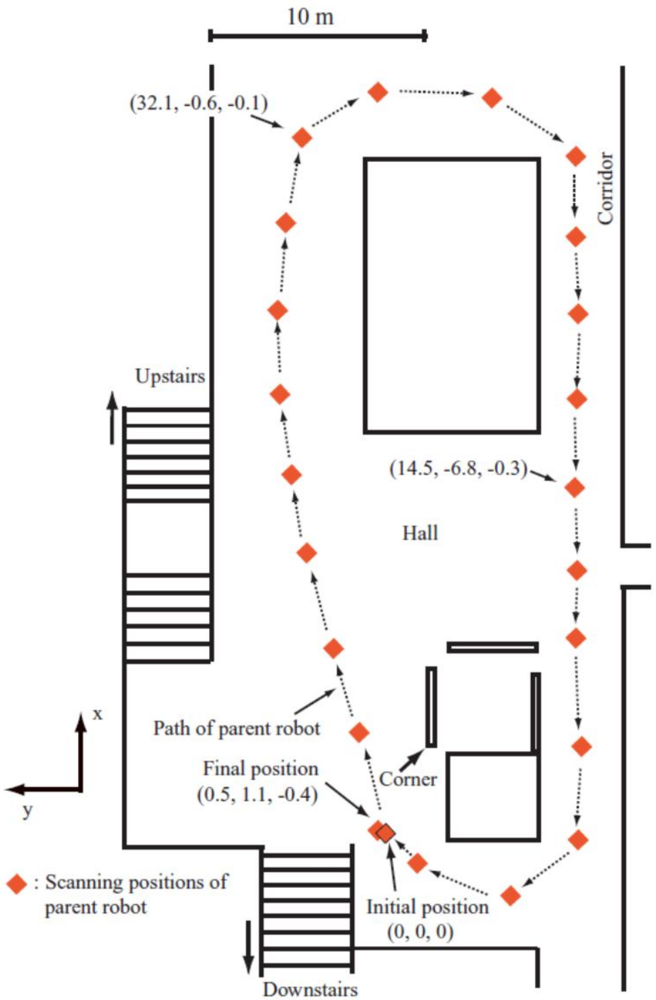

- Total distance: 86.21m
- Number of scans: 23
- Positioning error: 1.17m (1.36%)

Alignment

- Estimation of relative positions using overlapping areas

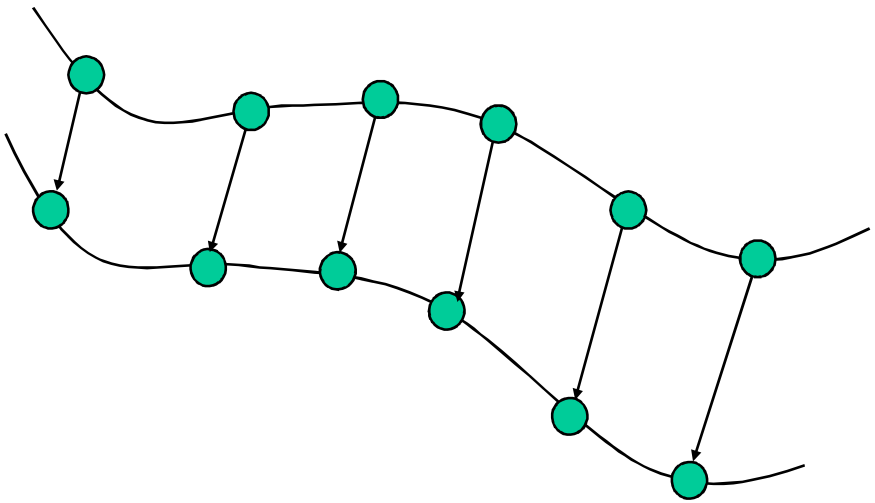

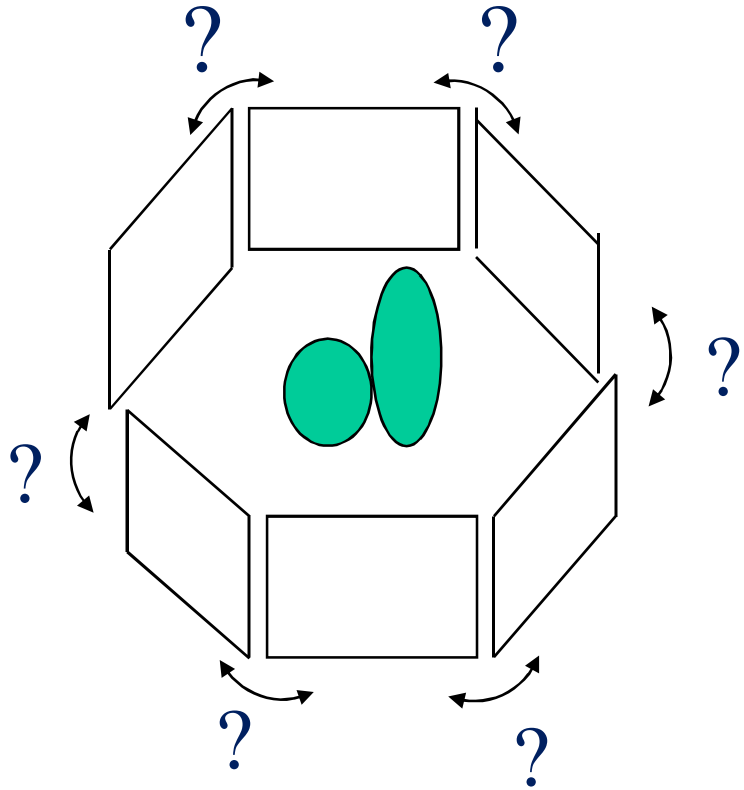

Category of alignment method

- With and without features
  - Global features (EGI, SAI), Local features (Spin image)
  - ICP (Iterative Closest Point), many extensions of ICP
- Pair-wise vs. Simultaneous
  - In order to avoid error accumulation, errors have to be globally minimized

Global features

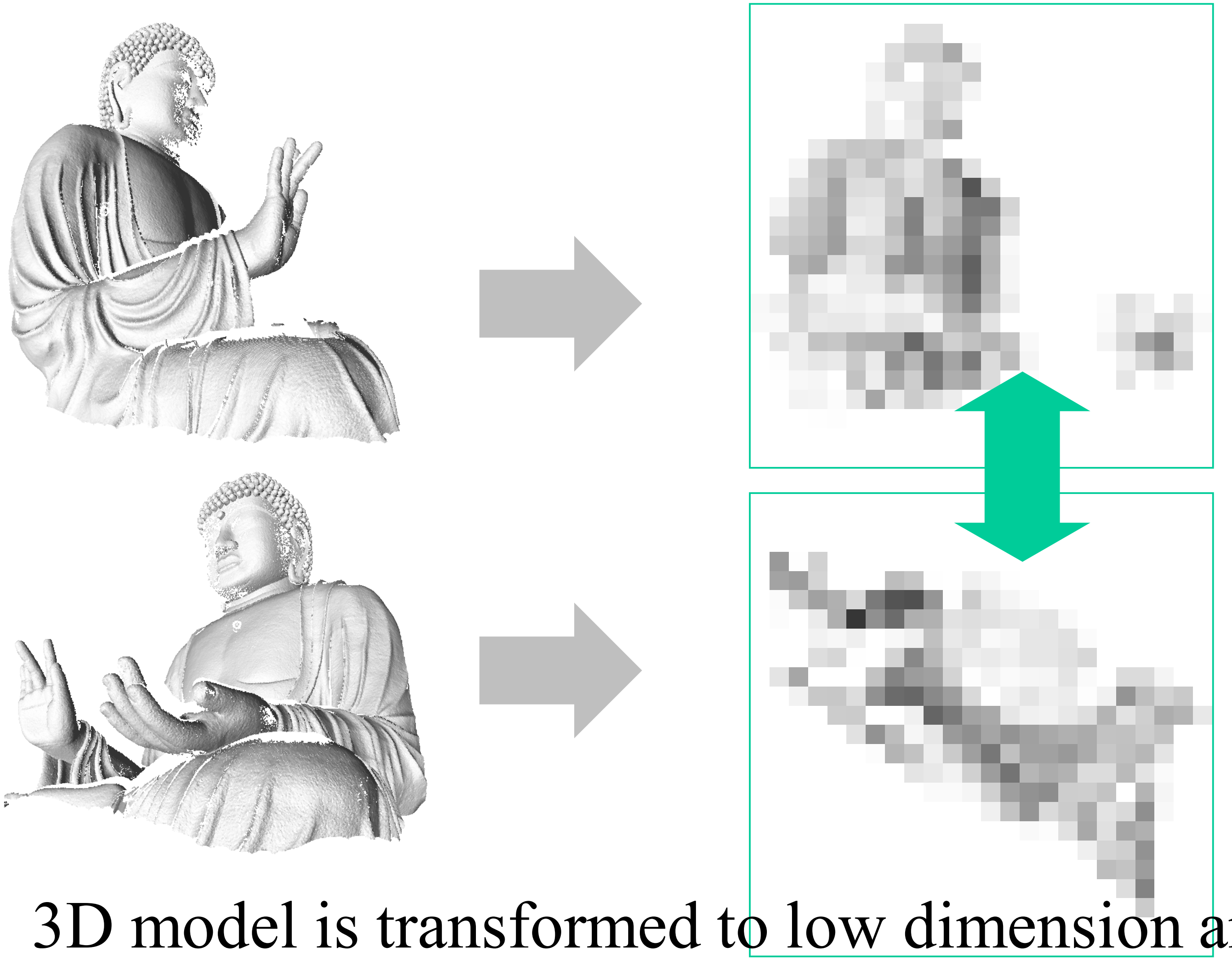

- 3D model is transformed to low dimension and rotation-scale invariant vectors

Extended Gaussian Image (EGI)

[Horn & Ikeuchi]

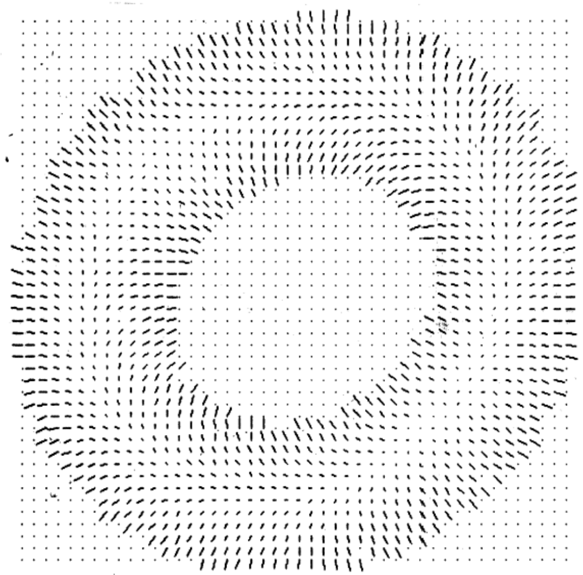

Needle map

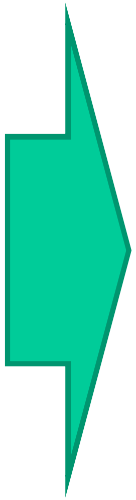

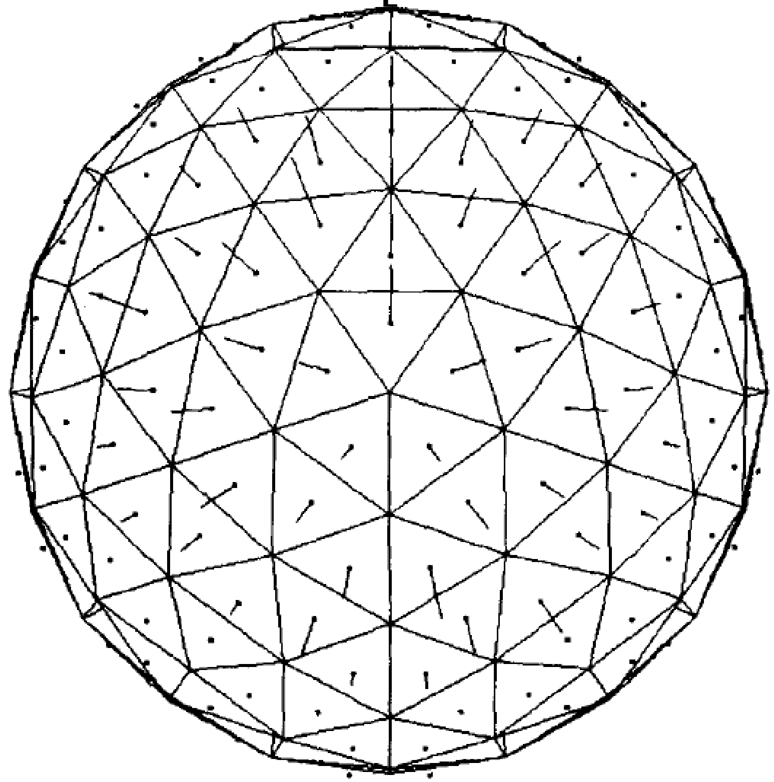

EGI (Geodesic dome)

Spherical Attribute Image (SAI)

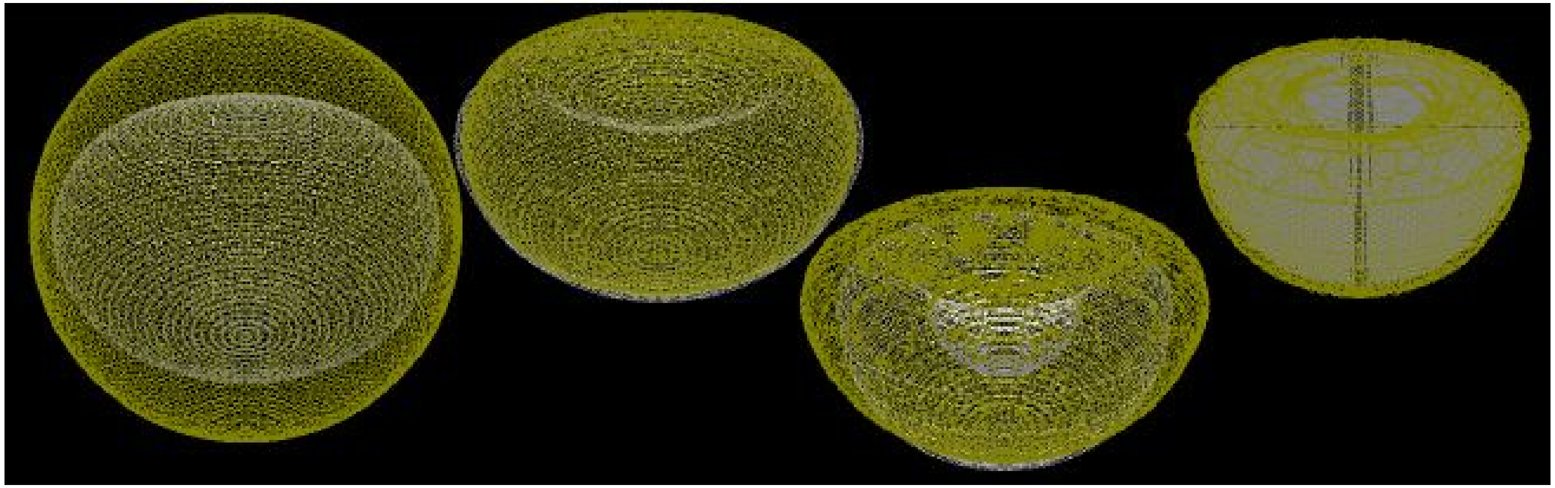

[Delingette et al. '93]

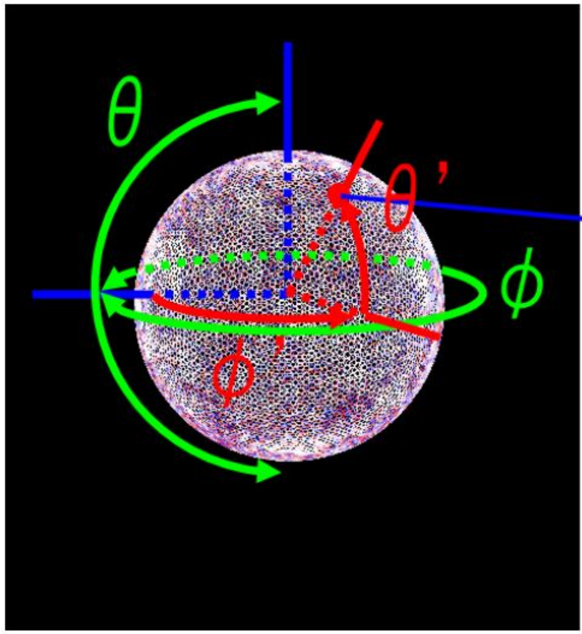

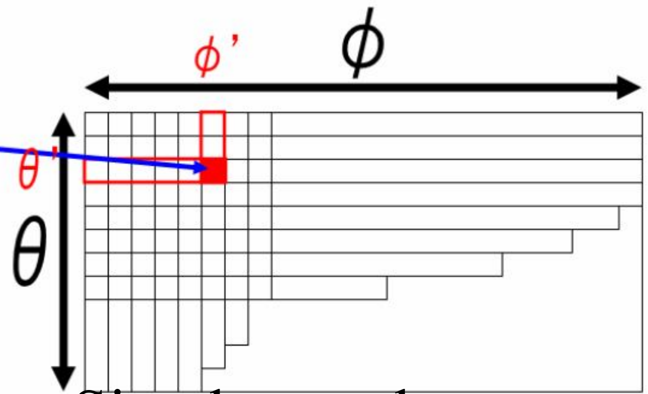

Simplex angle

Simplex Angle

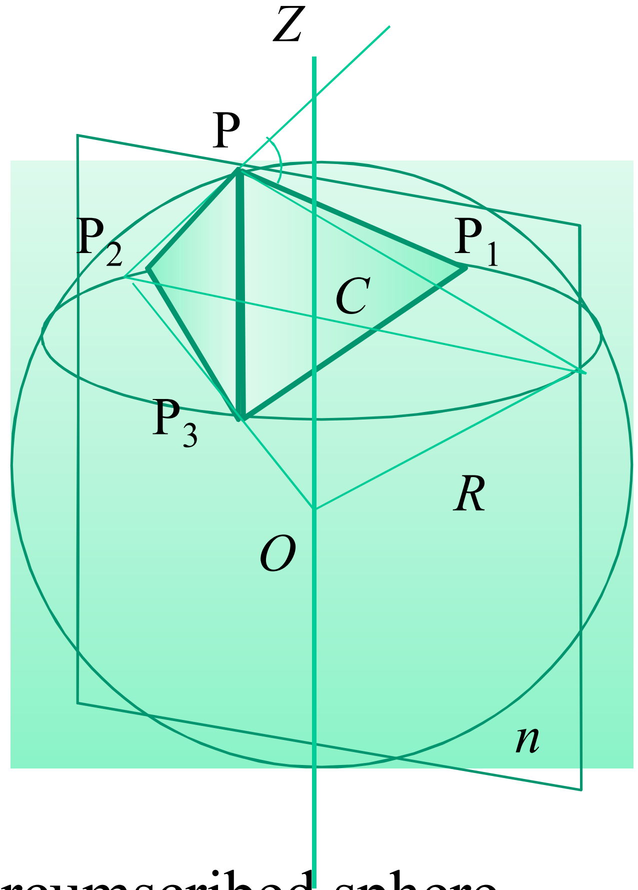

Circumscribed sphere

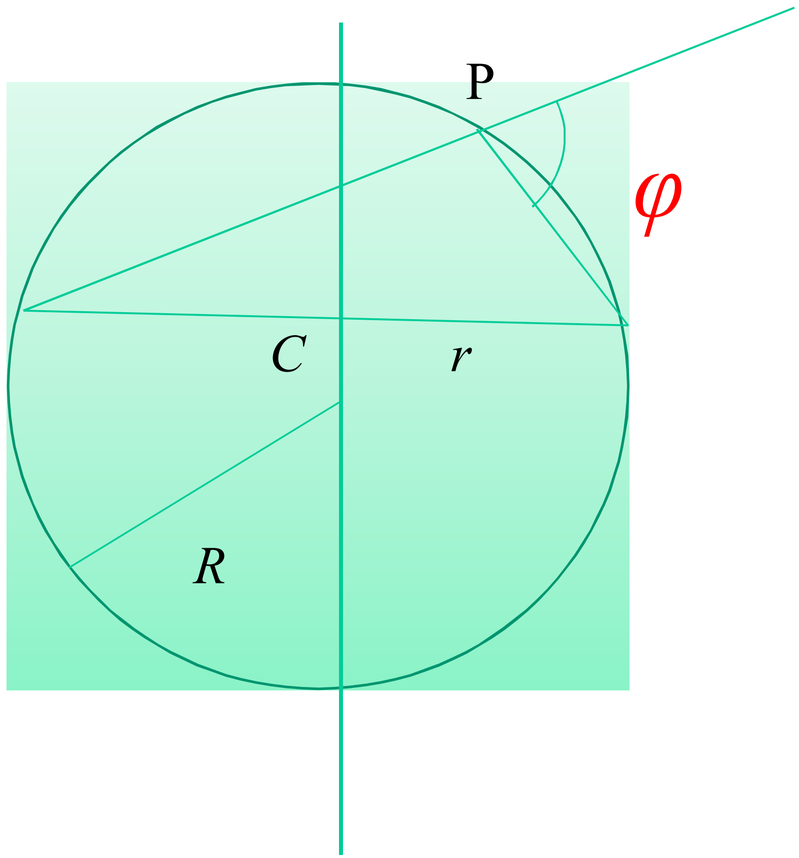

Rotation and Scale invariant

SAI matching

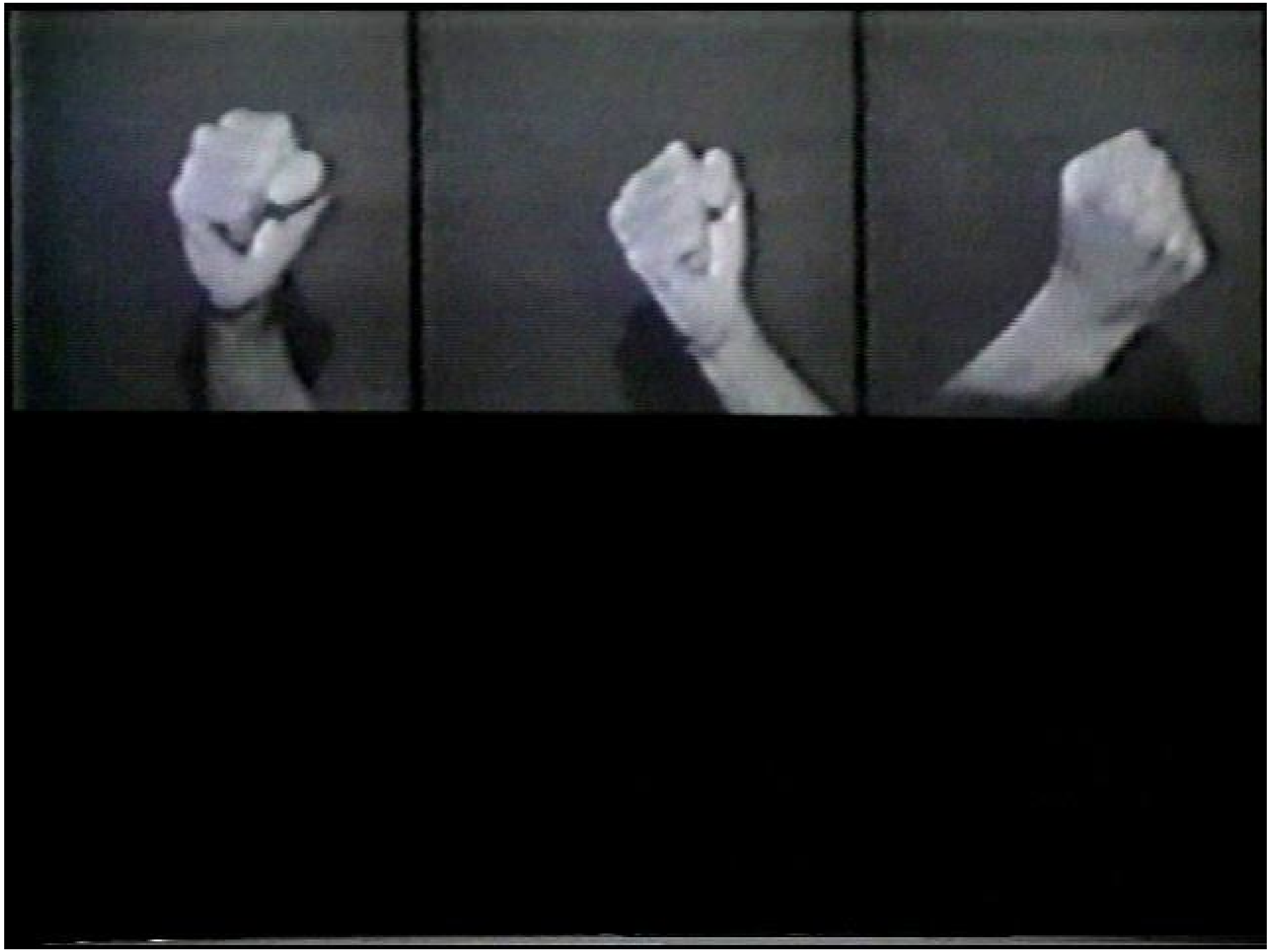

Local features

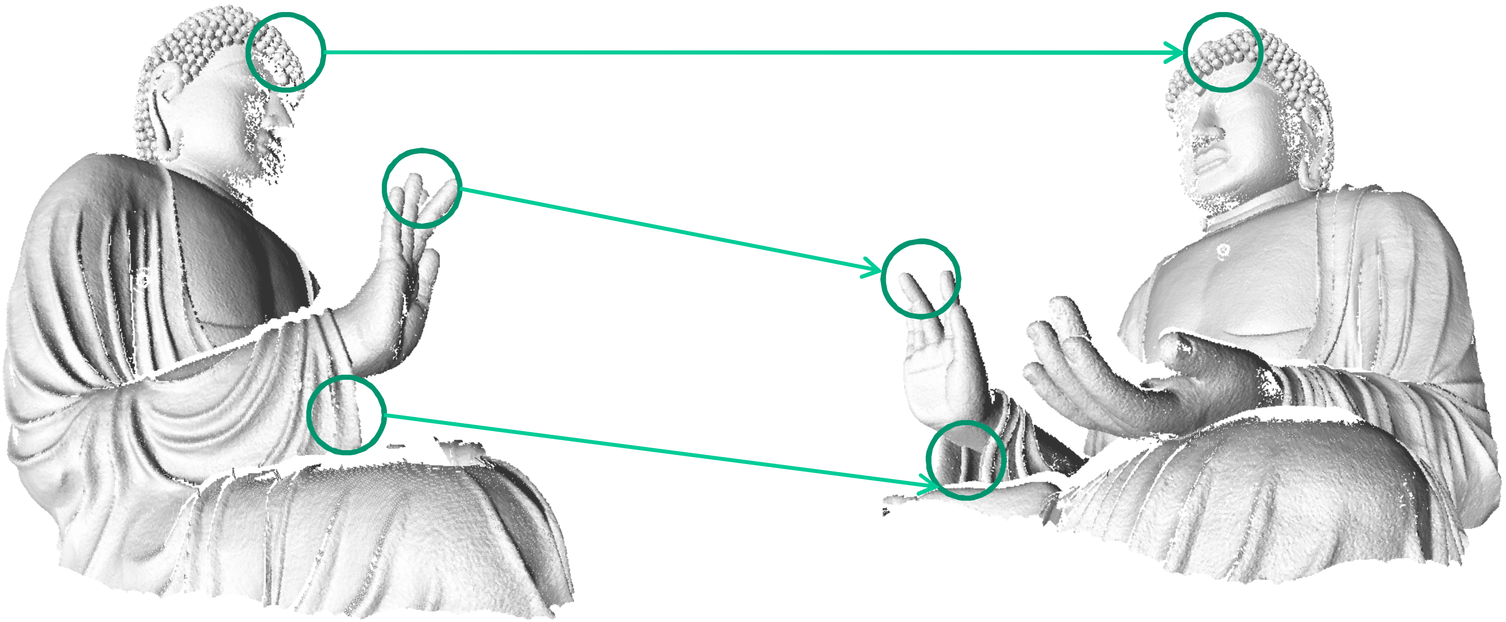

- Relative pose of two range images can be estimated from 3 or more matching points

Spin image

[Johnson & Hebert '96]

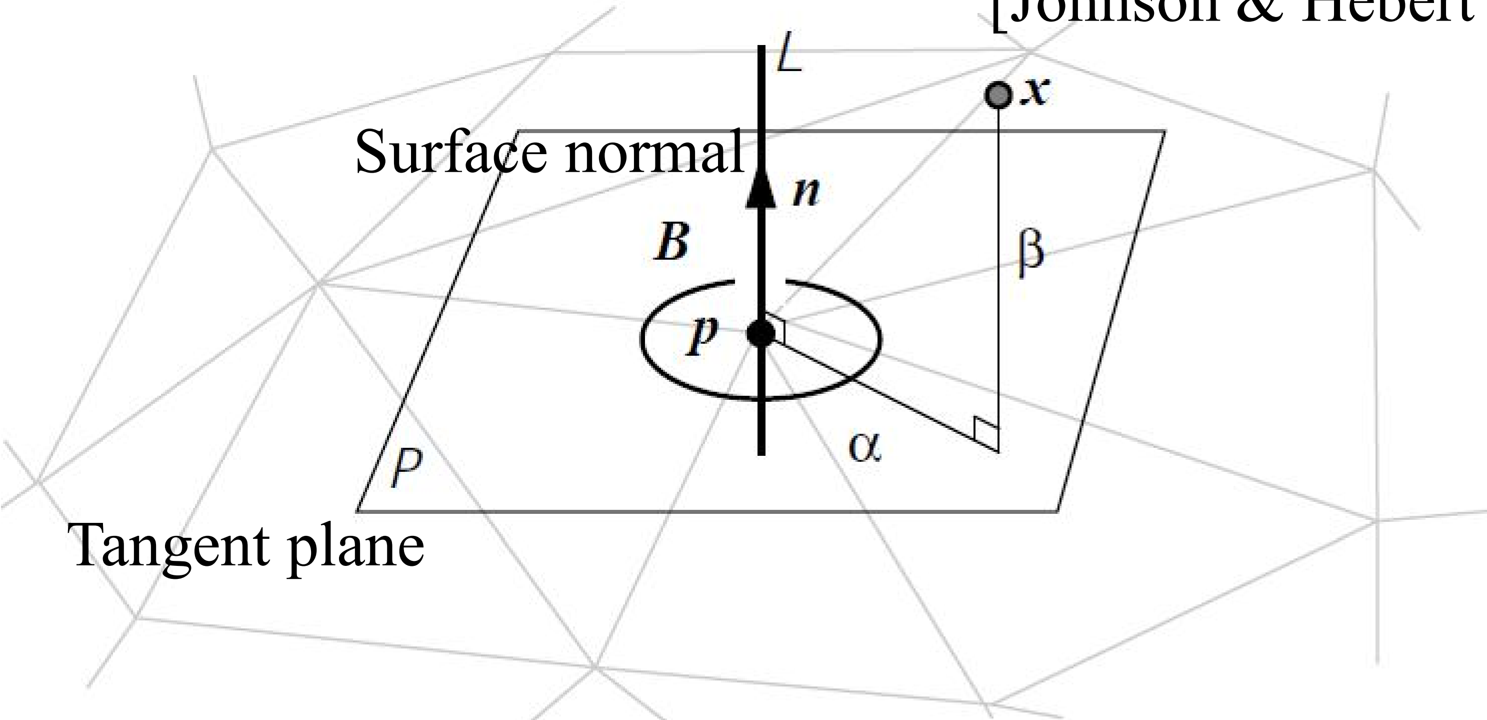

α: *the radial distance to the surface normal line L*

β: *the axial distance above the tangent plane P*

Rotation invariant

Spin image examples

[Johnson & Hebert '96]

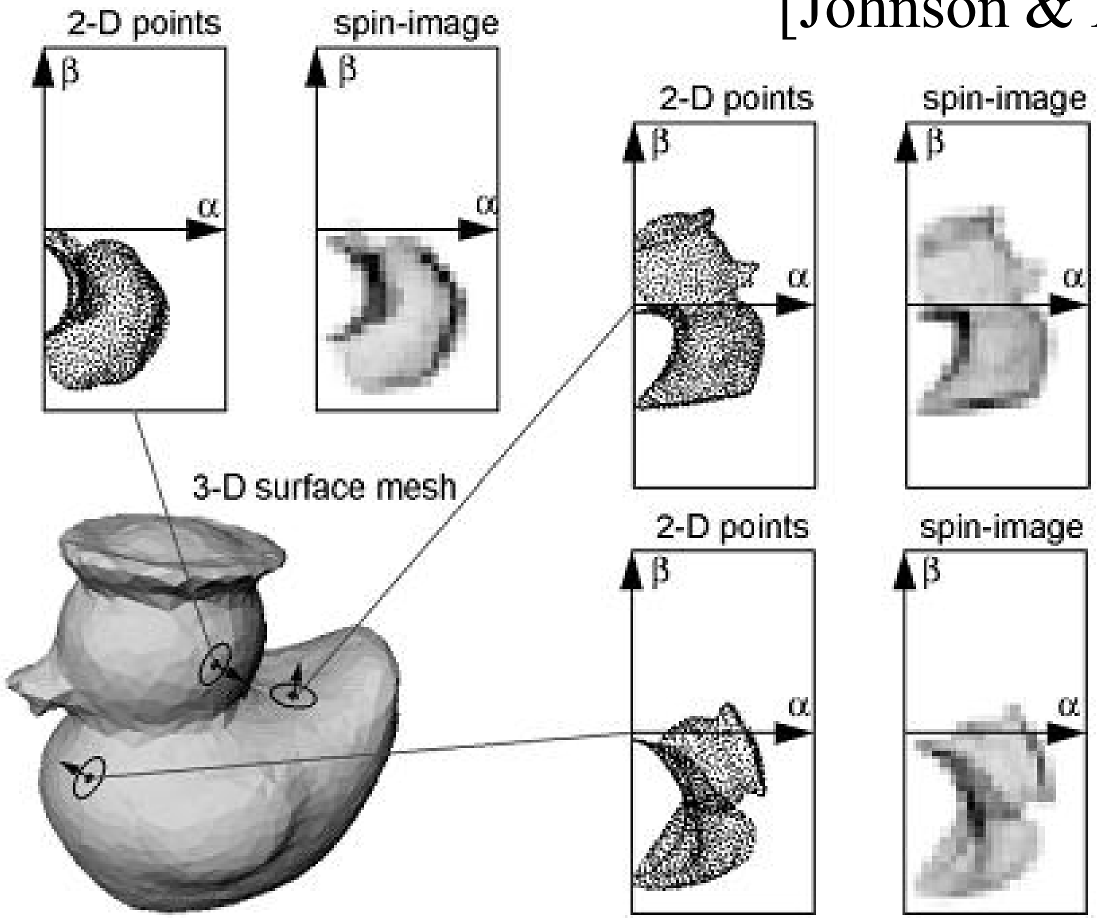

Matching result by Spin image

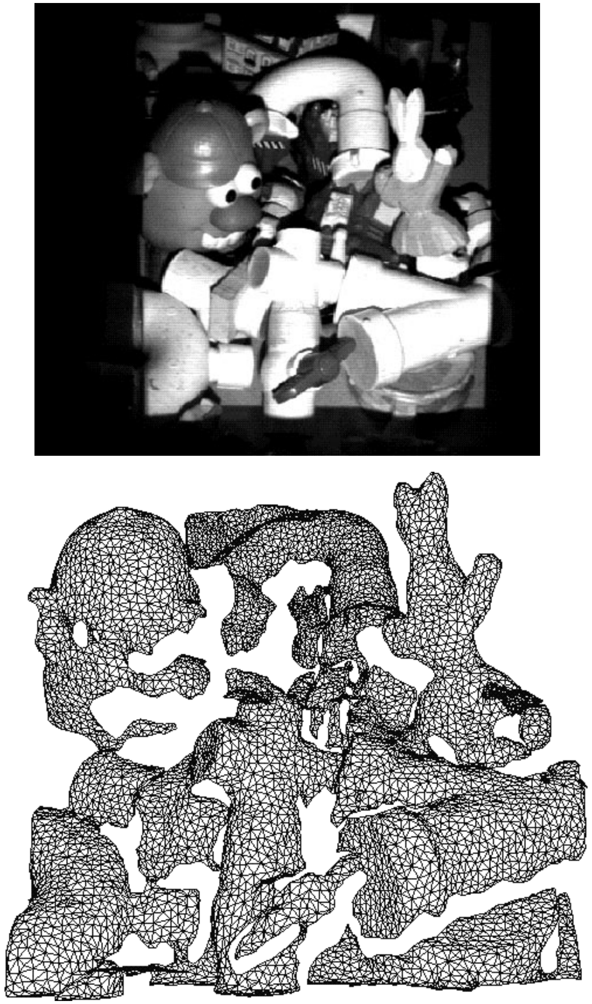

Range image

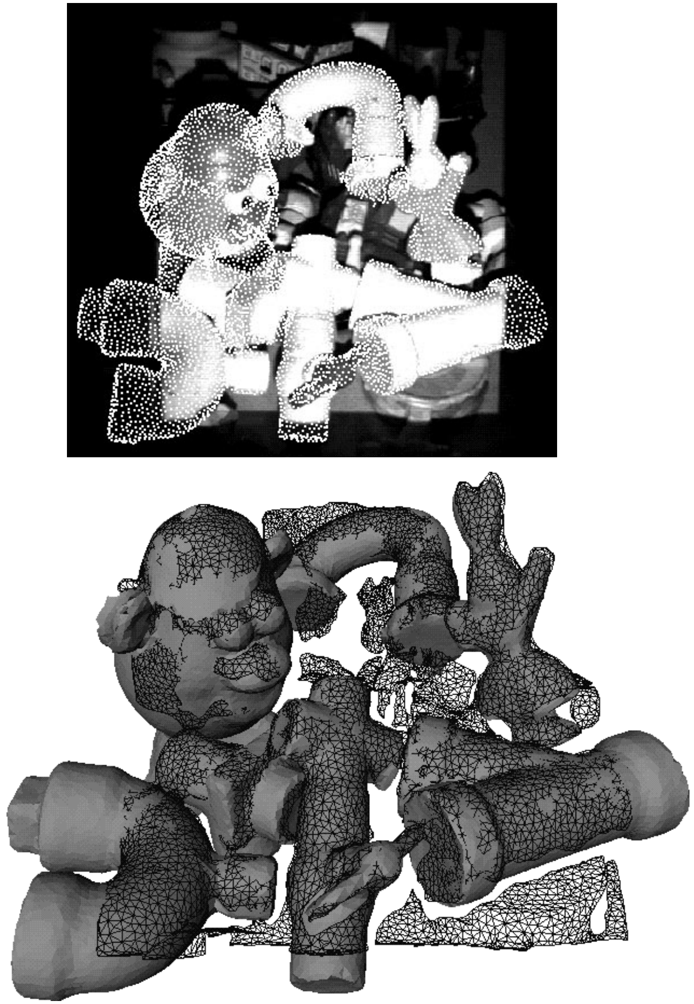

Recognition result

ITERATIVE METHOD

Alignment method without features

- Iterative Closest Point (ICP) [Besl et al. '92]

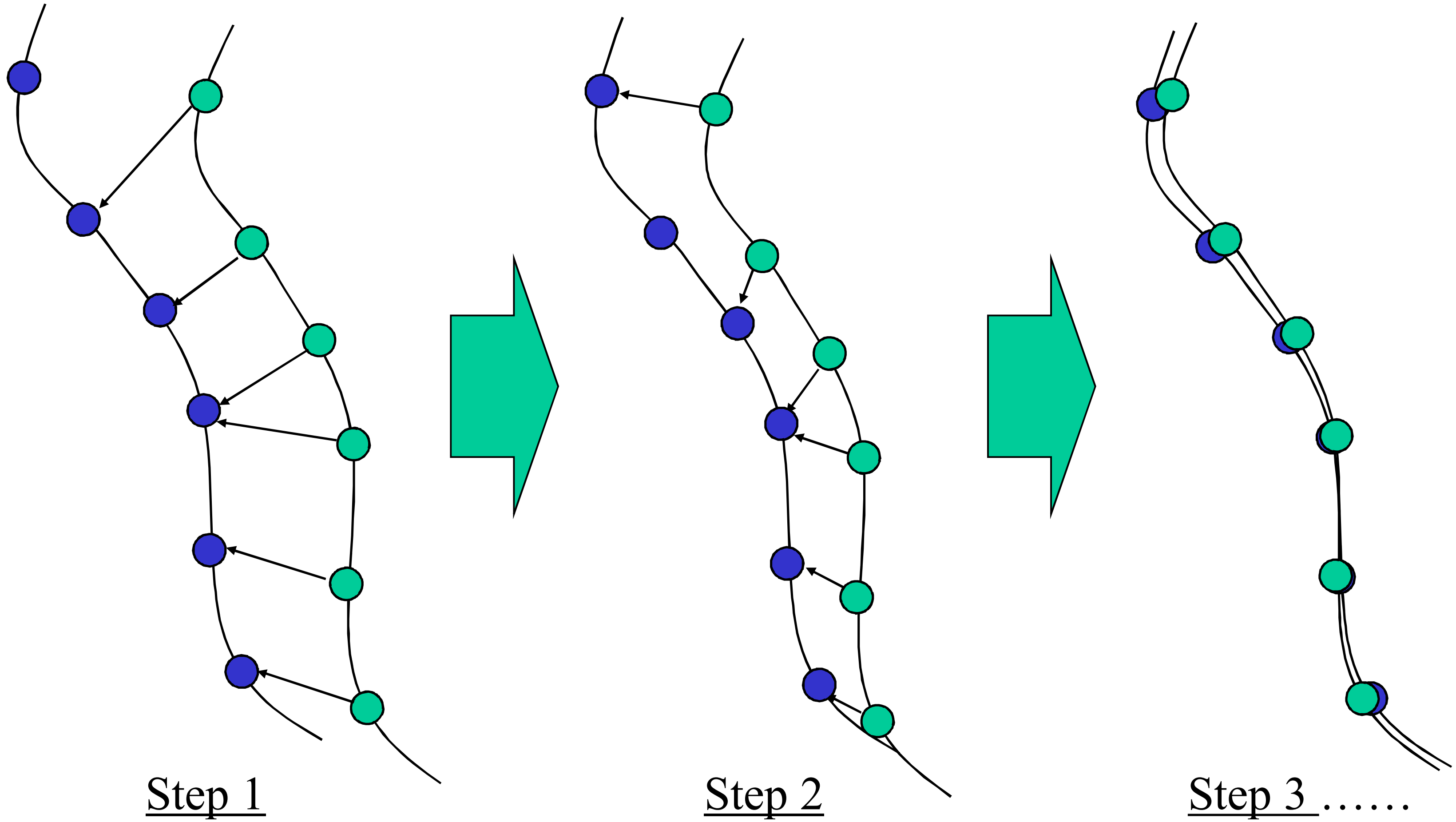

Procedures of ICP

1. Find corresponding (nearest neighbor) points between 2 range images
2. Take sum of the errors between correspondences
3. Compute transformations so as to minimize the error

- Iterate the processes until termination criteria is fulfilled

ICP variants

[Rusinkiewicz et al. '01]

1. Selecting source points
2. Finding corresponding points
3. Weighting the correspondences
4. Rejecting certain (outlier) point pairs
5. Assigning an error metric to the current transform
6. Minimizing the error metric

1. SELECTION OF SOURCE POINTS

Selection of source points

- All points [Besl et al. ‘92]
- Uniformly sampled points[Turk ‘94]
- Randomly sampled points [Masuda ‘96]
- Normal vectors are uniformly distributed [Rusinkiewicz ‘01]

Normal space sampling

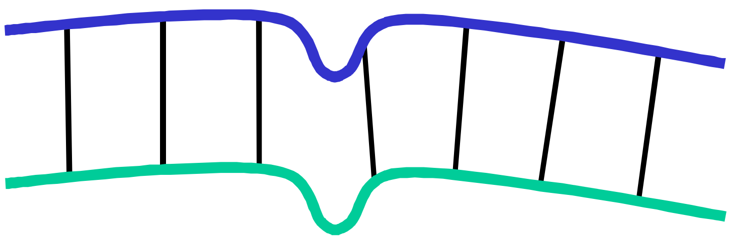

Uniform sampling

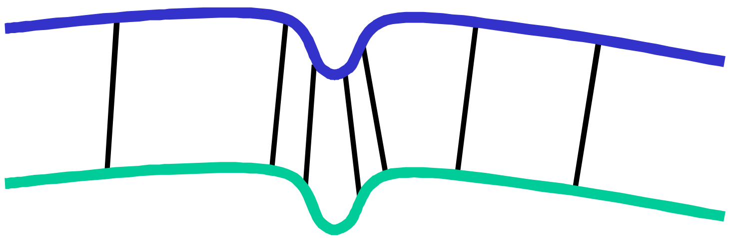

Normal space sampling

Comparison (Sampling)

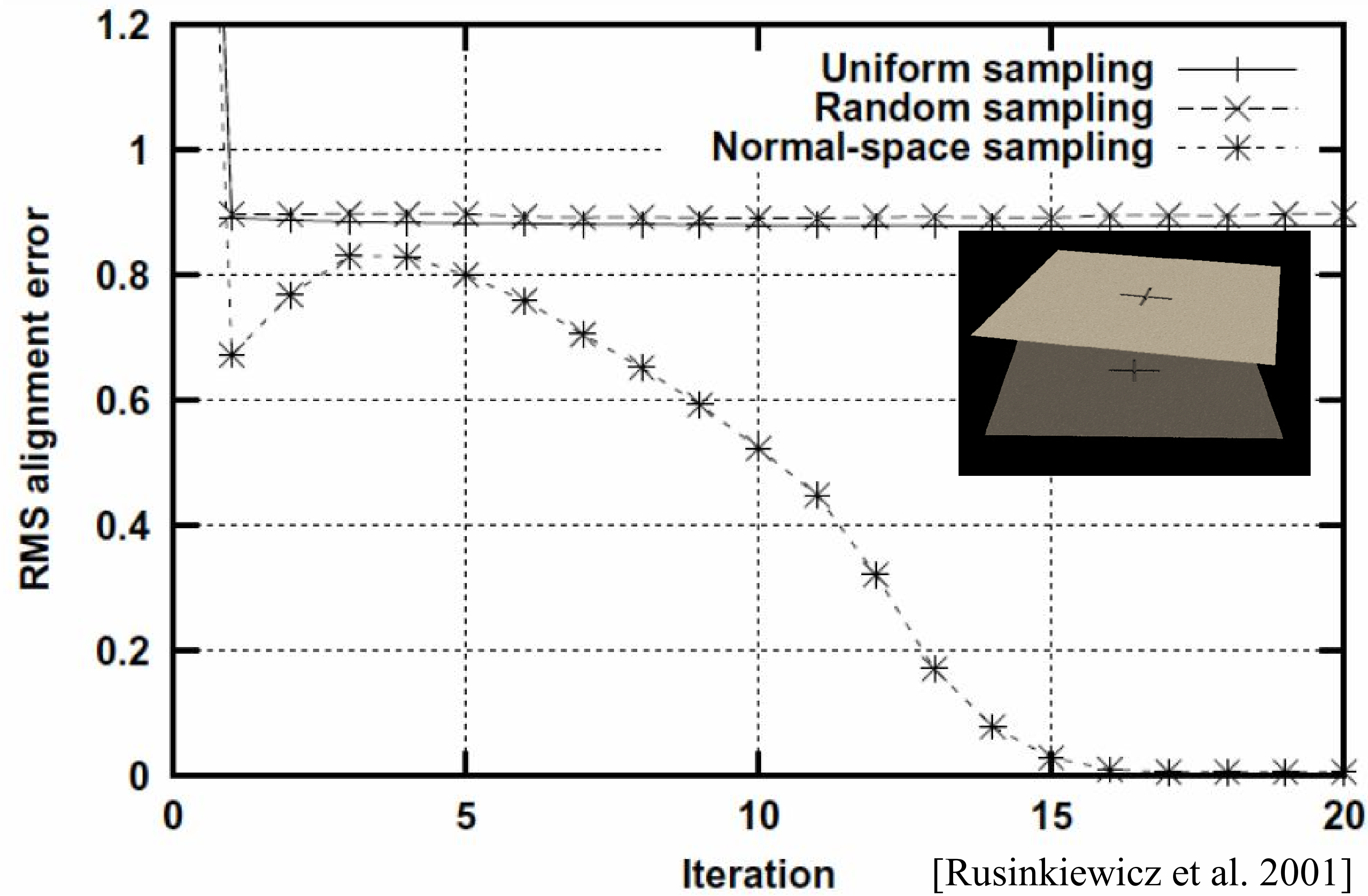

[Rusinkiewicz et al. 2001]

2. CORRESPONDENCE SEARCH

Matching method

- Closest point (Nearest Neighbor)
- Normal shooting
- Projection

Closest point

[Besl and McKay '92]

- Advantages
  - Correspondences are given independently to the initial positions
  - Robust to noises
- Disadvantages
  - Computational cost is high
  - Weak to sliding

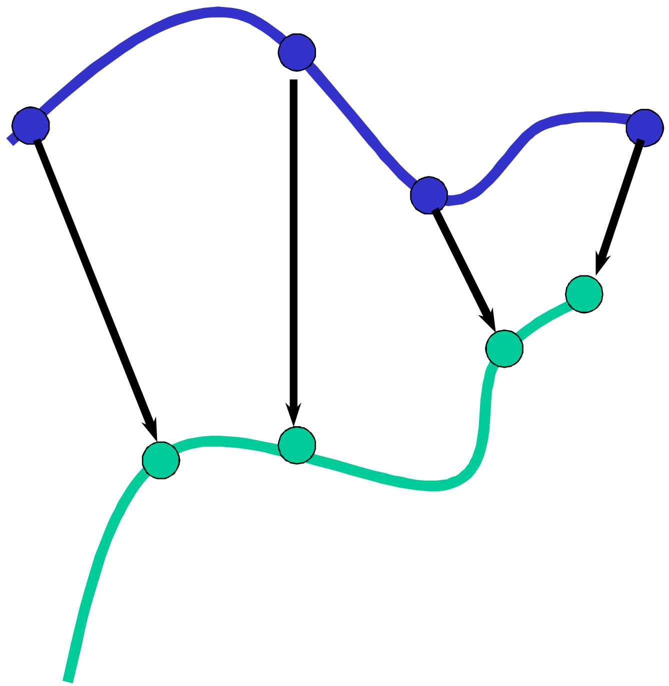

Nearest neighbor search

- *k*-d tree (Binary search tree)

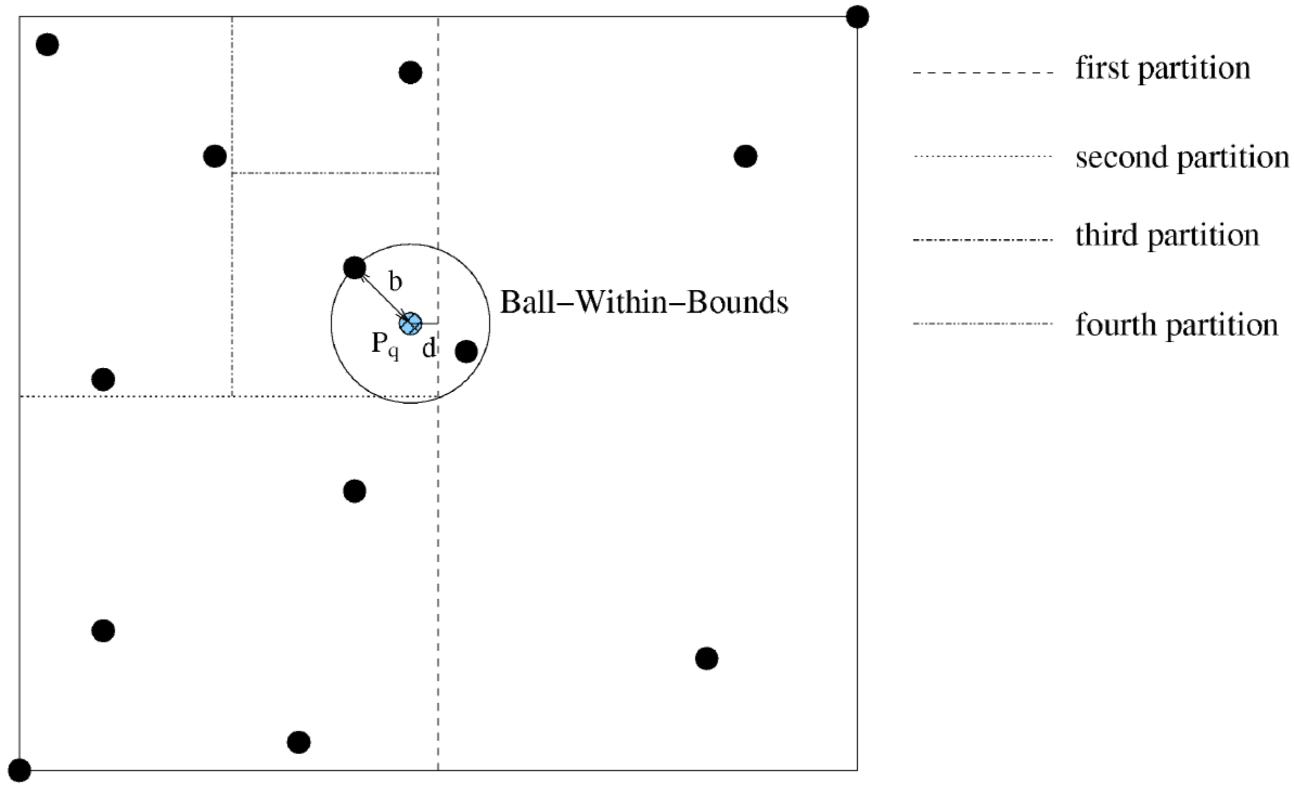

Approximate Nearest Neighbor search [Arya et al. 94]

- (1+ε)-approximate nearest neighbor

$$||\mathbf{p} - \mathbf{p}_q|| \leq (1+\varepsilon)\, ||\mathbf{p}^* - \mathbf{p}_q||$$

$$||\mathbf{p}_q - \mathbf{p}|| \,/ (1+\varepsilon)$$

$$\varepsilon > 0$$

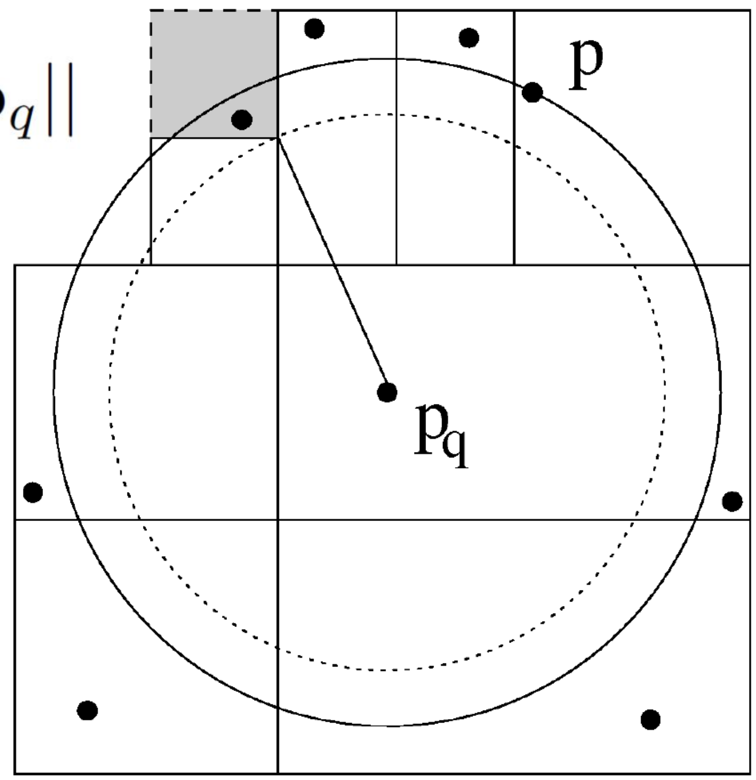

Cached k-d tree search for ICP

[A. Nüchter et al. 3DIM'07]

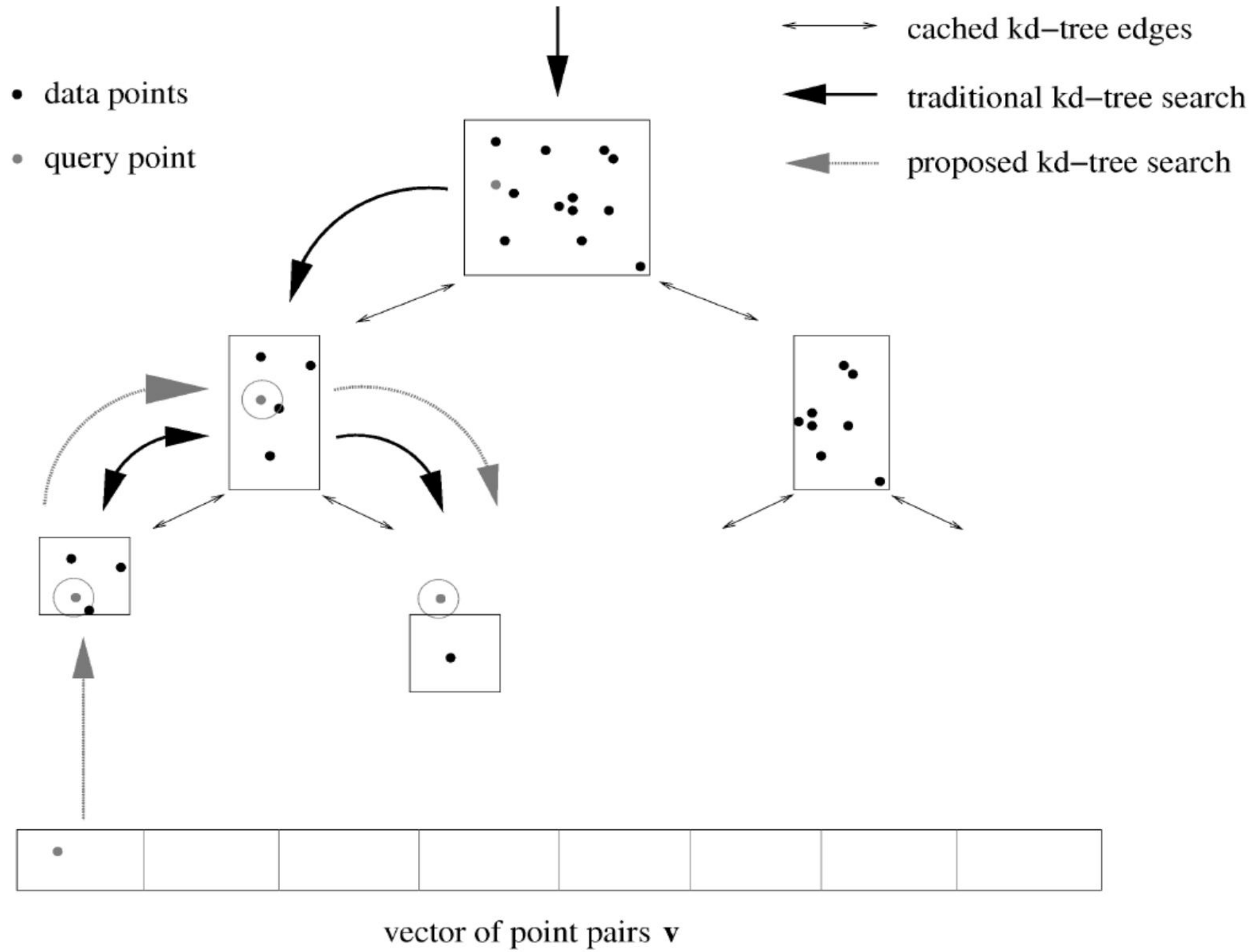

Evaluation

- 3D laser range sensor based on SICK

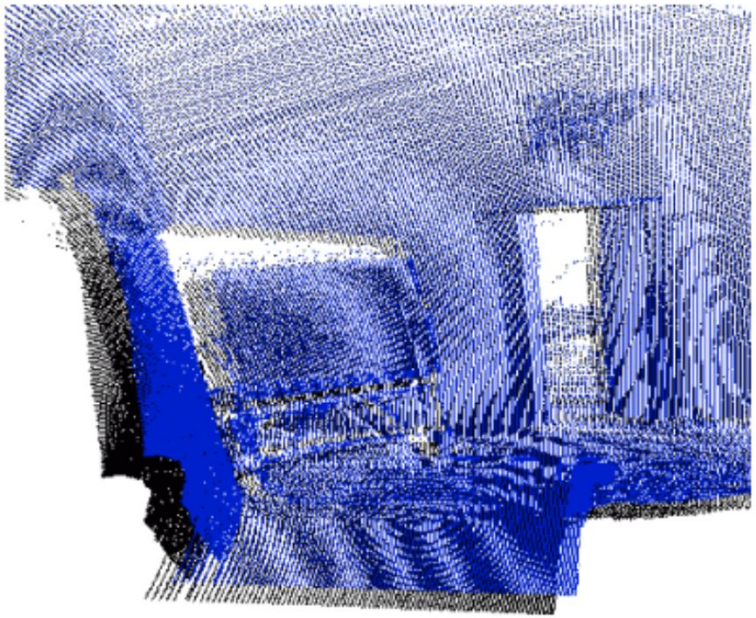

Cluttered indoor environment

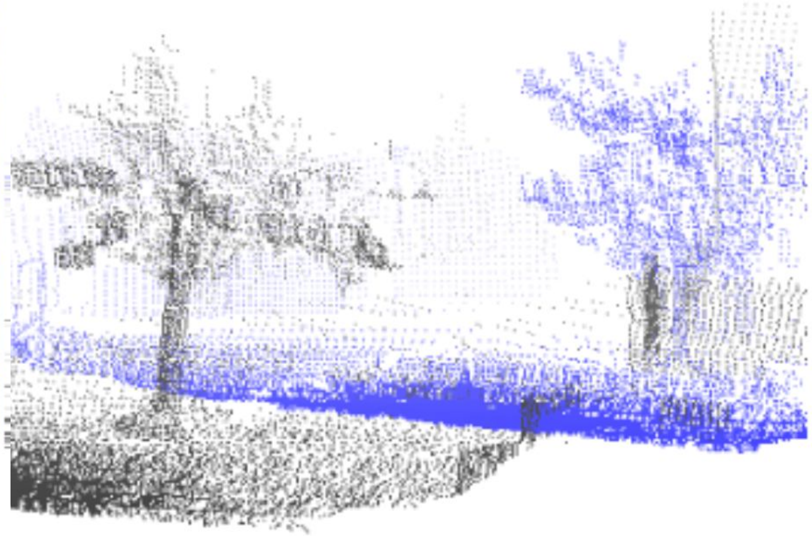

Outdoor environment

Search time / iteration

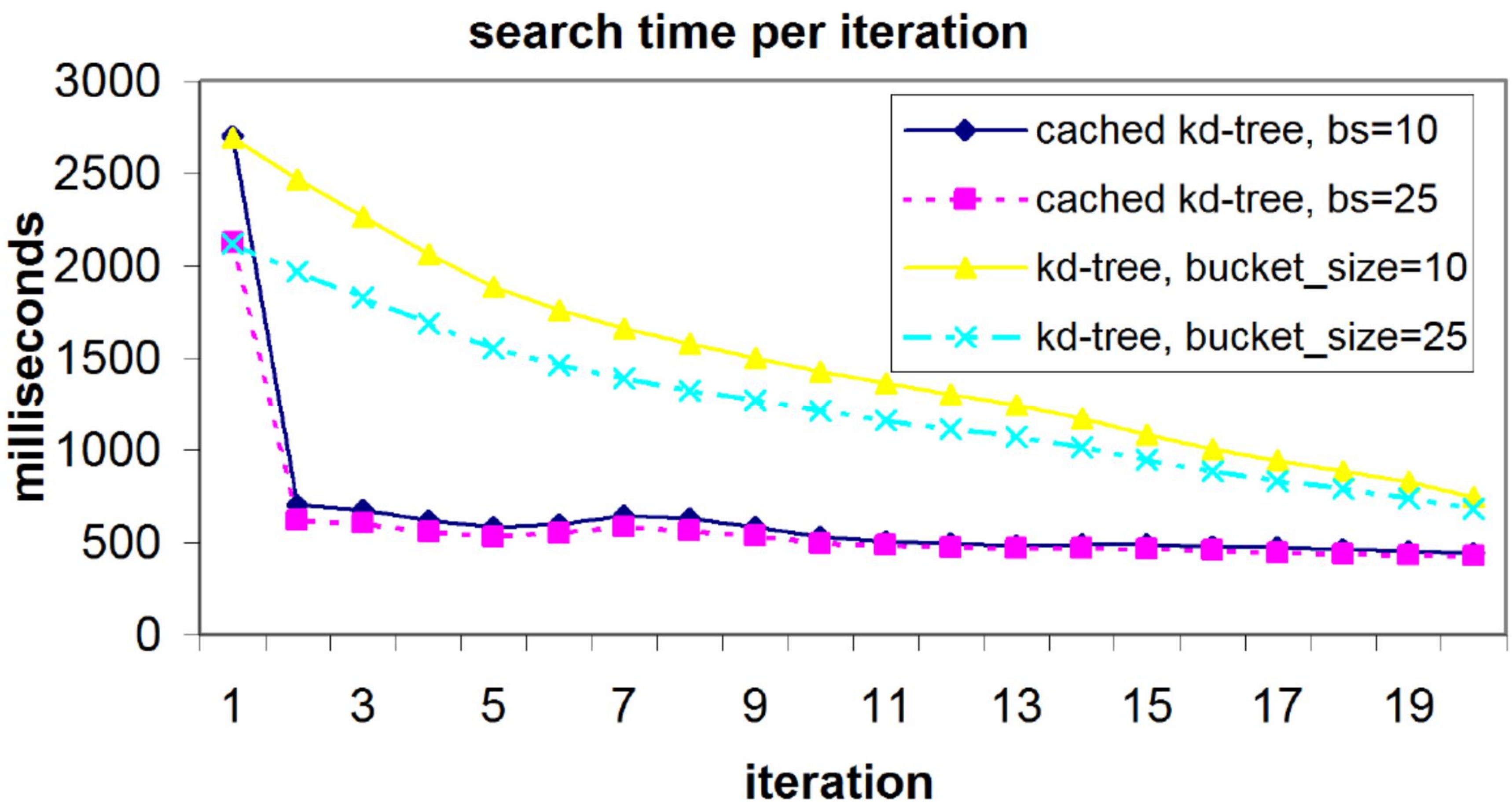

Overall comparison

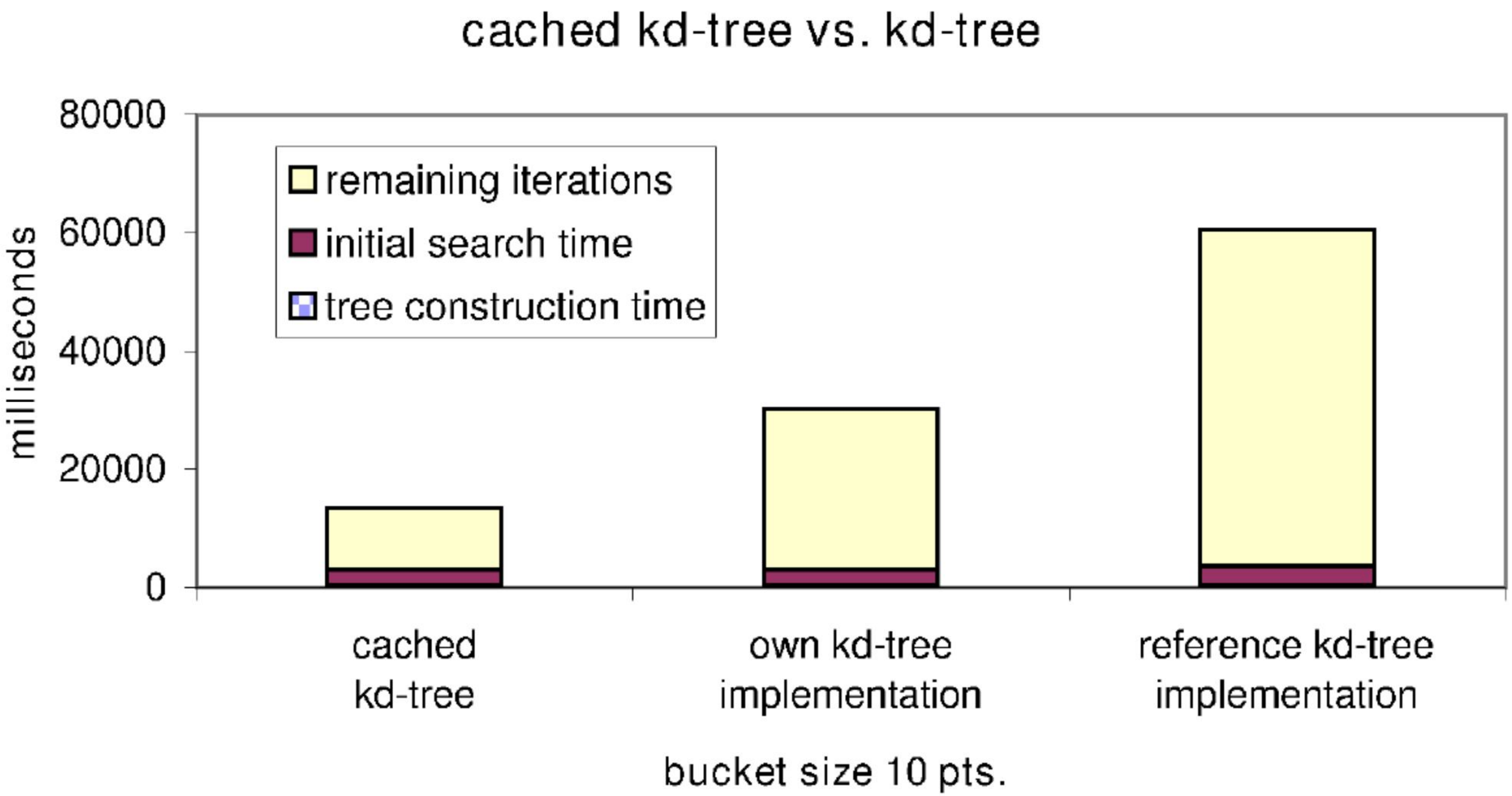

Projection

[Blais '95]

- Advantages
  - Low computational cost
- Disadvantages
  - Correspondences depend on the initial positions

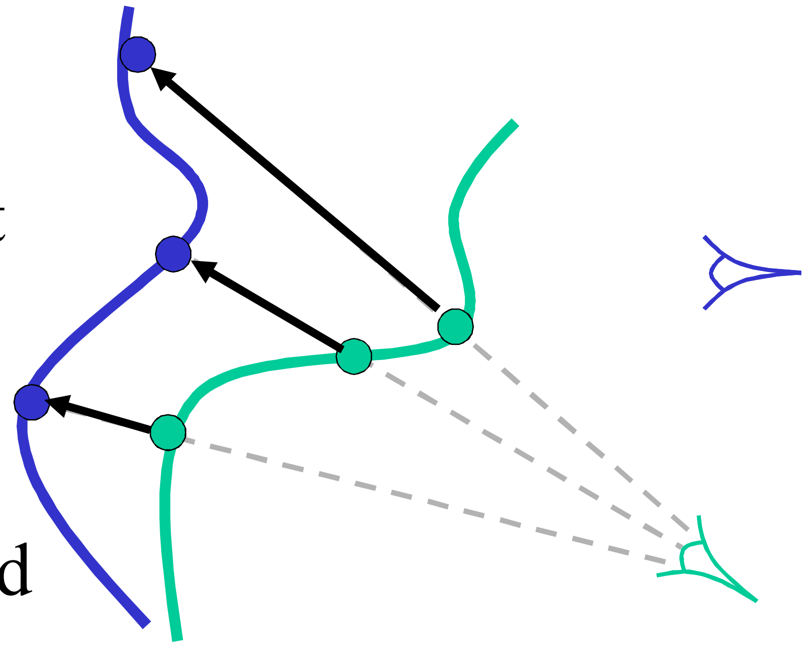

Normal shooting

[Chen and Medioni ‘91]

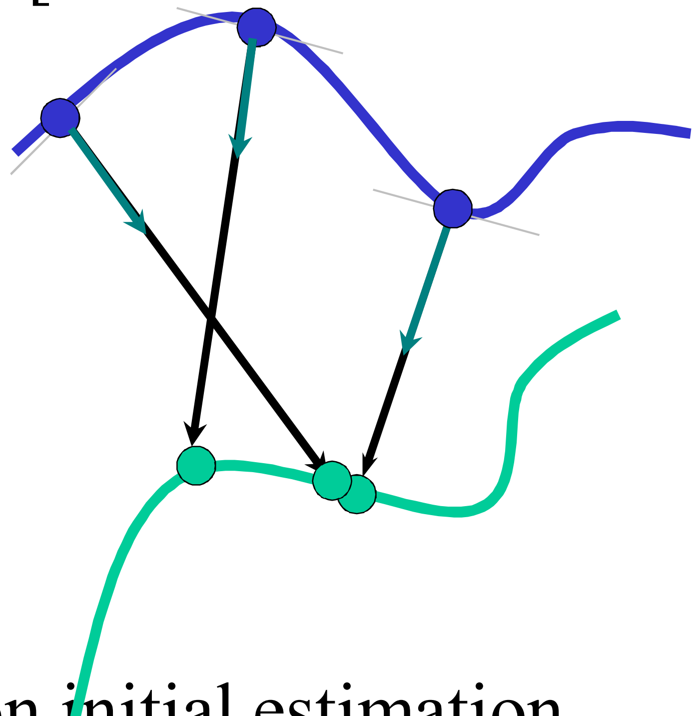

- Advantages
  - Fast convergence
- Disadvantages
  - High computational cost
  - Correspondences depend on initial estimation
  - Weak to noises

3. WEIGHTING CORRESPONDENCES

Weighting method

- Constant weight
- Inner product of normals $Weight = n_x \bullet n_y$
- Accuracy of sensors
- Confidence obtained from other modalities (color, reflectance, etc.)
- Distance between correspondences

$$Weight = f\left(1 - \frac{Dist(x, y)}{Dist_{\max}}\right)$$

Weight functions

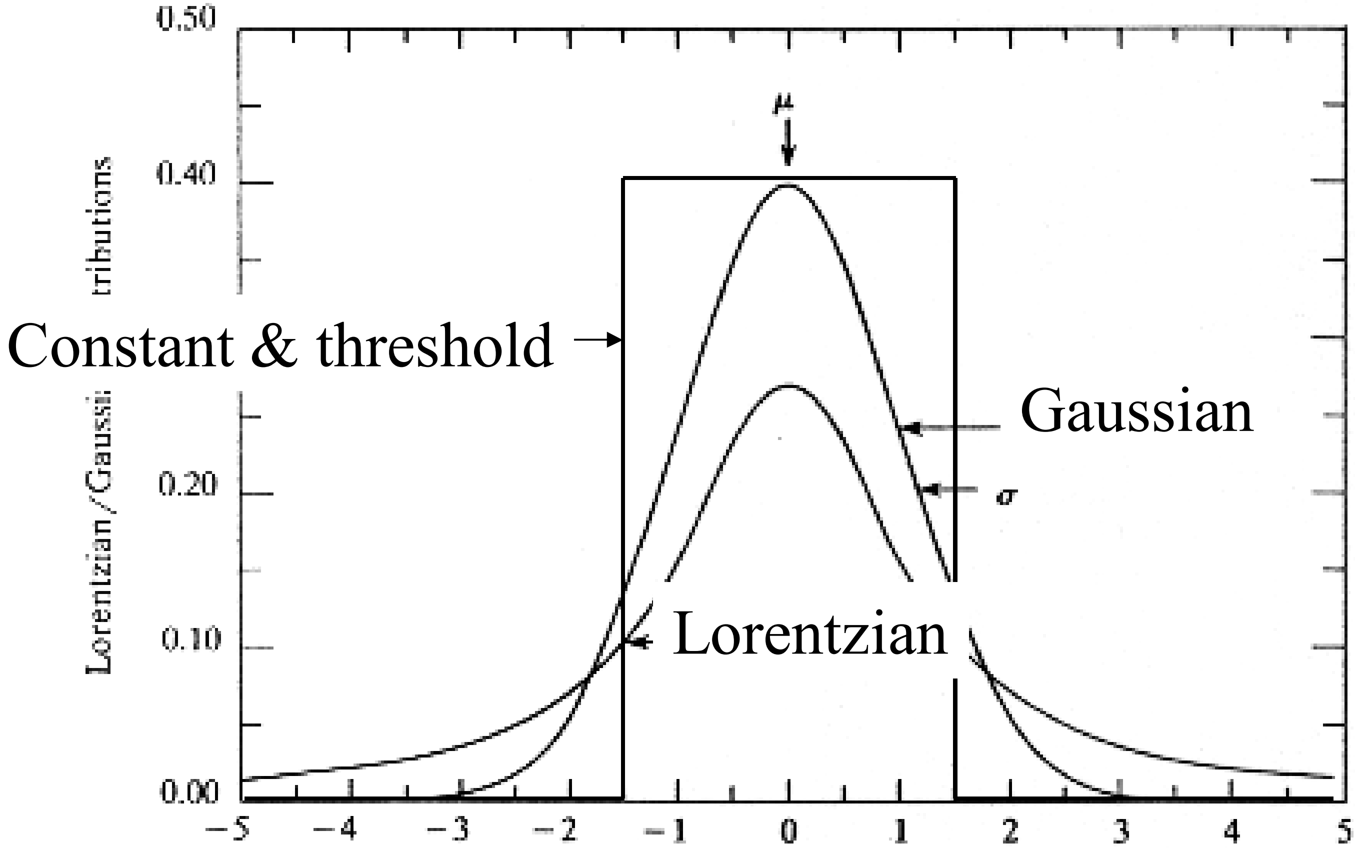

- Distances between correspondences

Comparison (Weighting)

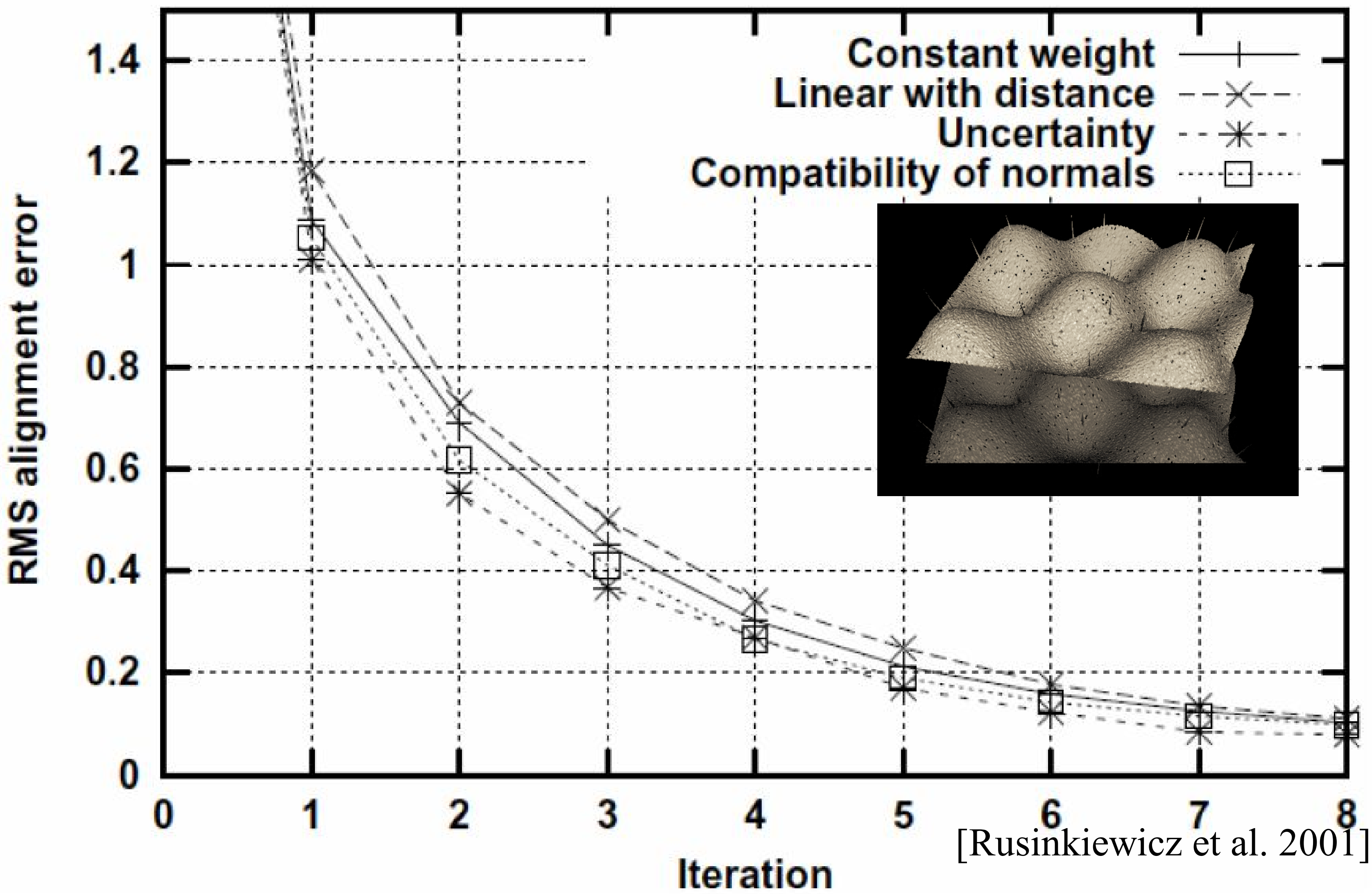

[Rusinkiewicz et al. 2001]

Using photometric properties

[Nishino & Ikeuchi ‘02]

- Reflectance obtained by laser range sensors
  - Robust to illumination changes

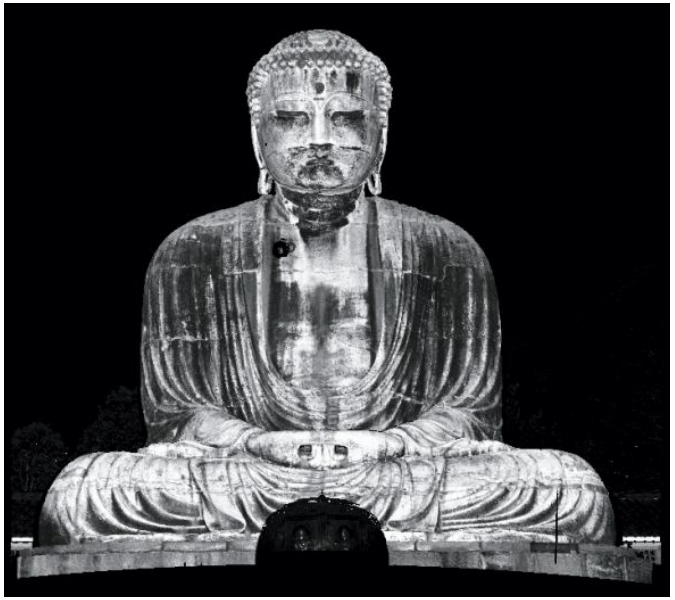

Robust Range Image Registration Using Local Distribution of Albedo

Diego Thomas, Akihiro Sugimoto

Issues

- Range images of symmetrical objects

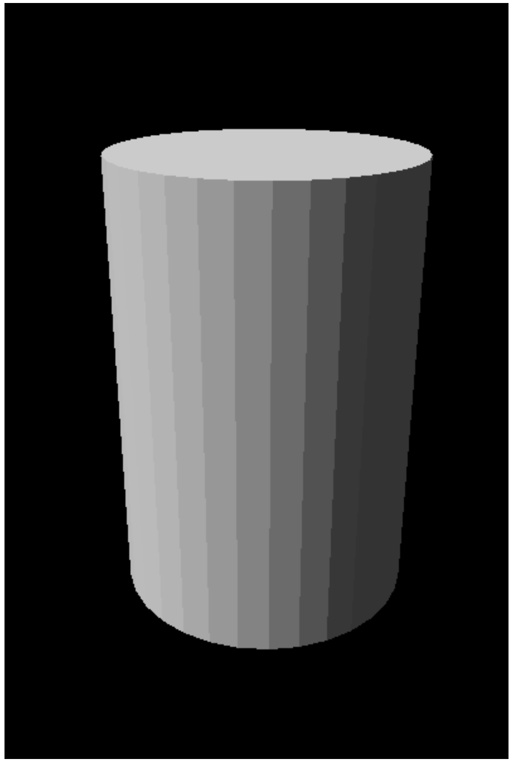

Approach

- Similarity evaluation using albedo
- Region-based approach using Level Set method

Albedo (True Color)

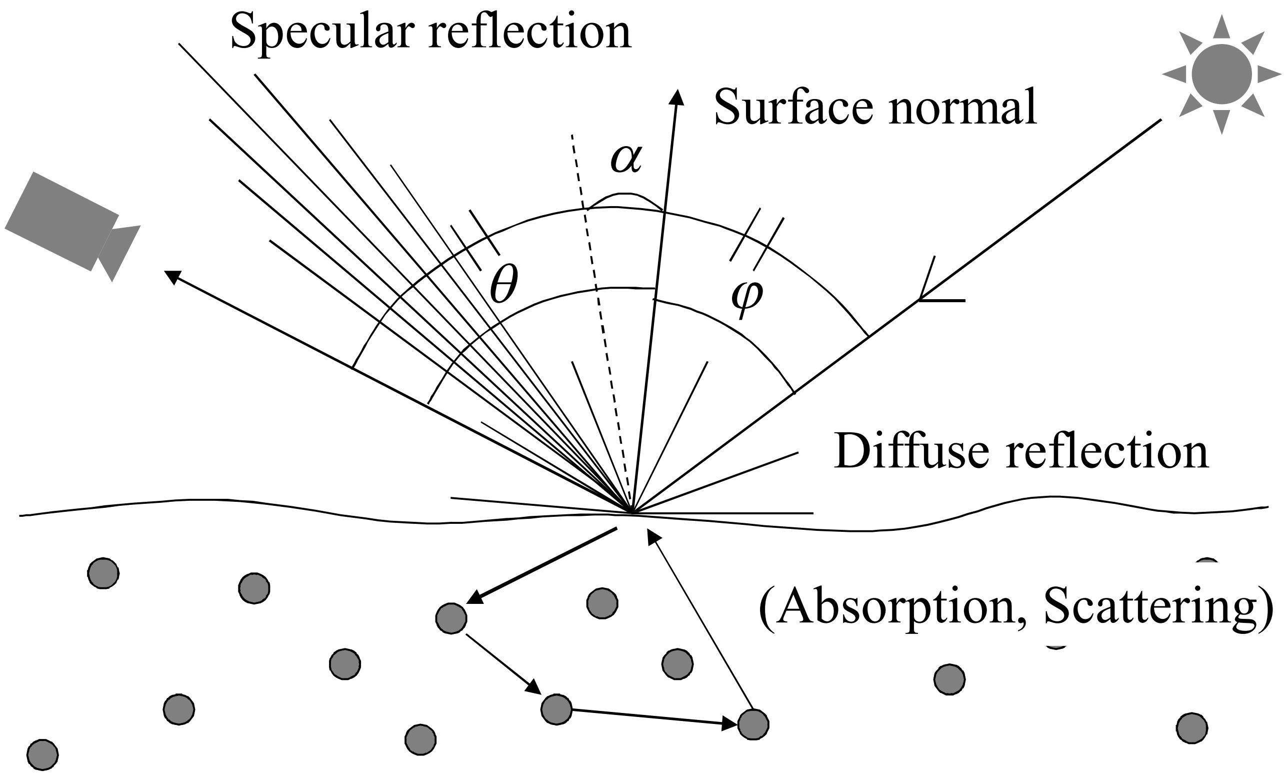

Albedo -> Surface reflectance

$$\overrightarrow{alb(m)} = \frac{\overrightarrow{c(m)}}{\overrightarrow{n(m)}^{\top} M \overrightarrow{n(m)}}$$

Region growing

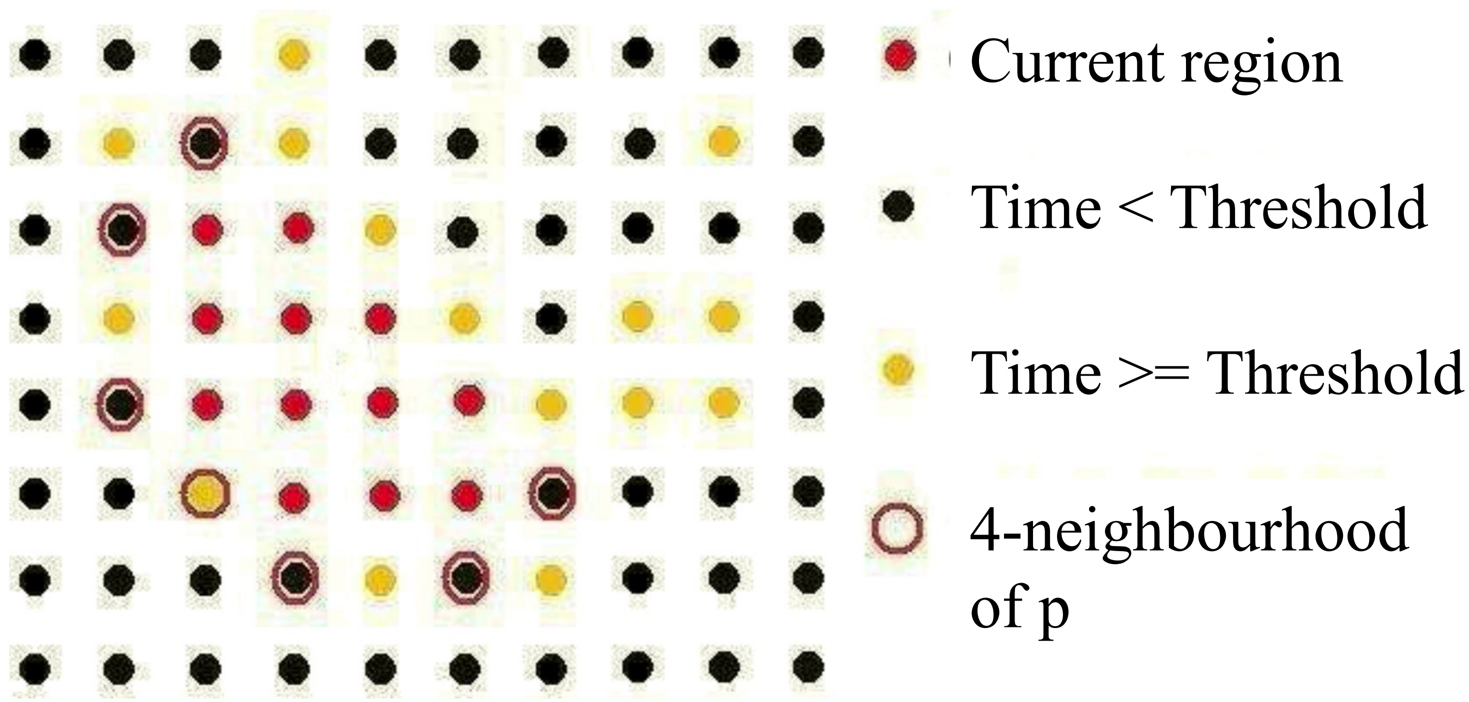

(3) 3rd step

Level set method

$$\frac{d}{dt}\psi = -P(x)\|\nabla\psi\|$$

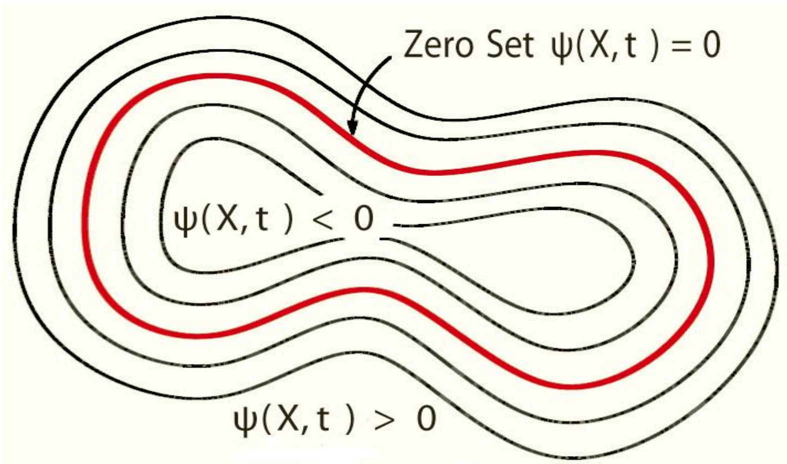

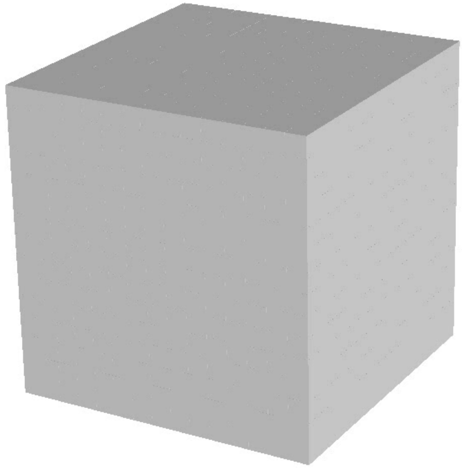

[Fast level set method
Kurazume et al. 03]

Correspondence search

Searching for the corresponding point of *m*

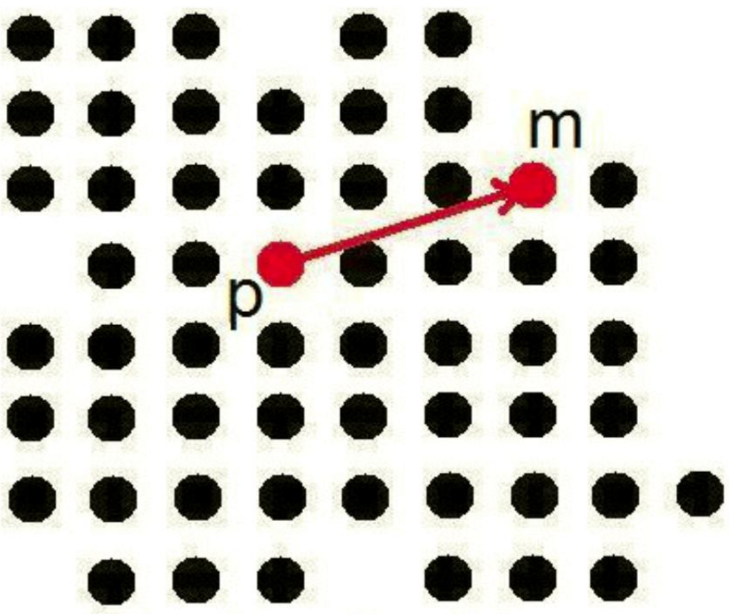

Region of point p

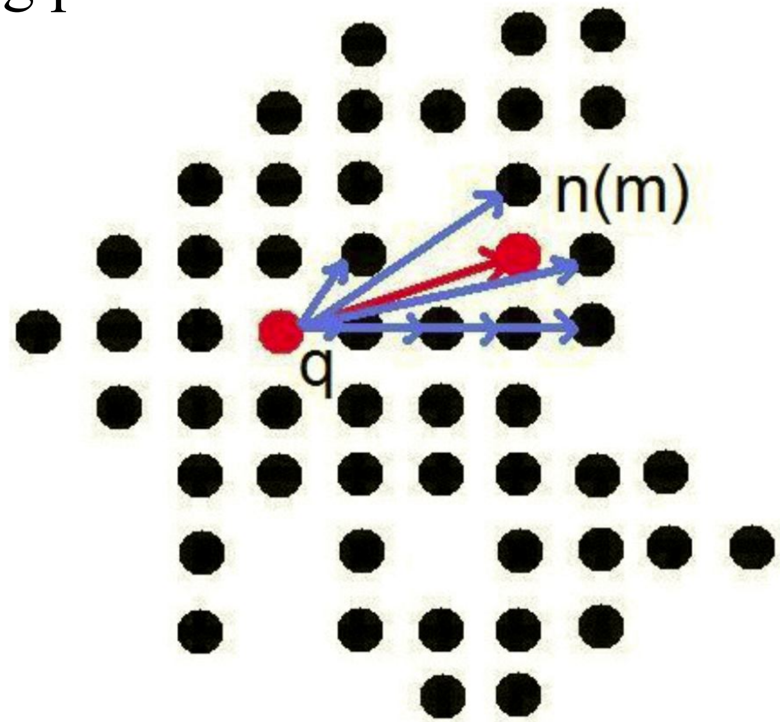

Region of point q

Similarity evaluation using Albedo

$$L(p,q) = \frac{size(R(p)) + size(R(q))}{(\sum_{m\in R(p)} \omega_{(m,q)} + \sum_{m\in R(q)} \omega_{(m,p)})^2}$$

$$\times \left\{ \sum_{m\in R(p)} \omega_{(m,q)} \|\overrightarrow{alb(m)} - \overrightarrow{alb(n(m)_q)}\|_2^2 + \sum_{m\in R(q)} \omega_{(m,p)} \|\overrightarrow{alb(m)} - \overrightarrow{alb(n(m)_p)}\|_2^2 \right\},$$

Size of the regions

Weight by distance

Albedo

Rigidity constraint

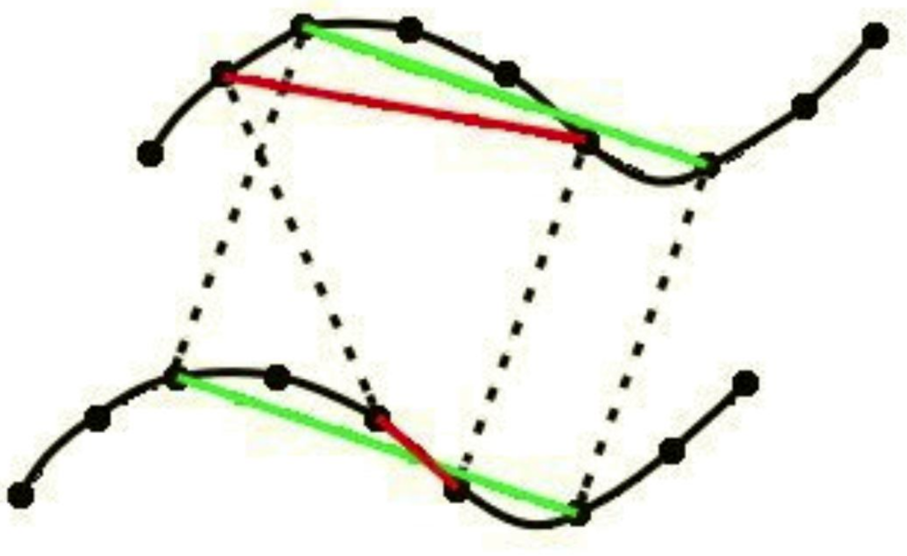

- Pairs satisfying rigidity constraint
- Pairs violating rigidity constraint

Evaluation with synthetic data

(a) First image.

(b) Second image.

(c) Albedo image.

Comparison with previous method

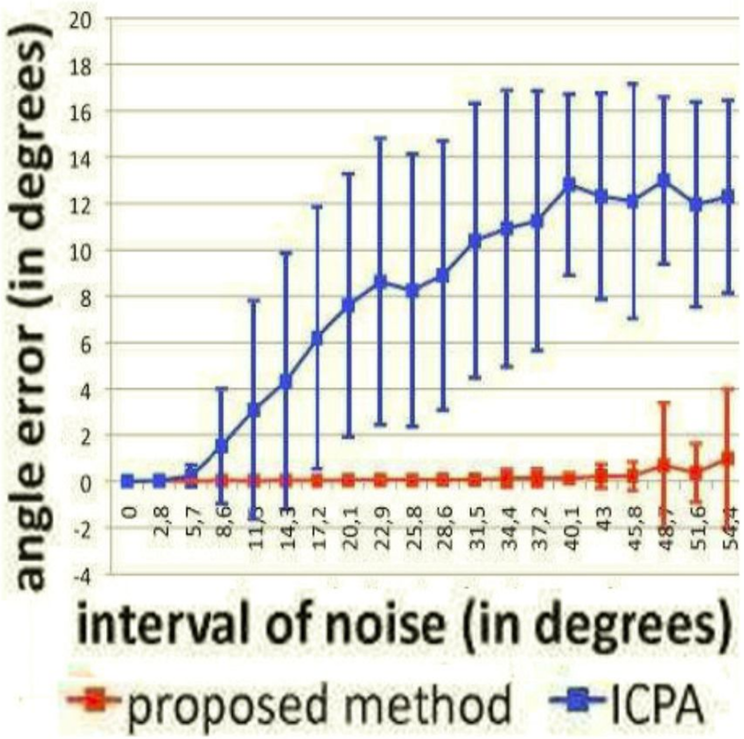

(a) Angle error.

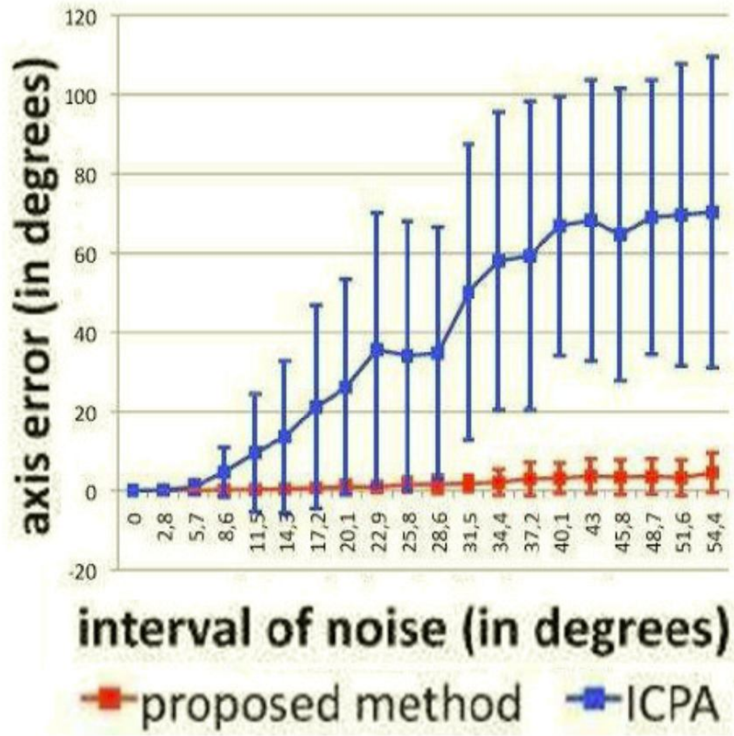

(b) Axis error.

Evaluation with real data

- Range images captured from differenct viewpoints

(a) First image.

(b) Second image.

(c) Superimposed.

Albedo and Speed image

- Illumination conditions and region generation

(a) Albedo image.

(b) Gradient map.

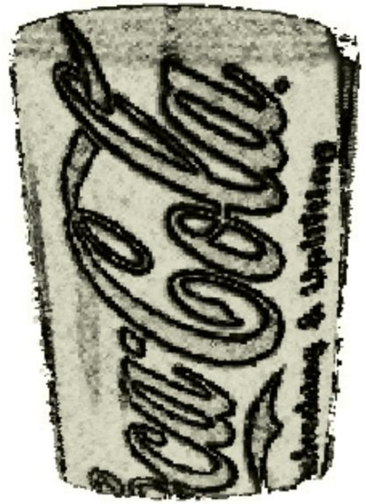

(c) Speed map.

Experimental result 1

Proposed method | ICPA | ICP-CG

Experimental result 2

Proposed method ICPA ICP-CG

Summary

- Robust range images registration method

- Similarity evaluation using albedo
- Region-based approach by Level Set method

4. OUTLIER REJECTION

Outlier rejection

- Point to point distance is more than a threshold
- N % of pairs that have large distances
- Point to point distance is larger than the median (Lmeds) [Masuda et al. ’96]
- Point to point distance is inconsistent with the neighboring pairs [Drai ‘98]
- Pairs include points on boundaries [Zhang ‘94] (Nearest neighbor search)

Threshold values

- Given by users
  - Generally used because ICP-based method is sensitive to initial positions

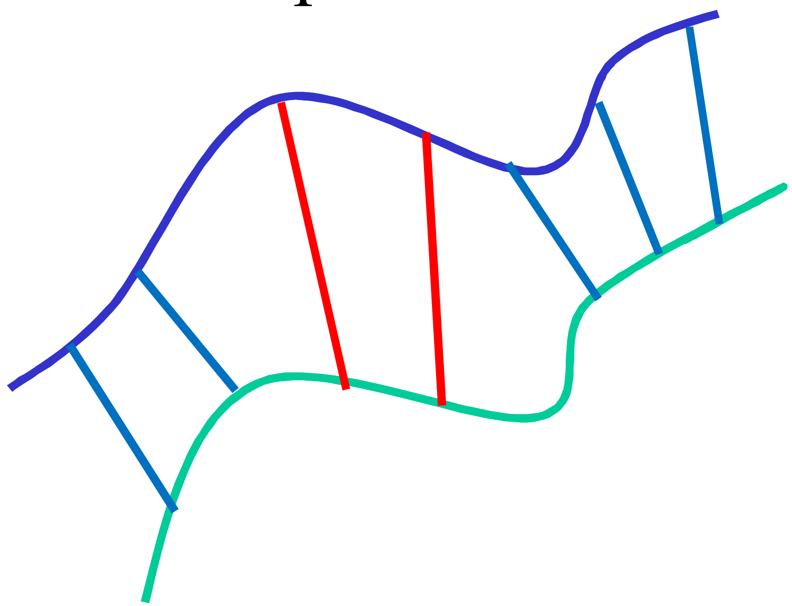

Consistency with neighbors

- Point to point distance is inconsistent with the neighboring pairs

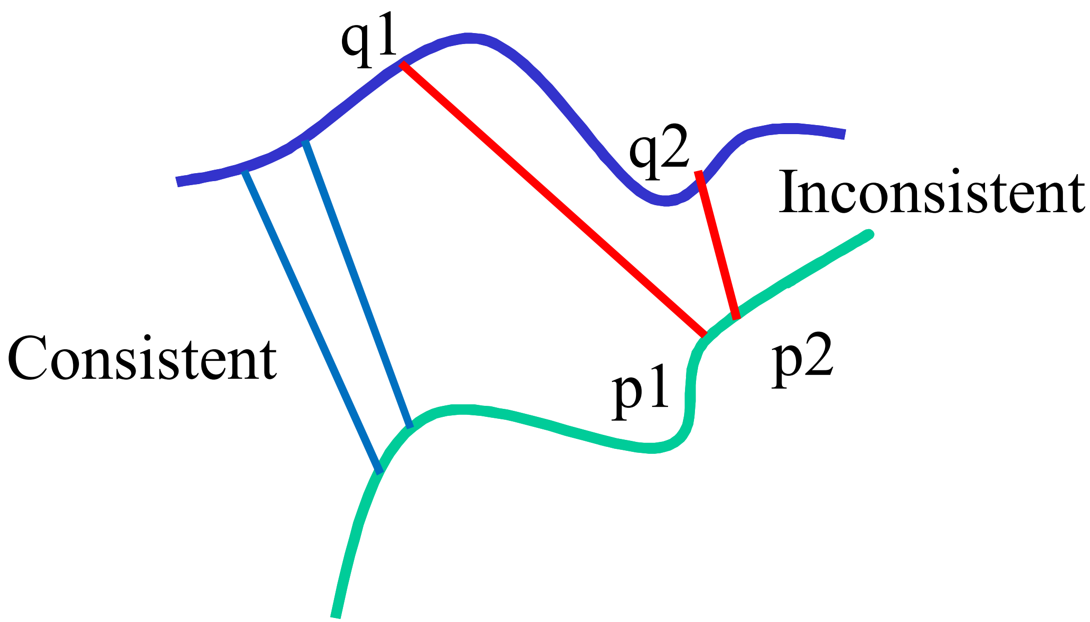

Comparison (Outlier rejection)

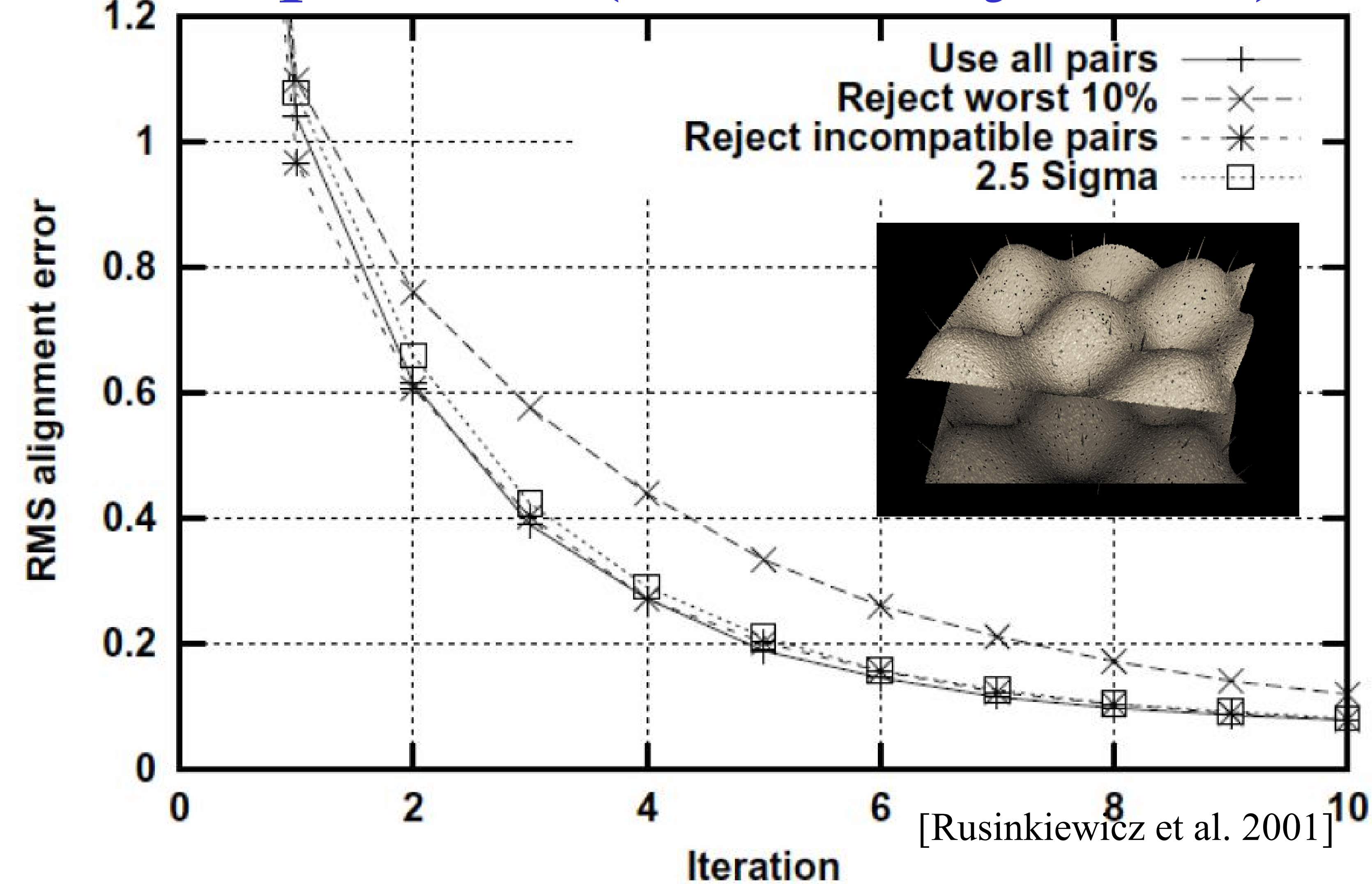

[Rusinkiewicz et al. 2001]

Points on boundary

[Zhang '94]

- A point on boundaries is matched with many points on non-overlapped areas

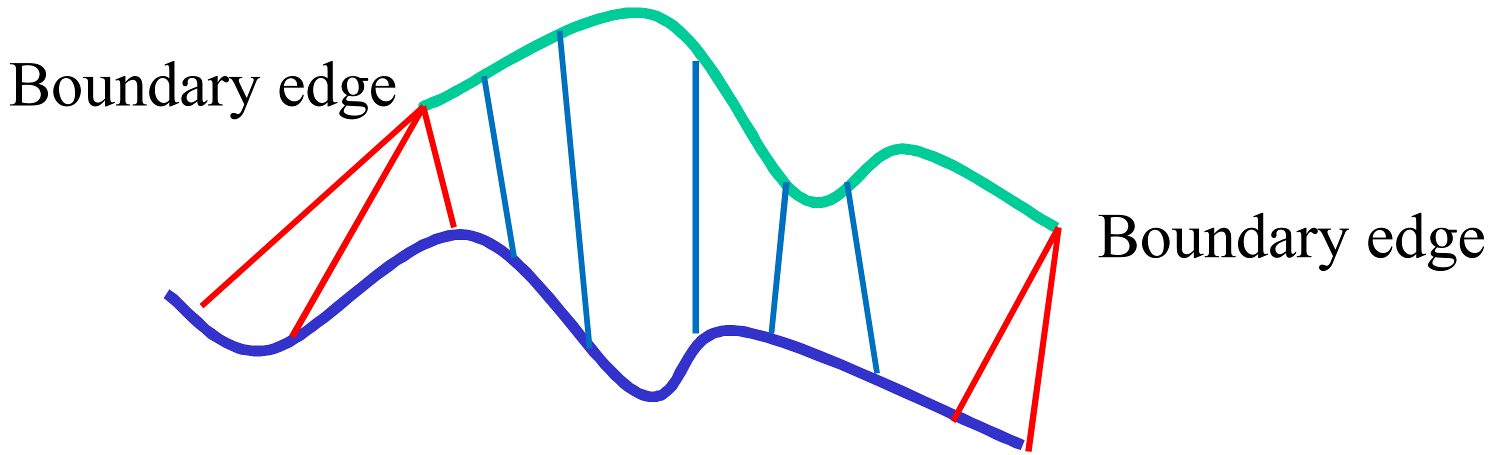

Outlier Robust ICP for Minimizing Fractional RMSD

J. M. Phillips, R. Liu and C. Tomasi
Duke University

Registration with outliers

- New data

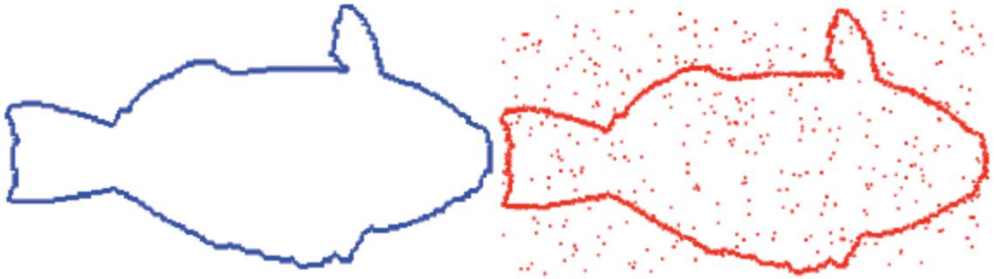

- Deformation

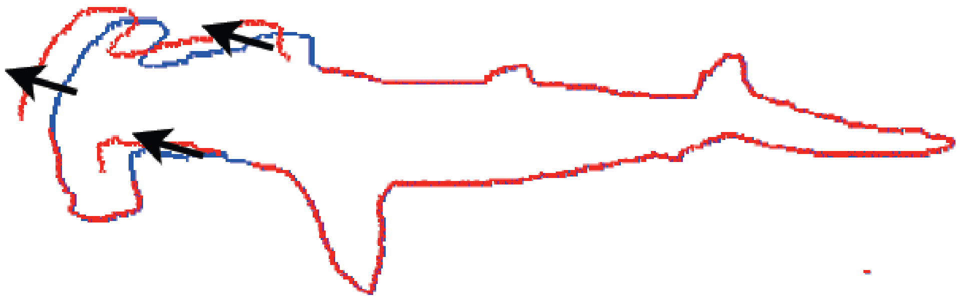

-Registration is often skewed by outliers
-Outlier detection depends on registration

Proposed method

- Register point sets and find outliers in one algorithm

- Using FRMSD (Fractional Root Mean Squared Distance)

Distance function

- RMSD (Root Mean Squared Distance)

$$\min_{T \in \mathcal{T}} \sqrt{\frac{1}{|D|} \sum_{p \in D} ||T(p) - \mu(p)||^2}$$

Align data point set D to model point set M

$\mathcal{T}$ = rotations, translations, scale, ...

μ = matching from D to M

Hard to optimize over both $\mathcal{T}$ and μ

susceptible to outliers

Fractional RMSD

Let D_f be $f|D|$ points $p \in D$ with smallest residuals $||p - \mu(p)||$.

$$\min_{\substack{T \in \mathcal{T} \\ f \in [0,1]}} \frac{1}{f^{\lambda}} \sqrt{\frac{1}{|D_f|} \sum_{p \in D_f} ||T(p) - \mu(p)||^2}$$

λ is empirically given

Algorithm

1: Compute $\mu_0 = \arg \min_{\mu_0 : D \to M} \text{RMSD}(D, M, \mu_0)$.

2: Compute $f_0 \in [0, 1]$ minning $\text{FRMSD}(D, M, f_0, \mu_0)$.

3: $i \leftarrow 0$.

4: **repeat**

5: Compute D_{f_i} minimizing $\text{RMSD}(D_{f_i}, M, \mu_i)$ such that $D_{f_i} \subseteq D$ and $|D_{f_i}| = \lfloor f_i |D| \rfloor$.

6: Compute $T \in \mathcal{T}$ minimizing $\text{RMSD}(D_{f_i}, M, \mu_i)$. $D \leftarrow T(D)$.

7: $i \leftarrow i + 1$.

8: Compute $\mu_i : D \to M$ minning $\text{RMSD}(D, M, \mu_i)$.

9: Compute $f_i \in [0, 1]$ minning $\text{FRMSD}(D, M, f_i, \mu_i)$.

10: **until** $(u_i = u_{i-1}$ and $f_i = f_{i-1})$

Optimal value of λ

Alg.	λ	time (s)	# iter.	RMSD	FRMSD	f
FICP	1	0.142	10.38	0.158	0.225	0.701
FICP	1.3	0.069	3.81	0.170	0.248	0.749
FICP	2	0.059	3.06	0.170	0.303	0.750
FICP	3	0.061	3.17	0.170	0.404	0.750
FICP	4	0.062	3.21	0.171	0.538	0.751
FICP	5	0.063	3.30	0.172	0.717	0.751

FRMSD is robust for $\lambda \in [1, 5]$

Experiments

- Stanford bunny
  - 25% deformation, 5° rotation

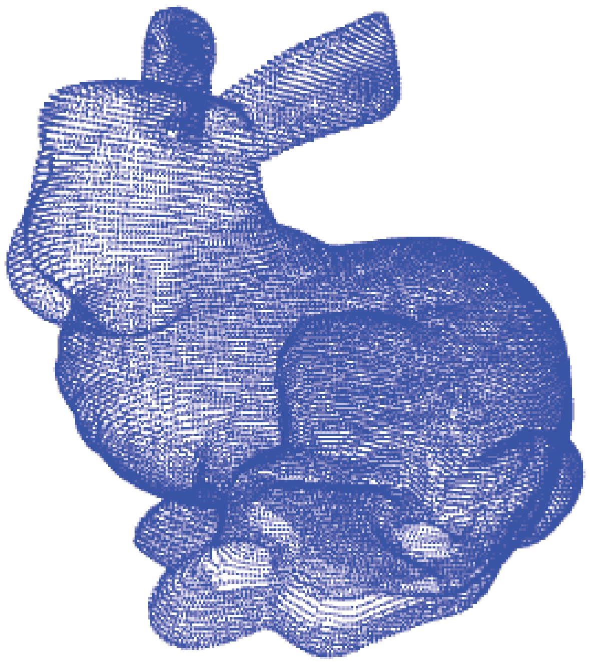

Model

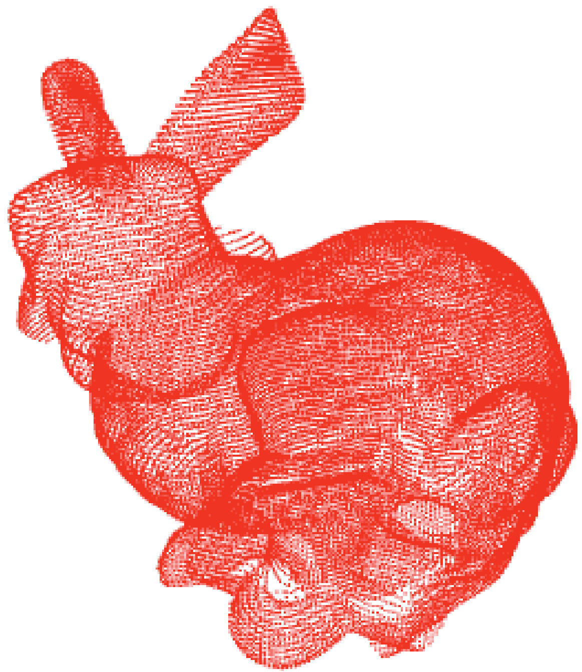

Data

Experimental result

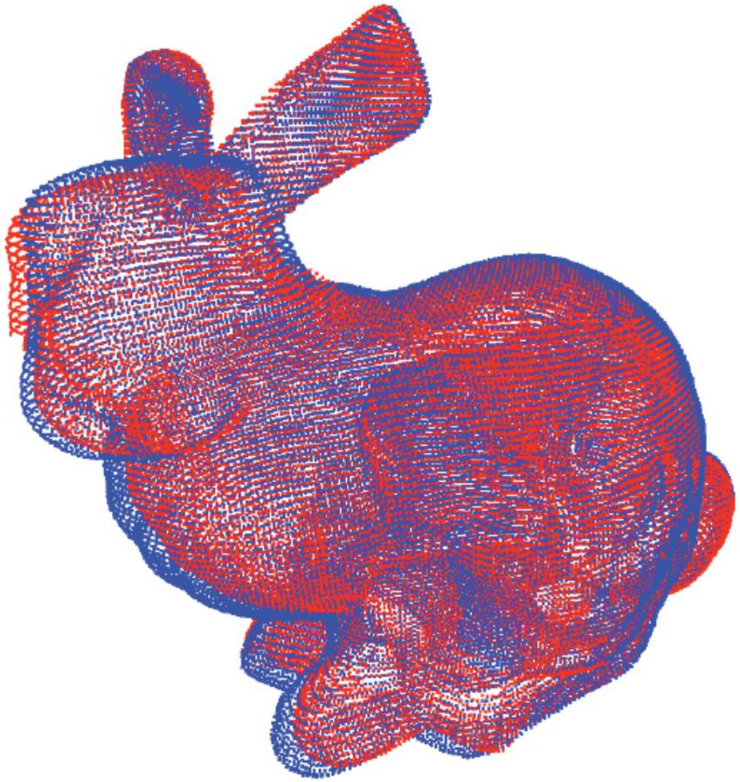

ICP

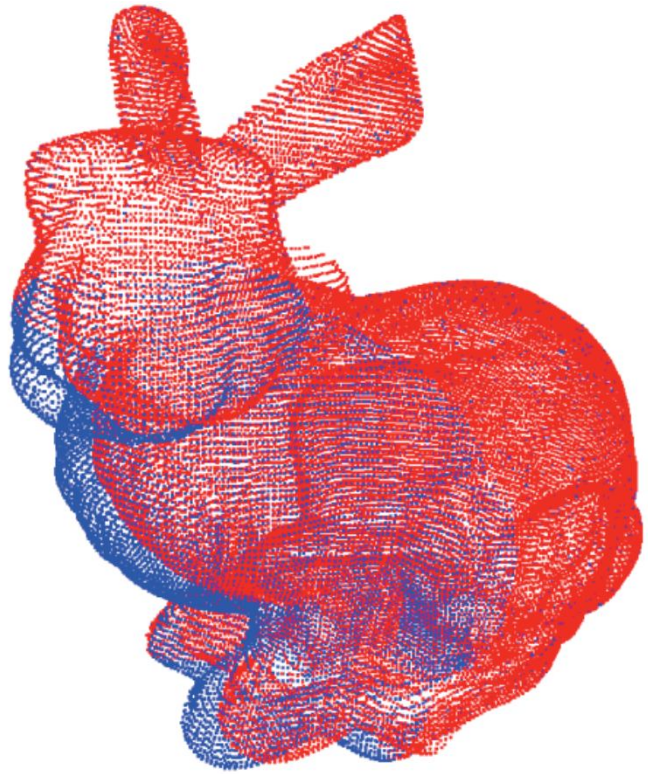

FICP

Comparison

time (s)	60.1
# iter.	78.8
RMSD	0.6668
FRMSD	0.6668
f	1.0

time (s)	16.5
# iter.	17.3
RMSD	0.0052
FRMSD	0.0124
f	0.750

ICP

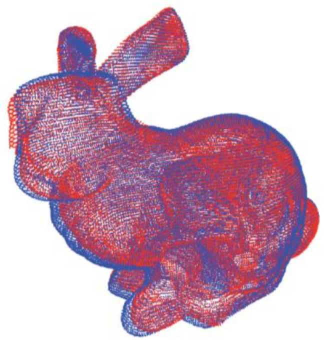

FICP

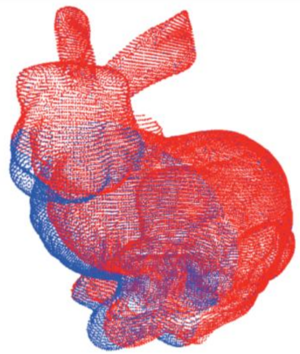

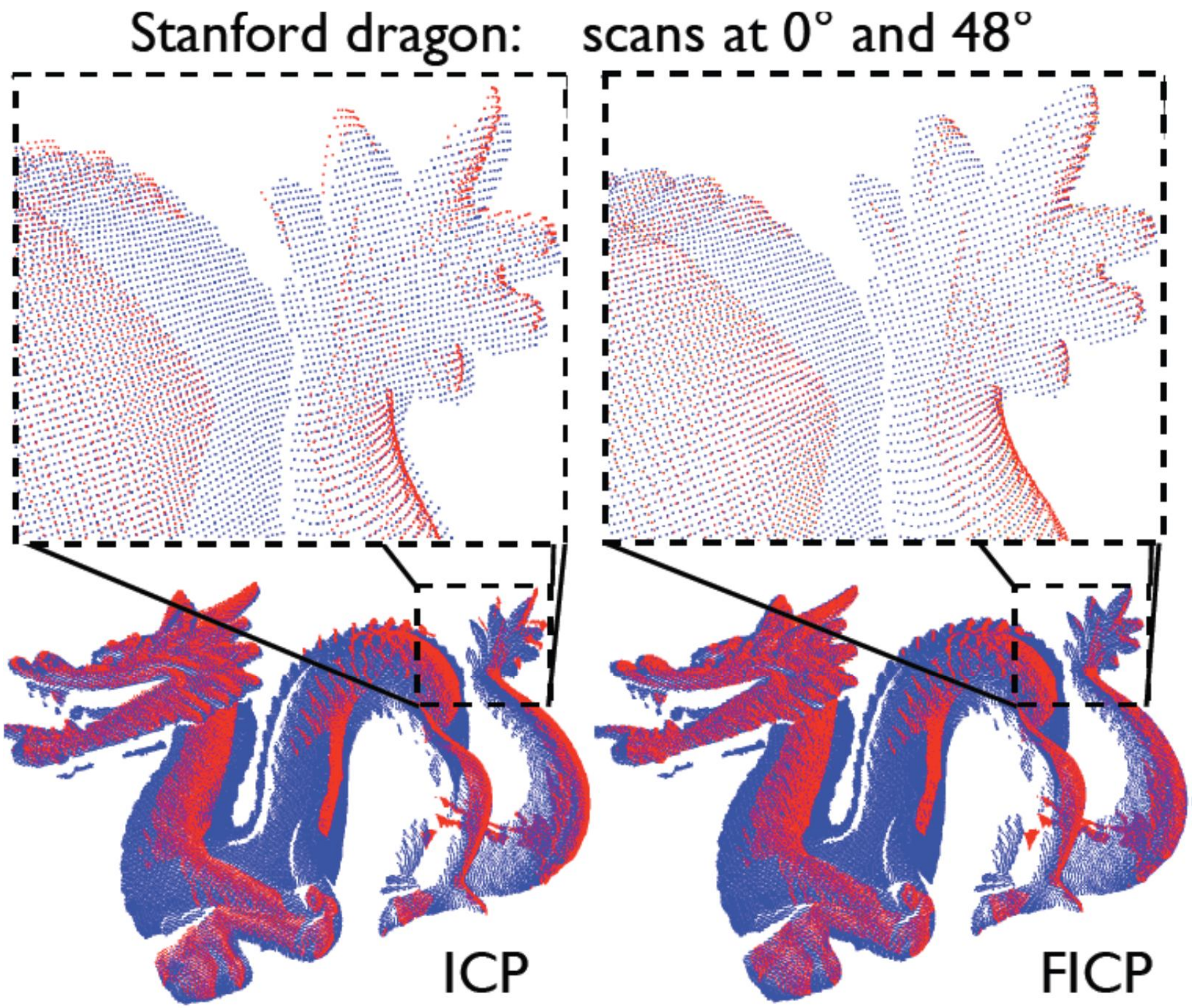
Stanford dragon: scans at 0° and 48°
ICP
FICP

5. ERROR METRIC

Error metric

- Point-to-Point [Besl & Mackey ’92]

$$\hat{\varepsilon} = \min_{R,t} \sum_{i \neq j,k} \left(\vec{y}_{ijk} - (R_i \vec{x}_{ik} + \vec{t}_i) \right)^2$$

- Point-to-Plane [Chen & Medioni ‘91]

$$\hat{\varepsilon} = \min_{R,t} \sum_{i \neq j,k} \left(R_i \vec{n}_{ik} \cdot \{ (R_j \vec{y}_{ijk} + \vec{t}_j) - (R_i \vec{x}_{ik} + \vec{t}_i) \} \right)^2$$

Point-to-Point

[Besl & Mackey '92]

- Guaranteed to converge to local minima
- Low convergence-speed
- Weak to horizontal movement

$$\|\boldsymbol{x} - \boldsymbol{y}\|$$

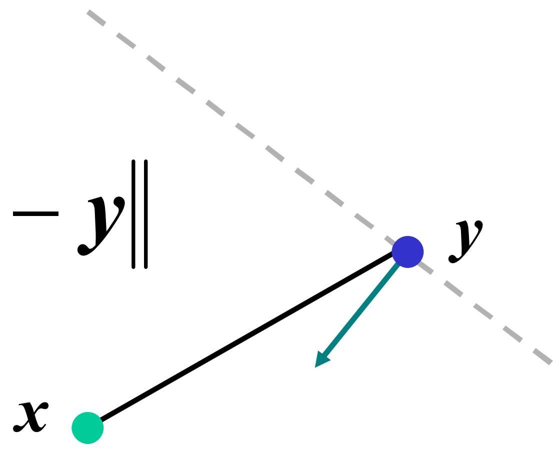

Point-to-Plane

[Chen & Medioni '91]

- Sensitive initial positions, noises, threshold
- Convergence speed is high

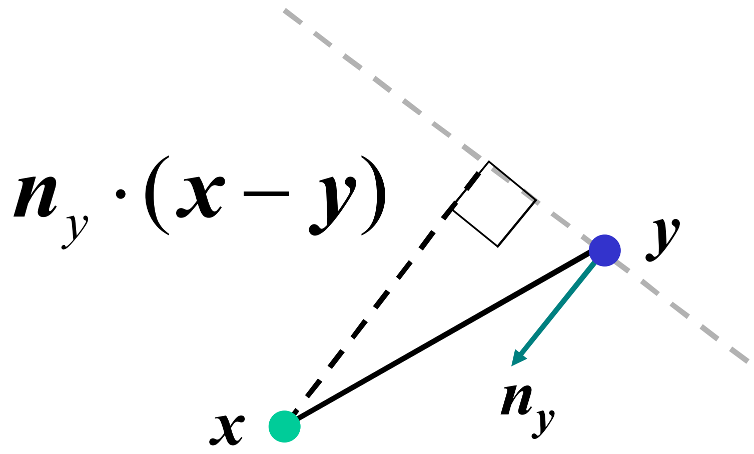

Comparison (Error metric)

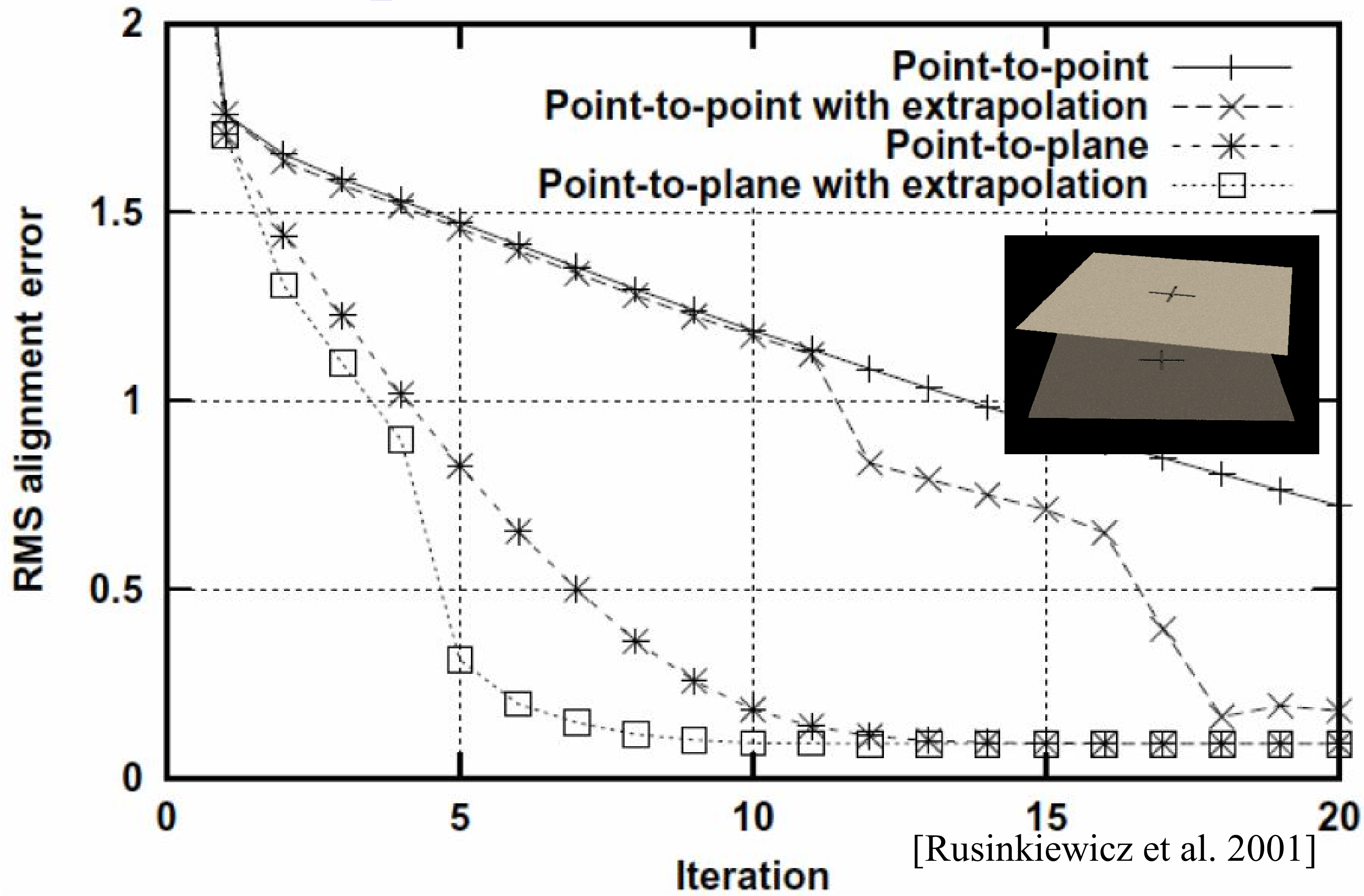

[Rusinkiewicz et al. 2001]

6. OPTIMIZATION

Optimization method

- Non-linear: Levenberg-Marquat method etc.

- Linear:
  - Point-to-Point: Closed form solution [Horn][Umeyama]
  - Point-to-Plane: Linealization by assumption of small angles[Neugebauer]

Closed form solution

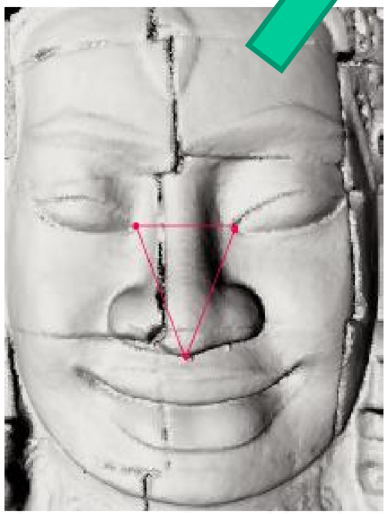

$$e^2(R, \mathbf{t}, c) = \frac{1}{3}\sum_{j=1}^{3} ||\mathbf{y}_{ji} - (cR\mathbf{x}_j + \mathbf{t})||^2$$

Rotation $R = USV^T$

Translation $\mathbf{t} = \mu_y - cR\mu_x$

Scaling $c = \frac{1}{\sigma_x^2}\mathrm{tr}(DS)$

Simultaneous alignment

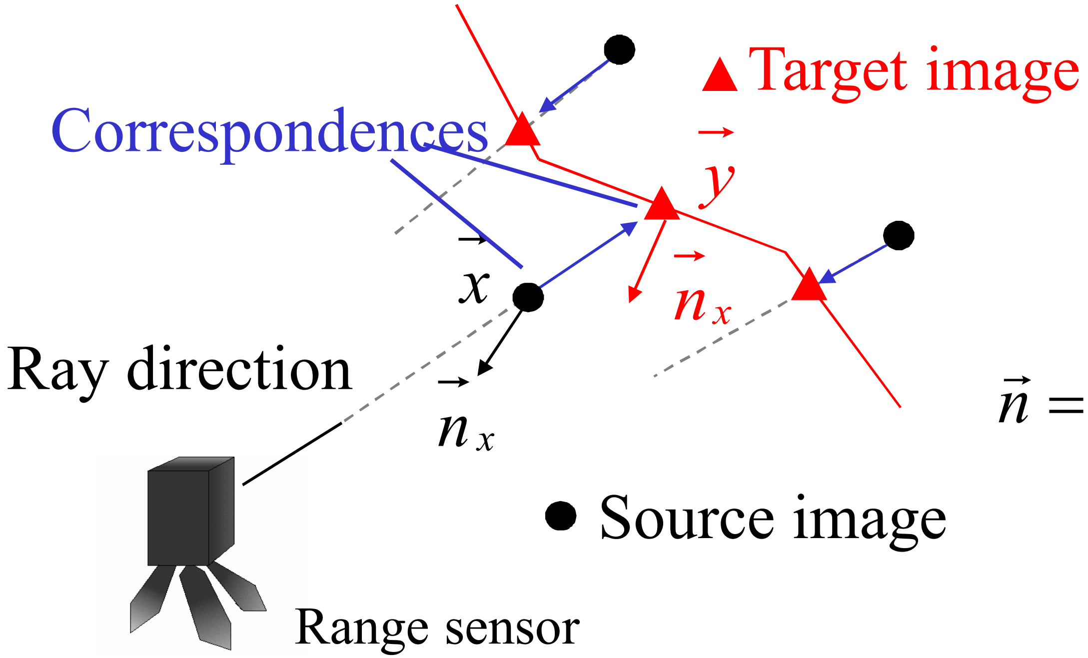

$$\vec{n} = \frac{\vec{n}_x + \vec{n}_y}{\left\| \vec{n}_x + \vec{n}_y \right\|}$$

$$\hat{\varepsilon} = \min_{R,t} \sum_{i \neq j,k} \left(R_i \vec{n}_{ik} \cdot \{ (R_j \vec{y}_{ijk} + \vec{t}_j) - (R_i \vec{x}_{ik} + \vec{t}_i) \} \right)^2$$

$$\hat{\varepsilon} = \min_{\vec{\delta}} \sum_{i \neq j,k} \left\| A_{ijk} \vec{\delta} - s_{ijk} \right\|^2$$

Linealization

[Neugebauer '97]

- Assumption: rotation angles are enough small

$$\bar{\varepsilon} = \arg\min_{\vec{\delta}} \sum_{i \neq j,k} \left\| A_{ijk}\vec{\delta} - s_{ijk} \right\|^2$$

$$\begin{cases} \vec{\delta} = \left(m_0 \cdots m_{n-1} \right) \\ m_i = \left(c_{1i} \quad c_{2i} \quad c_{3i} \quad t_{xi} \quad t_{yi} \quad t_{zi} \right) \\ s_{ijk} = \vec{n}_{ik} \cdot \left(\vec{x}_{ik} - \overrightarrow{y_{ijk}} \right) \\ A_{ijk} = \left(\underbrace{0 \ldots 0}_{6i\times 1} \underbrace{C_{ijk}}_{6\times 1} \underbrace{0 \ldots 0}_{6(l-i-1)\times 1} \right) + \left(\underbrace{0 \ldots 0}_{6j\times 1} \underbrace{- C_{ijk}}_{6\times 1} \underbrace{0 \ldots 0}_{6(l-j-1)\times 1} \right) \\ C_{ijk} = \begin{pmatrix} \overrightarrow{n_{ik}} \times \overrightarrow{y_{ijk}} \\ -\overrightarrow{n_{ik}} \end{pmatrix} \end{cases}$$

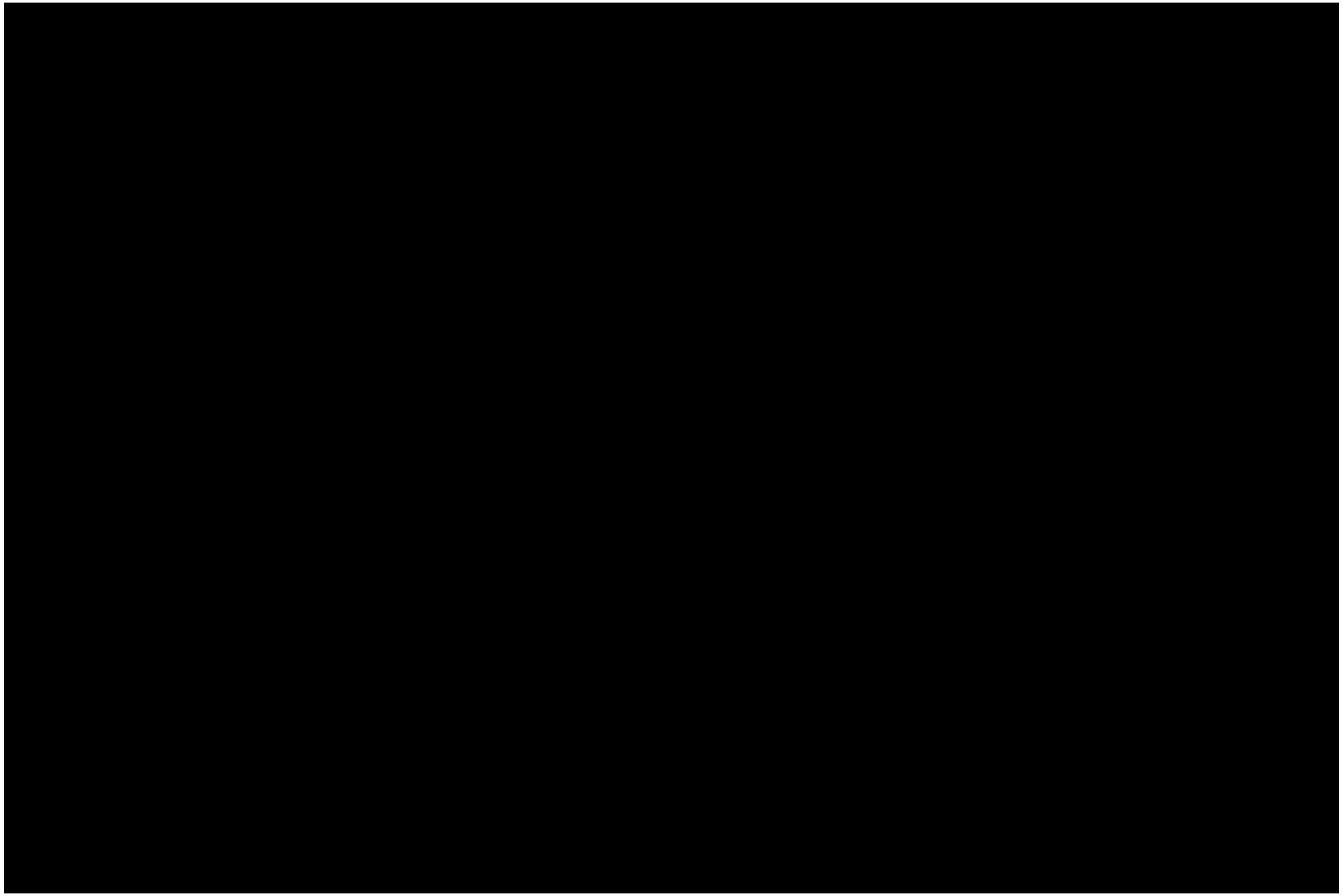

Alignment result (Nara Great Buddha)

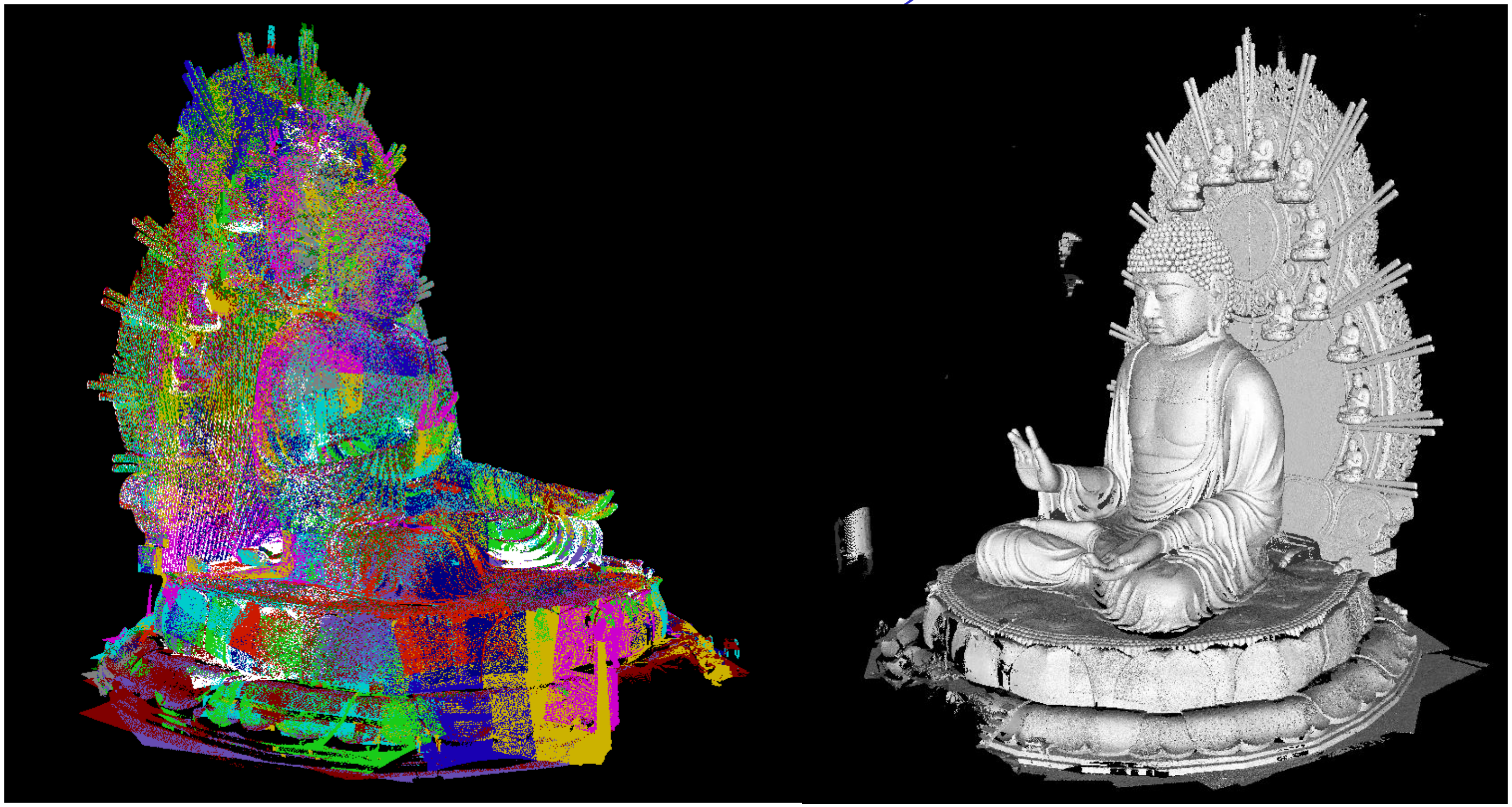

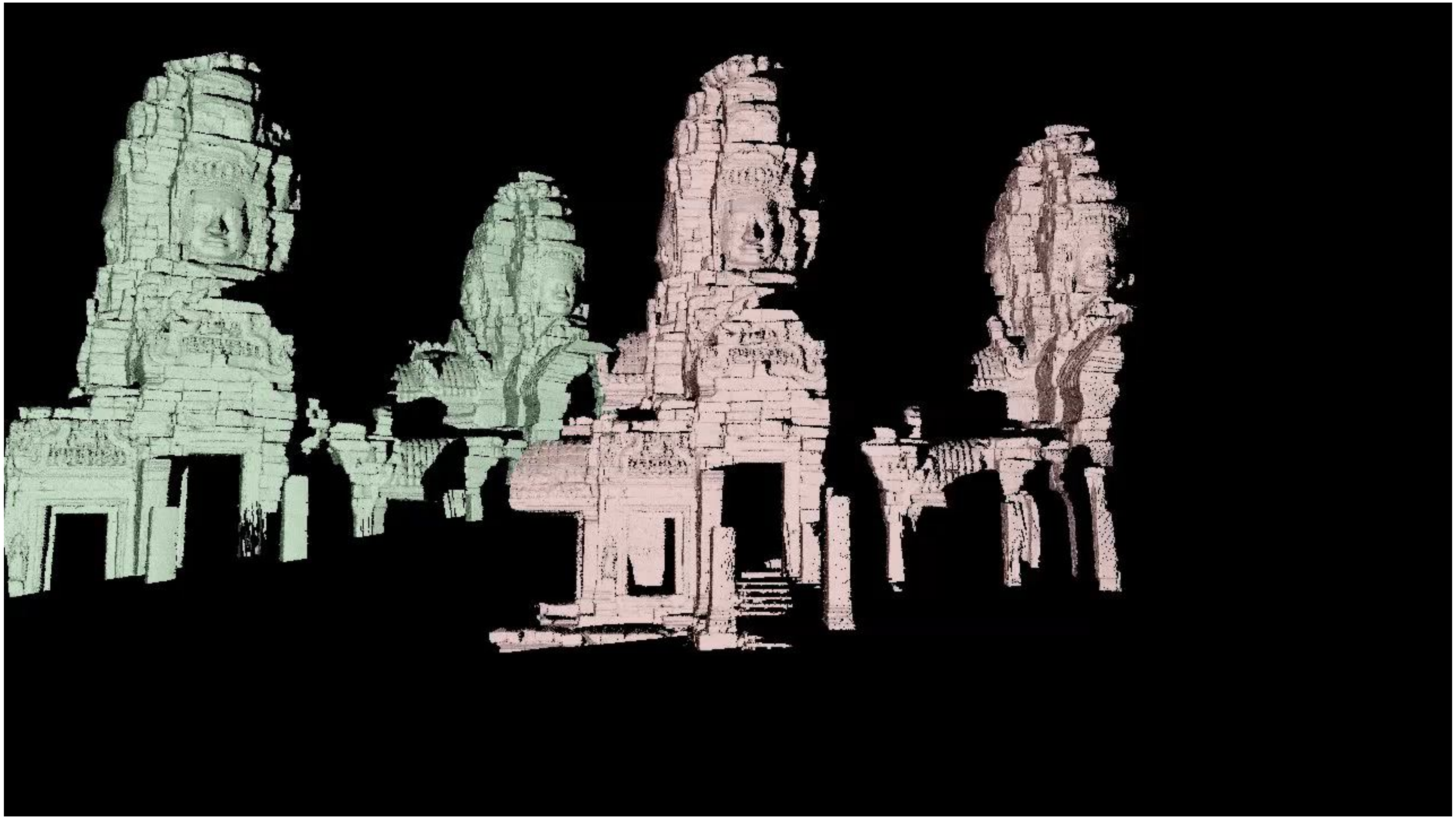

Alignment result (Bayon)

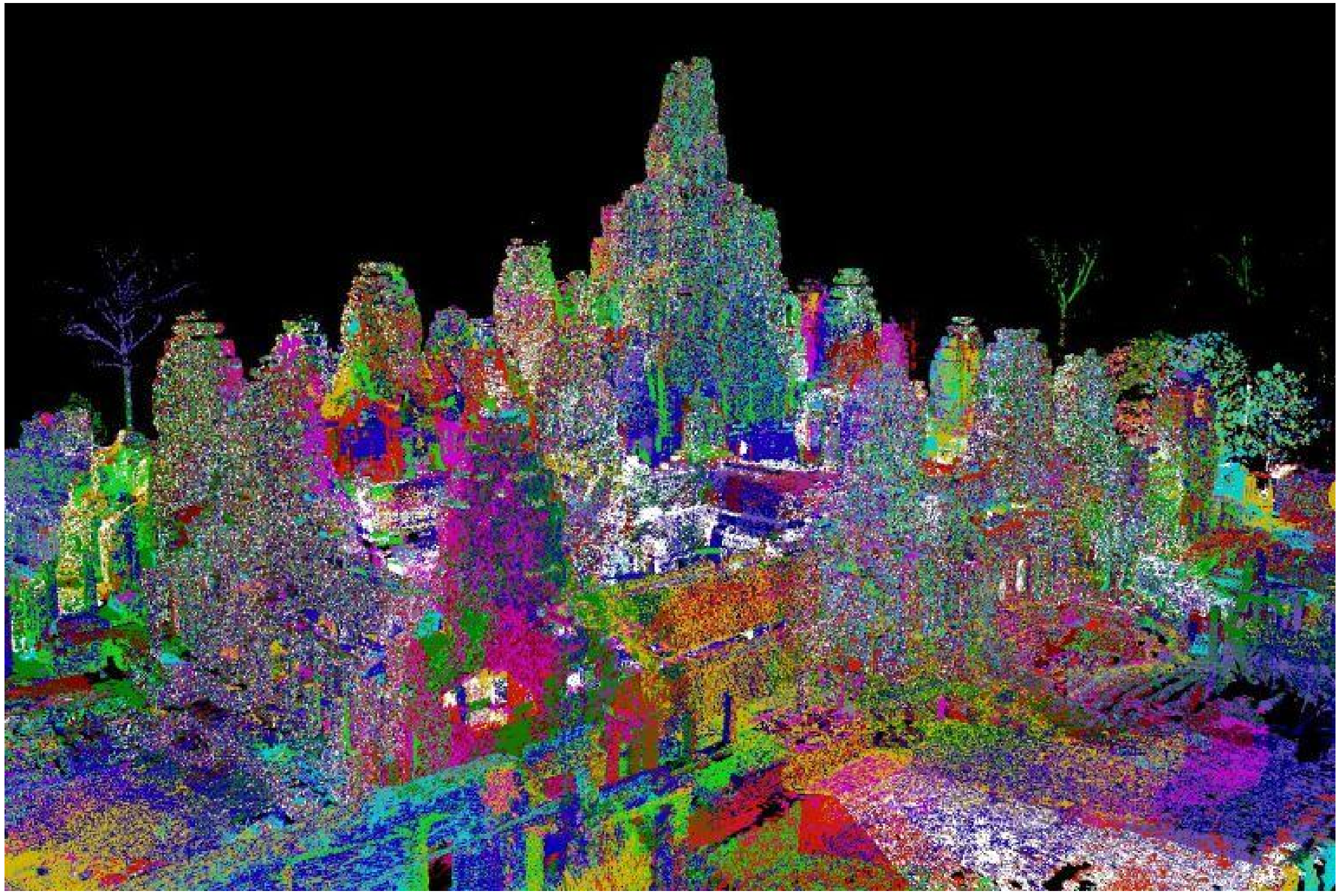

Modeling procedures